creative commons
COMMONS DEED

저작자표시-비영리-변경금지 2.0 대한민국

이용자는 아래의 조건을 따르는 경우에 한하여 자유롭게

- 이 저작물을 복제, 배포, 전송, 전시, 공연 및 방송할 수 있습니다.

다음과 같은 조건을 따라야 합니다:

저작자표시. 귀하는 원저작자를 표시하여야 합니다.

비영리. 귀하는 이 저작물을 영리 목적으로 이용할 수 없습니다.

변경금지. 귀하는 이 저작물을 개작, 변형 또는 가공할 수 없습니다.

- 귀하는, 이 저작물의 재이용이나 배포의 경우, 이 저작물에 적용된 이용허락조건을 명확하게 나타내어야 합니다.
- 저작권자로부터 별도의 허가를 받으면 이러한 조건들은 적용되지 않습니다.

저작권법에 따른 이용자의 권리는 위의 내용에 의하여 영향을 받지 않습니다.

이것은 이용허락규약(Legal Code)을 이해하기 쉽게 요약한 것입니다.

Disclaimer

dCollection

약학박사학위논문

어성초의 화학 성분과 대식세포 내 산화질소 생성 저해활성

Chemical Constituents from Aerial Parts of *Houttuynia cordata* and Their Inhibitory Activity against NO Production in Macrophage

2017 년 8 월

서울대학교 대학원

약학과 생약학전공

안 종 민

Abstract

Houttuynia cordata Thunb, belonging to the family of Saururaceae, is a plant used in traditional medicine for the treatment of fever, poisoning and inflammation-related disorders. In previous phytochemical studies, it has been reported that the aerial parts of *H. cordata* contained various types of compounds including simple phenolic compounds, flavonoids, flavonoid glycosides, ionones and some alkaloids containing benzamide and isoquinoline moieties.

Alkaloids are nitrogen-containing compounds found in plants, microorganism and marine organisms. They contain one or more nitrogen atoms, and they have various structures, including quinoline, isoquinoline, indole alkaloid and benzamide. The alkaloids in nature have been reported for diverse biological and pharmacological activities.

A few alkaloids have been reported from aerial parts of *H. cordata*, and their anti-inflammatory activities have not been reported previously. This report investigated the alkaloids from the aerial parts of *H. cordata* and explored the biological activity of the isolates to determine their anti-inflammatory properties. In detail, twenty-one alkaloids were isolated and their structures were elucidated. Of which, two benzamides (**1**, **2**) and a *β*-carboline alkaloid (**14**) were isolated from nature for the first time. The isolated alkaloids were tested for their inhibitory activity against NO production in RAW 264.7 cells stimulated by LPS. Of the tested compounds, perlolyrine (**15**) showed the significant inhibitory activity with

an IC_{50} value of 8.7 μM.

In addition, further isolation was performed in order to investigate the constituents of aerial parts of *H. cordata*. As a result, thiry-eight compounds were further isolated from a methanolic extract of aerial parts of *H. cordata* including 8 flavonoids, 4 megastigmanes, 8 phenylpropanoid derivatives, 3 benzoic acid derivatives, 2 lignans, 5 neolignans, a bisphenylpropanol, 5 glycosides and 2 macrolides. Among them, a neolignan (**50**) was firstly isolated from nature.

Keyword : *Houttuynia cordata*, Saururaceae, Alkaloids, Anti-inflammatory

Student Number : 2011-21735

Contents

List of Schemes

List of Tables

List of Figures

List of Abbreviations

DOPA : 3,4-Dihydroxyphenylalanine

DMSO : Dimethyl sulfoxide

CD_3OD : Tetradeuteromethanol

CC : Column Chromatography

HPLC : High Performance Liquid Chromatography

RPMI : Roswell Park Memorial Institute medium

LPS : Lipopolysaccharide

CD : Circular Dichroism

UV : Ultraviolet

FT-IR : Fourier Transform Infrared

TLC : Thinlayer Chromatography

HR-ESI-QTOF-MS : High resolution-electrospray ionization-Quadrupole-Time-of-flight mass spectrometry

NMR : Nuclear Magnetic Resonance

MPLC : Medium Pressure Liquid Chromatography

RP : Reverse phase

ECD : Electronic circular dichroism

aq. MeOH : aqueous methanol

aq. MeCN : aqueous acetonitrile

MTT : 3-(4,5-dimethylthiazol-2-yl)-2,5-diphenyltetrazolium bromide

ELISA : enzyme-linked immunosorbent assay

HMBC : heteronuclear multiple bond correlation

HSQC : heteronuclear single quantum coherence

COSY : correlation spectroscopy

NOESY : nuclear overhauser enhancement spectroscopy

d : doublet

dd : doublet of doublet

m : multiplet

t : triplet

s : singlet

Glc : glucose

Rha : rhamnose

1. Introduction

1.1. *Houttuynia cordata* Thunb.

Houttuynia cordata Thunb., belonging to the family of Saururaceae, is distributed throughout Asian countries, including Korea, China, Japan and Thailand. This plant, called *Eoseongcho*, is used in traditional medicine for the treatment of inflammation-related disorders, fever and constipation . The leaves of *H. cordata* also consumed as a vegetable in China .

In previous phytochemical studies, it has been reported that the aerial parts of *H. cordata* contained various types of compounds including simple phenolic compounds, flavonoids, flavonoid glycosides, ionones and some alkaloids containing benzamide and isoquinoline moieties (Figure 1 and 2) . The extracts of *H.cordata* showed beneficial properties, including anti-allergic, antivirus, anti-inflammatory and anticancer activities (Table 1).

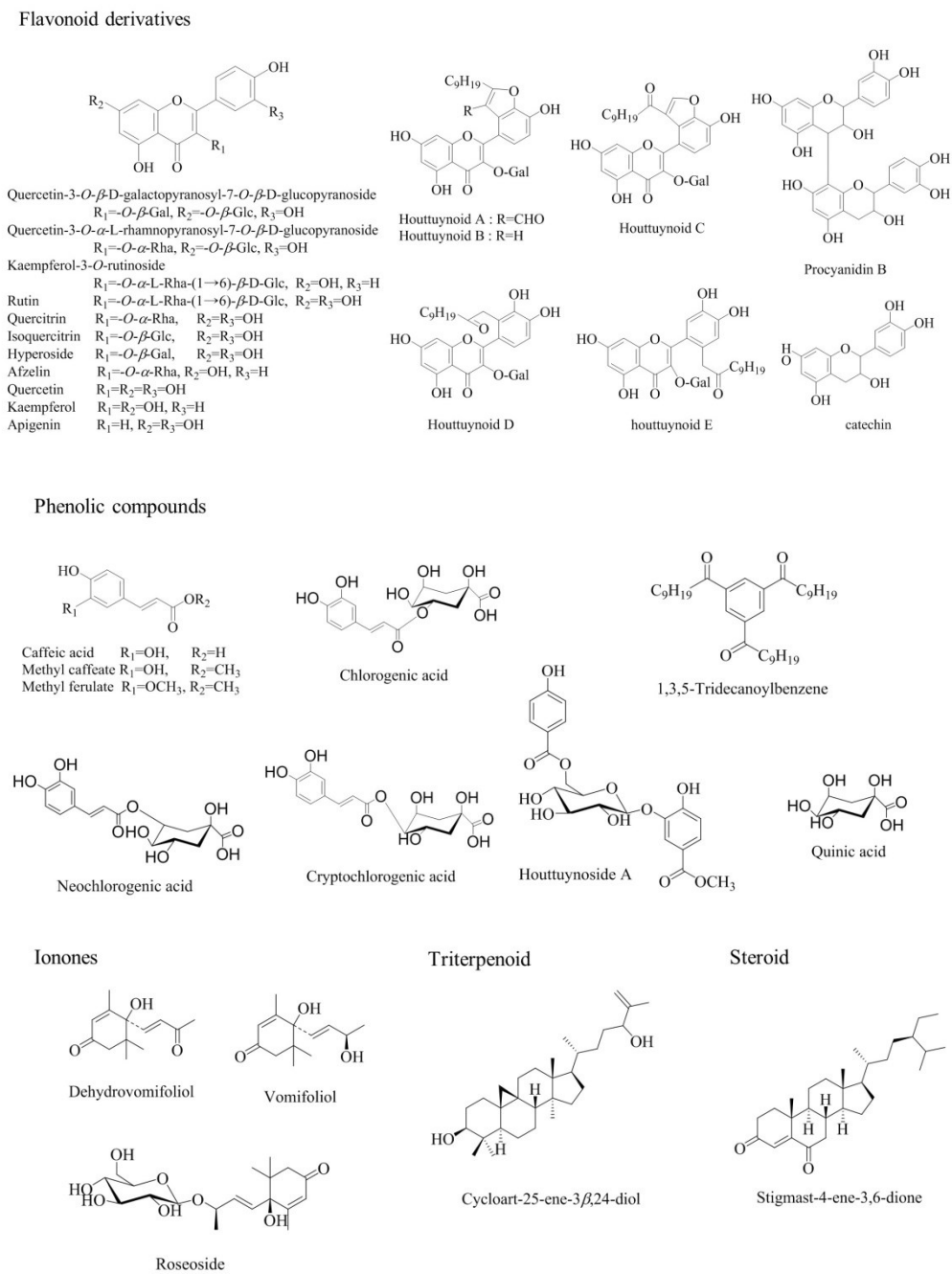

Figure 1. Structures of chemical constituents reported in *H. cordata* (1)

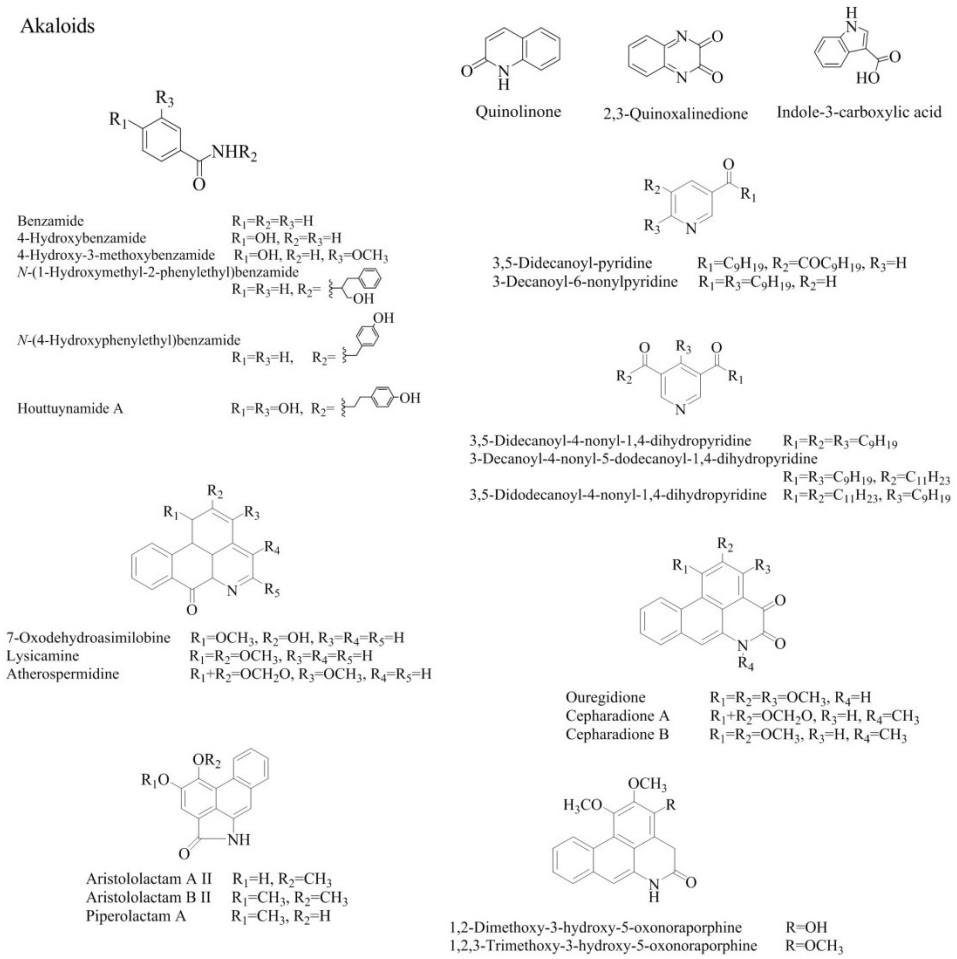

Figure 2. Structures of chemical constituents reported in *H. cordata* (2)

Table 1. Pharmacological studies reported in *H. cordata*.

Therapeutic target	In vitro/vivo assay	Extracts/ Active constituents	References
Anti-allergic	RBL-2H3 cells	Water extract	(Han et al. 2009; Shim et al. 2009)
	human basophilic KU812F cells		
	Anaphylactic reaction (mouse)		
Antiviral	Herpes Simplex Virus-1 (HSV-1)	Water extract, piperolactam A, roseoside, afzelin, houttuynoids A-E	(Chen et al. 2012)
	HSV-2	Water extract, quercetin, quercitrin, isoquercitrin,	(Chou et al. 2009)
	BCC-1/KMC cells infected with HSV-1 and HSV-2	Water extract	(Chiang et al. 2003)
	SARS (mouse)	Water extract	(Lau et al. 2008)
	Dengue virus serotype 2 (DEN-2)	Aqueous extract	(Leardkamolkarn et al. 2012)
Antibacterial	Bacterial pathogen Salmonella (RAW264.7)	Water extract	(Kim et al. 2008)
Genotoxicity	Reverse mutation assay (Salmonella typhimurium)	Methanol extract	(Kang et al. 2012)
	Chromosome aberration assay (Chinese hamster ovary cell)		
Anticancer (Apoptosis)	HL-60 cells, A549 cells,	Ethanol extract	(Y. F. Chen et al. 2013; Prommaban et al. 2012)
	Human leukemic Molt-4 cells		
	HER2/neu-overexpressing cancer cells, mouse	houttuyninum	

Antiobesity	mouse	Water extract	(Miyata et al. 2010)
Immunologic	HMC-1	Ethanol extract	(Lee et al. 2008)
	Mouse	Decanoyl acetaldehyde	(Yang & Jiang, 2009)
Anti-inflammatory	COX-assay (from sheep seminal vesicle microsomes)	Hexane extract, linoleic acid, linolenic acid	(Bauer et al. 1996)
	Raw 264.7	Supercritical extract	(Shin et al. 2010)
	HMC-1 cells	Ethanol extract, Ethylacetate fraction	(Kim et al. 2007)
Antioxidant	DPPH	Quercitrin, quercetin-3-*O*-*β*-D-galactopyranoside	(Chou et al. 2009)
Hepatoprotective	PTP1B	Aporphine alkaloids	(Ma et al. 2017)

1.2. Alkaloids

1.2.1. Benzamides

Benzamides are defined as alkaloids containing an amide group, which is a derivative of benzoic acid. They have been found in seaweed *Bostrychia radicans* (Montagne), plants *Houttuynia cordata*, *Swinglea glutinosa*, *Goniothalamus tapisoides*, *Glycyrrhiza glabra*, *Naravelia zeylanica*, *Cerbera manghas* and *Schinus terebinthifolius* and an endophytic fungus *Colletotrichum gloeosporioides* from *Michelia champaca* (De Oliveira et al. 2012; Braga et al. 2007; Fu et al. 2013; Chapla et al. 2014; Kim et al. 2013; Vijayalakshmi & Shourie 2013; Dibinlal et al. 2015; Zhang et al. 2010; Moustafa et al. 2007) and their pharmacological activities including antifungal, antitumor, acetylcholinesterase inhibitory, gastrointestinal prokinetic and antipsychotic activity have been reported (Keinath & Kousik 2011; Horsman 1995; Braga et al. 2007; Chapla et al. 2014; Briejer et al. 1995; Oltmanns et al. 2009).

1.2.2. Aporphine alkaloids

Aporphine alkaloids belong to isoquinoline type alkaloids. The precursor of isoquinoline alkaloids is a norlaudanosoline biosynthesized from a tyrosine and a DOPA (Figure 3) (Dewick 2009). In general, aporphine alkaloids have similar substituents including hydroxy, methoxy and methyl groups (Chen et al. 2013).

Aporphine alkaloids are generally known as the components of Lauraceae, Magnoliaceae, Menispermaceae, Papaveraceae and other families, and many pharmacological activities including hepatoprotective, anti-viral, anti-tyrosinase, antitumor and antimalarial activity have been reported (Ma et al. 2017; Chou et al. 2009; Chen et al. 2013).

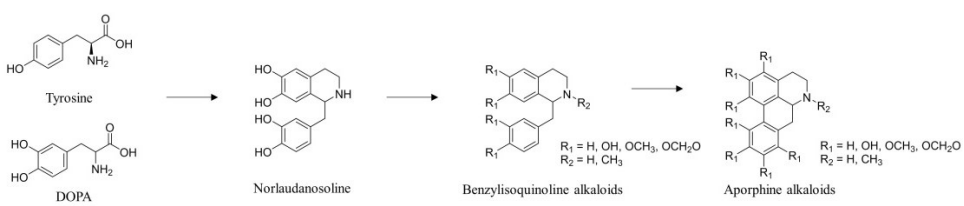

Figure 3. Biosynthetic pathway of aporphine alkaloids

Aporphine alkaloids have general MS fragmentation patterns, which are key evidence to identify these structures. These characterized fragmentation patterns were shown in Figure 4. Aporphine alkaloids without substituent at *N* atom could give a fragment ion of $[M+H-17]^+$, while the fragment ion peak at $[M+H-31]^+$ could be detected for those with methyl group at the *N* atom. Neutral losses of 17

and 31 u were assigned to the elimination of NH_3 and NH_2CH_3 from the protonated ions, respectively (Zhang et al. 2015).

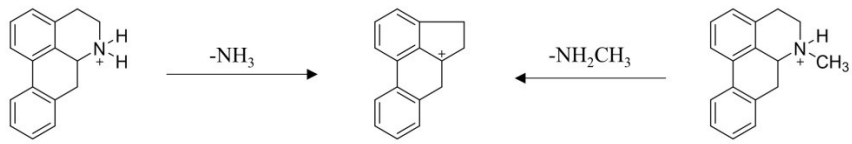

Figure 4. The fragmentation pathway of aporphine alkaloids

1.2.3. *β*-carboline alkaloids

Alkaloids based on a *β*-carboline system are indole alkaloids with a wide range of pharmacological activities. Various biological activities were reported for these kind of alkaloids, including hypothermic, antimicrobial, antiplatelet, antitumor, antipalsmodial, antifungal and psychopharmacological effects (Ahmadinejad & Tari 2017; Herraiz et al. 2010; Carvalho et al. 2017; Ang et al. 2000).

β-Carbolines are characterized by a core indole structure combined with a pyridine ring (Wagner et al. 2017). These alkaloids are naturally generated from tryptamine and aldehyde (or keto acid) (Figure 5) (Dewick 2009). They can be found in marine organism as well as in plants and micro-organisms (Yan et al. 2017).

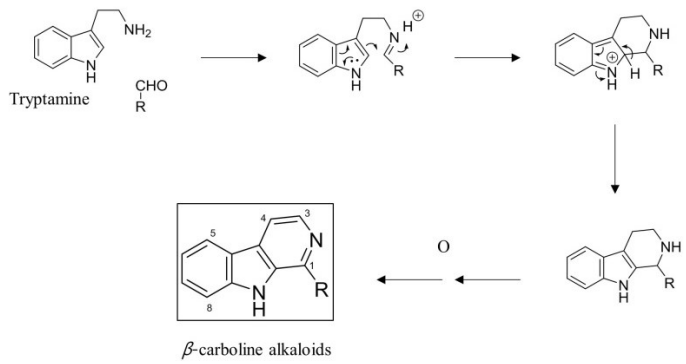

Figure 5. Biosynthetic pathway of β-carboline alkaloids

1.3. Nitric oxide production in macrophage and its inhibitory agents (alkaloids) from natural products

Inflammation is one of the most important host defense systems against tissue injuries and invading pathogens. Inflammation is also a key feature of various desease including metabolic syndrome, cancer, infections and wound (Hotamisligil 2006; Hopkinson-Woolley et al. 1994).

Macrophages play a significant role in almost all inflammatory responses. They are involved in the inflammatory response by releasing cytokines, chemokines and growth factors that recruit and activate additional leukocytes to injury site. In addition, activated macrophages activate the expression of genes responsible for the synthesis of reactive oxygen and nitrogen species (NO, O_2^-, H_2O_2) and bioactive lipids. These agents make for the regulation of the inflammatory response (Boscá et al. 2005; Guo & DiPietro 2010).

Nitric oxide is a gaseous molecule that perform a dual role on cell viability. Moderate levels of NO function as a protective role as well as a regulatory role of the additional pro-inflammatory cytokines, such as TNF-α, protecting the cell against stimulus-dependent apoptosis, whereas high concentration of NO promotes apoptotic, like those characteristic of the inflammatory response. In addition, excessive NO production prevent the recruitment and activation of more circulating cells and give rise to a wide range of inflammatory diseases, such as sepsis, psoriasis and systemic lupus erythematosus (Boscá et al. 2005; Vodovotz et al. 1993; Williams et al. 1999; Lee et al. 2000).

LPS-activated RAW 264.7 cells have been widely used to evaluate the anti-inflammatory effect of compounds. Previously reported alkaloids presented anti-inflammatory effect in RAW 264.7 cells are shown in Table 2, and their structures are shown in Figure 6.

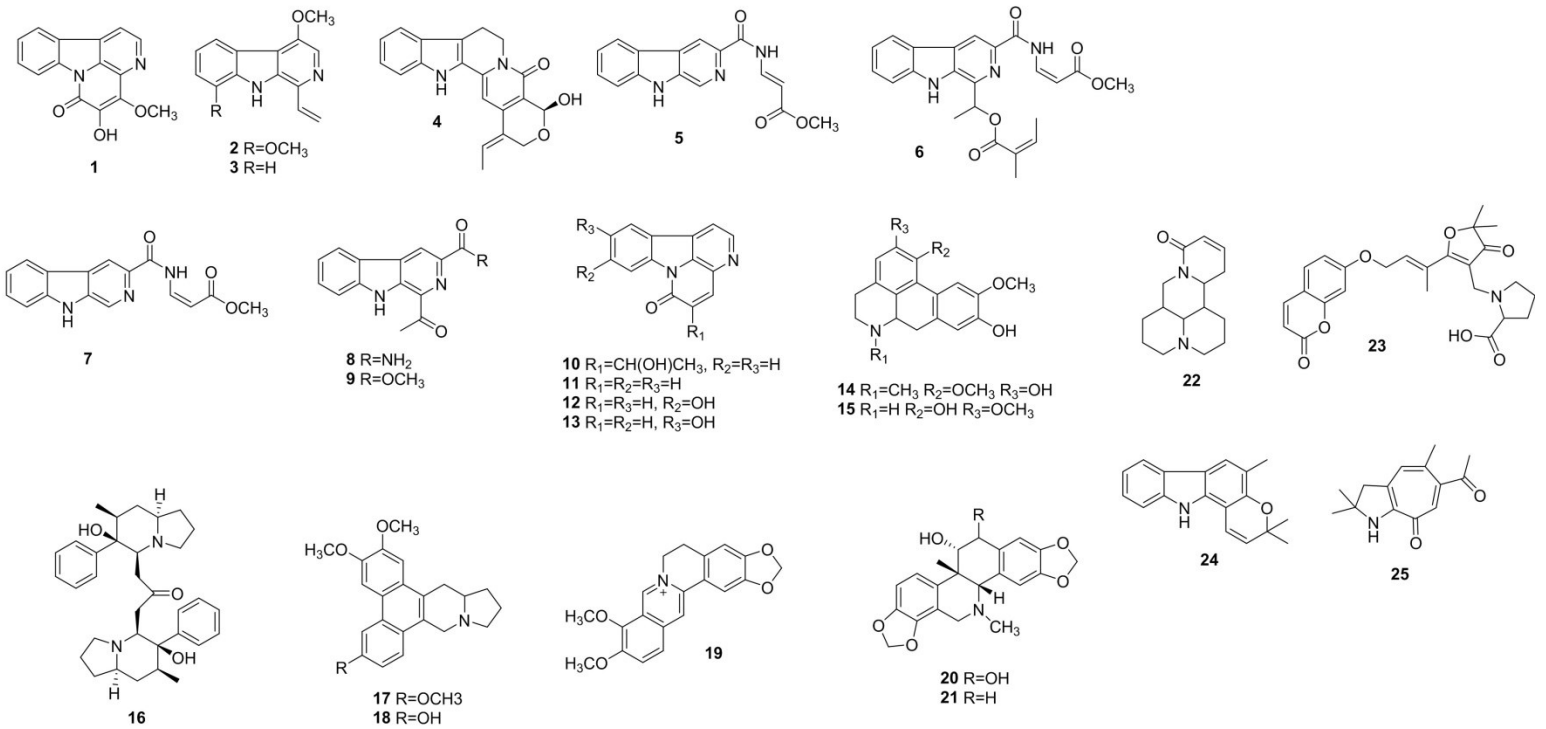

Figure 6. The anti-inflammatory agents (alkaloids) from natural products

Table 2. The anti-inflammatory agents (alkaloids) from natural products

Compounds	Activity (RAW 264.7 cells)	Plant source	References
4-Methoxy-5-hydroxycanthin-6-one (**1**)	inhibit the production of NO, TNFα	*Picrasma quassioides*	(Fan et al. 2013)
4,8-Dimethoxy-1-vinyl-*β*-carboline (**2**) 4-Methoxy-1-vinyl-*β*-carboline (**3**)	decerease iNOS, PGE_2, COX-2, NF-κB	*Melia azedarach*	(Lee et al. 2000; Yoon et al. 2005)
17-*O*-Methyl-19-(*Z*)-naucline (**4**)	inhibit NO production	*Nauclea officinal*	(Liu et al. 2017)
Dichotomide III (**5**) Dichotomide X (**6**) Stellarines B (**7**) Stellarines A (**8**) 1-Acetyl-3-methoxycarbonyl-*β*-carboline (**9**)	inhibit NO production	*Illigera luzonensis*	(Chen et al. 2010)
(*R*)-5-(1-Hydroxyethyl)-canthine-6-one (**10**) Canthin-6-one (**11**) 9-Hydroxycanthin-6-one (**12**) 10-Hydroxycanthin-6-one (**13**)	inhibit NO production	*Ailanthus altissima*	(Kim et al. 2016)
Boldine (**14**)	inhibit NO, IL-6 IL-17, TNFα, p-STAT3	*Peumus boldus*	(Pandurangan et al. 2016)
Norisoboldine (**15**)	inhibit NF-κB-p65 reduced VEGF mRNA expression and ARNT-HIF-1α complex accumulation	*Lindera aggregata* (root)	(Wei et al. 2015)
(+)-Homocrepidine A (**16**)	inhibit NO production	*Dendrobium crepidatum*	(Hu et al. 2016)

Antofine (**17**) 6-*O*-Desmethylantofine (**18**)	inhibit NO production	the *Cynanchum*, *Pergularia*, and *Tylophora* species that belong to the Asclepiadaceae family	(Min et al. 2010)
Berberine (**19**)	suppress IL-1β, TNFα, ROS	*Coptidis Rhizoma*	(Dinesh & Rasool 2017)
12-Hydroxycorynoline (**20**) Corynoline (**21**)	inhibit NO, IL-6, IL-10, TNFα	*Corydalis bungeana*	(Dong et al. 2015)
Sophocarpine (**22**)	decrease NO, TNFα, IL-6, COX-2	*Sophora alopecuroides* L.	(Gao et al. 2012)
Parvifloranine A (**23**)	inhibit NO production	*Geijera parviflora*	(Shou et al. 2013)
Girinimbine (**24**)	decerease NO, NF-κB	*Murraya koenigii*	(Iman et al. 2017)
Oleracone (**25**)	inhibit NO production	*Portulaca oleracea* L	(Meng et al. 2016)

1.4. Purpose of research

The purpose of this research was investigation of the alkaloids from the aerial parts of *H. cordata* and discovery of new bioactive alkaloids. Herein, the alkaloids from *H. cordata* were isolated and their structures were elucidated through the analysis of extensive spectroscopic data and comparison with previously reported data. The inhibitory effects of isolated alkaloids on LPS-induced NO production in RAW 264.7 cells were also evaluated in order to determine the anti-inflammatory activities of isolated alkaloids.

2. Experimental Section

2.1. Materials

2.1.1. Plant material

The dried aerial parts of *H. cordata* were purchased from the Kyung-dong oriental herbal market, Seoul, Republic of Korea, in March, 2013 and identified by Prof. Dr. Jehyun Lee (Dongguk University, Korea). The voucher specimen (SNUPH2013-02) was deposited in the Herbarium of the Medicinal Plant Garden, College of Pharmacy, Seoul National University.

2.1.2. Reagents

DMSO-d_6 and CD_3OD (Cambridge Isotope Laboratories, Inc. USA) were used as NMR solvents. Column chromatography (CC) was carried out with Diaion HP-20 (Mitsubishi chemical corporation, Japan), Sephadex LH-20 (25–100 μm; Pharmacia, USA) or Kiesegel 60 silica gel (40-63 μm, 230-400 mesh, Art. 9385; Merck, Germany). Thin-layer chromatography (TLC) was conducted on pre-coated Kiesegel 60 silica gel F_{254} plates (Art. 5715; Merck, Germany). Formic acid was purchased from Wako Pure Chemical Industries, Ltd. (Japan) HPLC grade solvents were purchased from Fisher Scientific Korea Ltd. (Korea). HCl, NH_4OH, H_2SO_4,

Na_2CO_3 and first grade solvents for extraction, fractionation and isolation were purchased from Daejung Chemical & Metals Co. Ltd. (Korea). L-cysteine methyl ester hydrochloride and *o*-tolylisothiocyanate were purchased from Tokyo Chemical Industry (Japan). RPMI, penicillin and streptomycin were purchased from HyClone (Logan, USA). Bovine serum albumin and LPS were purchased from Sigma (St. Louis, USA). All other reagents were purchased from Sigma-Aldrich (USA).

2.1.3. Equipments

Polarimeter : Jasco P- 2000 digital polarimeter, Japan

CD and UV : Chirascan plus Circular Dichroism spectrometer, UK

FT-IR : Jasco FT/IR-4200 spectrophotometer, Japan

HR-ESI-QTOF-MS : Waters Xevo G2 qTOF mass spectrometer, UK

MassLynx SCN 855 software for data acquisition

NMR : Jeol JMN-LA 300 Spectrometer, Japan

Bruker AVANCE 300 Spectrometer, Germany

Bruker GPX 400 Spectrometer, Germany

Bruker AVANCE 600 Spectrometer, Germany

Bruker AVANCE 800HD spectrometer coupled with cryoprobe, Germany

UV lamp : VL-4.LC, 365/254, Vilber Lourmat, France

MPLC : Combiflash companion, Isco, USA

MPLC column : RediSep 40 g, 80 g or 120 g silica flash column, Isco, USA

HPLC for isolation : Gilson HPLC equipped with Gilson 321 pump and UV.VIS 151 detector, USA

HPLC column :

Hypersil GOLD™ aQ (175 Å, i.d. 250 × 10 mm, 5 μm, Thermo Scientific™, Germany)

Inno C18 column (120 Å, i.d. 250 × 10 mm, 5 μm, Young Jin Biochrom co., Ltd., Korea)

Luna 5u C18 (2) (100 Å, i.d. 250 × 10 mm, 5 μm, Phenomenex Inc., USA)

Luna 5u C18 (2) (100 Å, i.d. 250 × 21.20 mm, 5 μm, Phenomenex Inc., USA)

Analytical RP-HPLC system :

Waters 2695 alliance system with a 996 Photodiode Array detector, USA

Hypersil™ BDS C18 column (130 Å, i.d. 150 × 4.6 mm, 5 μm, Thermo Scientific™, Germany)

Conformation search program : Conflex 7, Conflex Corp., Japan

ECD calculation program :

TmoleX 3.4 and Turbomole, COSMOLogic GmbH & Co., Germany

Analytical balance : Mettler ML 204, Switzerland

Evaporator : EYELA R-1000, Japan

Freeze-dryer : DURA-DRY, Fts system Inc., USA

Ultrasonicator : Branson 5510, UK

2.2. Methods

2.2.1. Extraction and Isolation of alkaloids

The dried aerial parts of *H. cordata* (36 kg) were ground and extracted three times with MeOH (200 L) at room temperature with sonication for 90 min. After removal of the solvent *in vacuo*, the chlorophylls were removed using HP-20 resin eluting with 90% aqueous MeOH. The crude extract was approximately 4.5 kg. A portion of crude extract (3.0 kg) was suspended in H_2O, then partitioned successively with *n*-hexane, $CHCl_3$, EtOAc and *n*-BuOH.

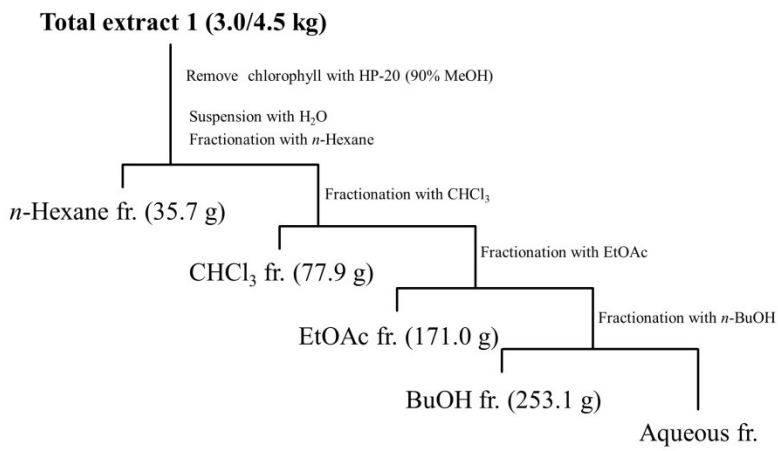

Scheme 1. The fractionation of a part of crude extract of *H. cordata*

The BuOH residue (253.1 g) was fractionated by Diaion HP-20 chromatography eluting stepwise with 20%, 40%, 60%, 80% and 100% aq. MeOH to yield 5 fractions (B1-5). A portion of fraction B2 (13.0 g) was subjected to silica gel chromatography eluting with $CHCl_3$/MeOH (15:1→0:1, step-gradient system) to give 13 fractions (B2a-B2m). B2e (645.0 mg) was separated into 10 fractions (B2e01-B2e10) on silica gel MPLC (80 g) eluting with $CHCl_3$/MeOH (12:1→0:1, step-gradient system). From B2e09, compound **19** (520.0 mg) was purified using a Hypersil GOLD HPLC column with the isocratic solvent of 20% aq. MeCN. B2g (1.03 g) was separated into 11 subfractions (B2g01-11) on an RP-MPLC column (120 g) eluting with aq. MeOH (5%→100%, step-gradient system). B2g03 (121.8 mg) was further fractionated by Sephadex LH-20 (50% aq. MeOH) and gave 4 subfractions (B2g03A-D). B2g03B was subsequently purified using an Inno HPLC column (10% aq. MeOH) to afford compound **20** (4.2 mg). B4 (5.0 g) was subjected to an RP-MPLC (120 g) eluting with aq. MeOH (25%→100%, step-gradient system) to yield 15 fractions (B4a-o). B4g (323.4 mg) was fractionated using Sephadex LH-20 with MeOH, followed by Luna 5u HPLC (24% aq. MeOH) to give compound **2** (1.0 mg). The alkaloid-rich fractions were prepared using an acid-base fractionation method from the fractions B2 (6.2 g) and B5 (36.0 g) and the chloroform residue. Two percent HCl and ten percent NH_4OH were used as the acid and base, respectively. The alkaloid-rich fractions B2A (116.8 mg) and B5A (1.71 g) were separated into 8 fractions (30:1→0:1, B2A1-8) and 9 fractions (50:1→0:1, B5A1-9), respectively, on a silica MPLC column (80 g) eluting stepwise with $CHCl_3$/MeOH. HPLC purification (Luna 5u, 8% aq. MeOH) of

B2A5 (17.8 mg) furnished compound **21** (1.5 mg). B5A3 (24.5 mg) was subjected to an RP-MPLC (40 g) eluting stepwise with aq. MeOH (30%→100%) to give 8 fractions (B5A3a-h). From B5A3f (17.5 mg), compounds **7** (5.1 mg) and **14** (3.7 mg) were isolated by HPLC separation (Inno, 40% aq. MeOH). B5A5 (300.8 mg) was subjected to an RP-MPLC column (80 g) and gave 15 fractions (B5A5a-o). B5A5e (20.0 mg) was further purified on a Luna column to yield compound **3** (15.0 mg, 40% aq. MeCN).

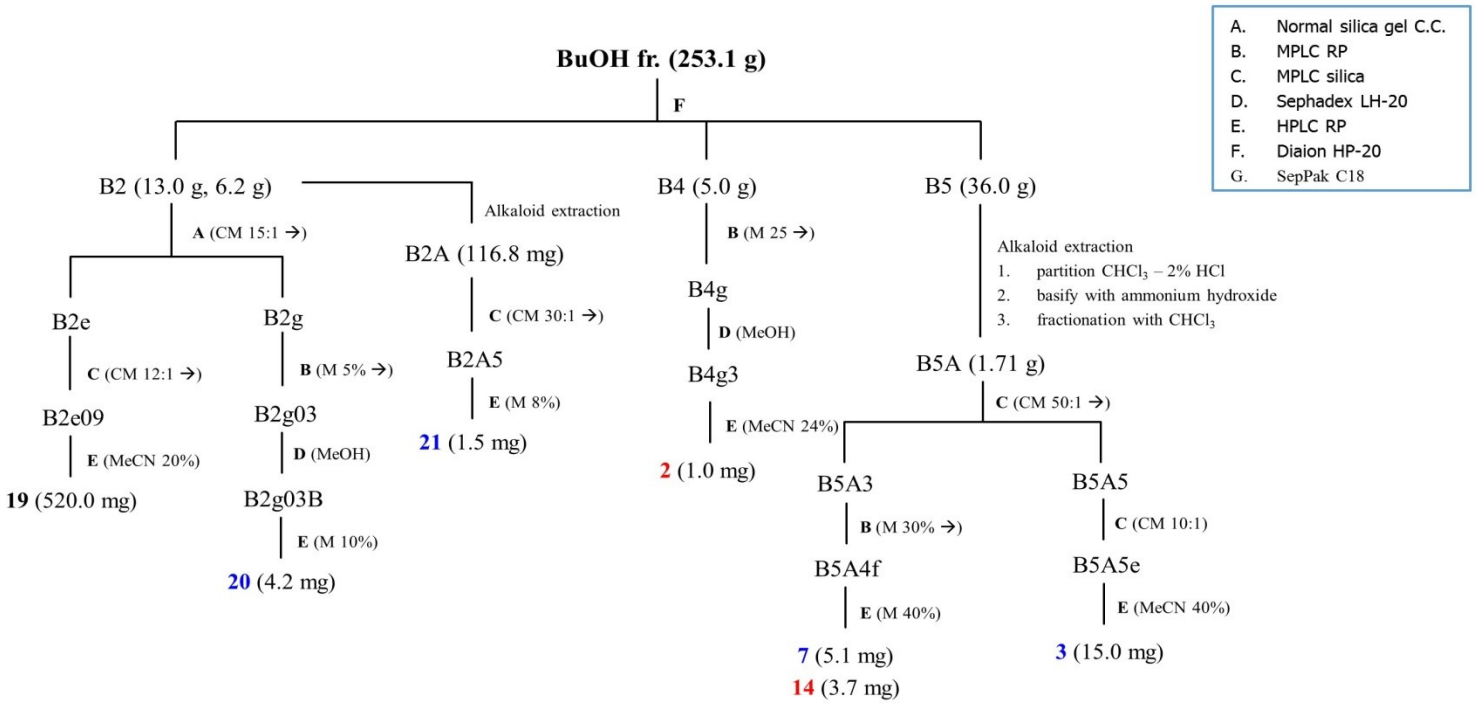

Scheme 2. Isolation of alkaloids from the *n*-BuOH fraction of *H. cordata*.

The alkaloid-rich fraction CA (823.5 mg), which was extracted from the chloroform residue (77.9 g), was separated by Sep-Pak C18 cartridge eluting stepwise with 20%, 50% and 100% aq. MeOH to give 3 fractions (CA1-3). CA2 (119.2 mg) was separated into 12 fractions (CA2a-l) on a silica MPLC (80 g) eluting with $CHCl_3$/MeOH (100:1→0:1, step-gradient system). Fractions CA2i (46.0 mg), CA2j (49.2 mg) and CA2k (62.5 mg) were further purified on a Hypersil GOLD column with the isocratic solvent (25%, 23% and 18% aq. MeCN, respectively) to yield compounds **6** (29.7 mg, from CA2i), **15**(15.0 mg, from CA2i), **8** (2.1 mg, from CA2j), **9** (2.2 mg, from CA2j), **10** (8.0 mg, from CA2k) and **11** (2.7 mg, from CA2k).

The ethyl acetate residue (32.2 g) was separated by silica gel column chromatography eluting stepwise with $CHCl_3$/MeOH (20:1→0:1) to give 12 fractions (E01-12). E04 (668.6 g) was chromatographed on a Sephadex LH-20 eluting with MeOH, yielding 9 fractions (E04a-i). From E04d (116.9 mg), E04f (18.3 mg) and E04h (17.6 mg), compounds **1** (11.6 mg, from E04d, 25% aq. MeCN), **4** (5.9 mg, from E04d, 25% aq. MeCN), **16** (5.8 mg, from E04f, 30% aq. MeCN) and **5** (4.0 mg from E04h, 40% aq. MeCN) were purified by a Luna 5u HPLC column.

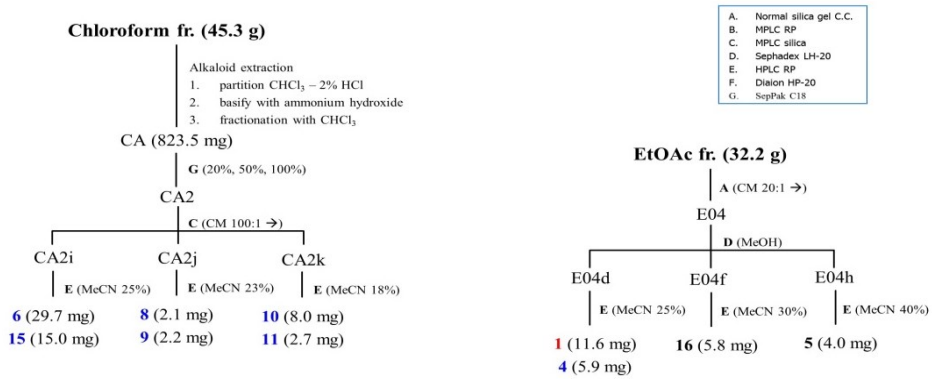

Scheme 3. Isolation of alkaloids from the $CHCl_3$ and EtOAc fractions of *H. cordata.*

Another total extract (0.6 kg) was fractionated by an RP-MPLC column (40 g) eluting with aq. MeOH (5%→100%, gradient system) to give 3 fractions. The alkaloid-rich fractions 1A-3A were prepared using an acid-base fractionation method from each fraction. Silica gel MPLC (120 g) for 1A (3.79 g) and 3A (1.12 g) was performed using step-gradient elution with $CHCl_3$/MeOH (100:1→0:1) to give 15 fractions (1A01-1A15) and 12 fractions (3A01-3A12), respectively. Fraction 1A12 (209.6 mg) was subjected to silica gel MPLC (40 g), eluted with $CHCl_3$/MeOH (40:1, isocratic system) and gave 6 fractions (1A12a-f). From 1A12e (60.4 mg), compound **18** (5.2 mg) was isolated by HPLC separation (Hypersil GOLD, 25% aq. MeCN). Compound **17** (29.6 mg) was obtained from 1A09 (33.4 mg) using an Inno column (25% aq. MeOH). Fractions 3A09 (35.6mg) and 3A11 (79.6 mg) were further purified on a Hypersil GOLD and Inno column, respectively, to give compounds **13** (0.5 mg, 30% aq. MeOH, from 3A09) and **12**

(2.4 mg, 40% aq. MeOH, from 3A11). All water and solvents used for HPLC were 0.05% formic acid buffer. The common flow rate for HPLC and MPLC chromatography was 2 and 40 ml/min, respectively.

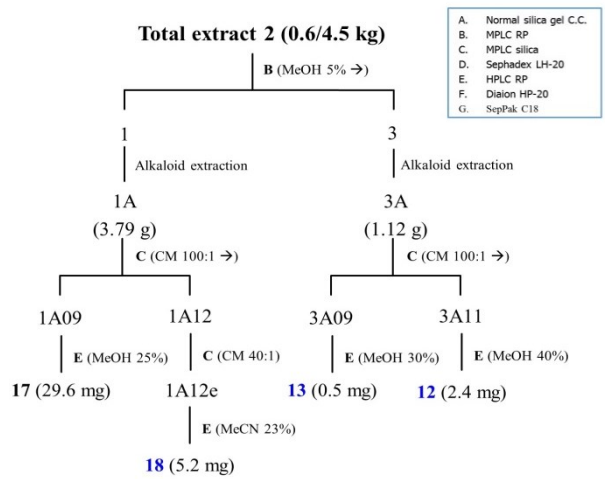

Scheme 4. Isolation of alkaloids from the portion of total extract of *H. cordata*.

Houttuynamide B (**1**)

Yellowish amorphous powder

$C_{15}H_{15}NO_3$

$[\alpha]_D^{21}$ -12.7 (*c* 0.30, MeOH)

UV (MeOH) λ_{max} nm (logε) 214 (3.31), 255 (3.36)

IR (neat) ν_{max} 3307, 1641, 1607, 1580, 1547, 1507, 1278, 1240, 1063 cm^{-1}

HRMS (ESI-TOF) *m/z* 258.1117 $[M+H]^+$ (calcd. for $C_{15}H_{16}NO_3$, 258.1130)

^1H NMR (CD_3OD, 400 MHz) : See Table 3

^{13}C NMR (CD_3OD, 100 MHz) : See Table 3

Houttuynamide C (**2**)

White amorphous powder

$C_{21}H_{25}NO_8$

$[\alpha]_D^{21}$ -5.4 (*c* 0.30, MeOH)

UV (MeOH) λ_{max} nm (logε) 210 (3.98), 291 (3.26)

IR (neat) ν_{max} 3335, 1641, 1583, 1545, 1449, 1305, 1244, 1078 cm^{-1}

HRMS (ESI-TOF) *m/z* 420.1645 $[M+H]^+$ (calcd. for $C_{21}H_{26}NO_8$, 420.1658)

^1H NMR (DMSO-d_6, 600 MHz) : See Table 3

^{13}C NMR (DMSO-d_6, 150 MHz) : See Table 3

N-(2-*β*-D-glucosidyl-2-phenylethyl)benzamide (**3**)

White amorphous powder

$C_{21}H_{25}NO_7$

$[\alpha]_D^{21}$ +8.2 (*c* 0.10, MeOH)

UV (MeOH) λ_{max} nm (logε) 201.6 (4.14)

IR (neat) ν_{max} 3357, 2917, 1641, 1577, 1541, 1490, 1313, 1159, 1076, 701 cm^{-1}

HRMS (ESI-TOF) *m/z* 426.1524 $[M+Na]^+$ (calcd. for $C_{21}H_{25}NO_7Na$, 420.1658)

^1H NMR (CD_3OD, 300 MHz) : See Table 3

^{13}C NMR (CD_3OD, 75 MHz) : See Table 3

Table 3. ^{1}H and ^{13}C NMR spectroscopic data of compounds **1-3**.

	1[a]		**2**[b]		**3**[c]	
No.	δ_C	δ_H (*J* in Hz)	δ_C	δ_H (*J* in Hz)	δ_C	δ_H (*J* in Hz)
C=O	170.4		166.3		170.3	
1	126.4		135.8		135.5	
2	130.3	7.68 d (8.7)	114.1	7.17 dd (1.9, 1.5)	128.3	7.78 m
3	116.1	6.80 d (8.7)	157.3		129.5	7.44 m
4	162.1		118.1	6.89 ddd (7.5, 1.9, 1.5)	132.6	7.51 dd (7.4, 7.4)
5	116.1	6.80 d (8.7)	129.3	7.21 m	129.5	7.44 m
6	130.3	7.68 d (8.7)	117.6	7.20 m	128.3	7.78 m
1'	48.6	3.62 dd (4.7, 13.5)	44.5	3.69 dd (13.7, 5.6)	46.7	3.80 dd (13.8, 4.3)
		3.50 dd (7.9, 13.5)		3.53 m		3.60 dd (13.8, 7.5)
2'	73.8	4.88 dd (4.7, 7.9)	79.0	4.88 t (5.6)	81.9	4.90 dd (4.2, 7.2)
1"	144.0		140.6		141.7	
2", 6"	127.2	7.42 d (7.2)	126.6	7.39 d (7.5)	127.7	7.44 m
3", 5"	129.4	7.34 t (7.2)	127.9	7.32 t (7.5)	129.1	7.30 t (7.1)
4"	128.6	7.25 t (7.2)	127.3	7.25 t (7.5)	128.7	7.27 t (7.1)
Glc-1			102.9	4.44 d (7.6)	104.8	4.55 d (7.2)
Glc-2			73.9	3.10 m	75.4	3.30 m
Glc-3			76.5	3.17 m	78.0	3.34 m
Glc-4			69.9	3.07 m	71.4	3.27 m
Glc-5			76.9	3.09 m	77.8	3.17 m
Glc-6			60.9	3.57 m	62.5	3.70 dd (2.3, 11.8)
				3.37 m		3.52 dd (5.3, 11.8)

[a] In CD_3OD, ^{1}H (400 MHz) and ^{13}C NMR (100 MHz) were measured.

[b] In DMSO-d_6, ^{1}H (600 MHz) and ^{13}C NMR (150 MHz) were measured.

[c] In CD_3OD, ^{1}H (300 MHz) and ^{13}C NMR (75 MHz) were measured.

4-[Formyl-5-(methoxymethyl)-1*H*-pyrrol-1-yl] butanoic acid (**4**)

Yellowish amorphous powder

$C_{11}H_{15}NO_4$

$[\alpha]_D^{21}$ -17.3 (*c* 0.10, MeOH)

UV (MeOH) λ_{max} nm (logε) 292 (4.09)

IR (neat) ν_{max} 2932, 1730, 1660 cm^{-1}

HRMS (ESI-TOF) *m/z* 224.0917 $[M-H]^-$ (calcd. for $C_{11}H_{14}NO_4$, 224.0928)

^{1}H NMR (DMSO-d_6, 400 MHz) : δ 9.45 (1H, s, CHO), 6.99 (1H, d, *J* = 4.0 Hz, H-3), 6.28 (1H, d, *J* = 4.0 Hz, H-4), 4.50 (2H, s, H-6), 4.37 (2H, m, H-1′), 3.36 (3H, s, 6-OCH_3), 2.32 (2H, t, *J* = 7.2 Hz, H-3′), 2.00 (2H, m, H-2′)

^{13}C NMR (DMSO-d_6, 100 MHz) : δ 181.1 (CHO), 176.8 (C-4′), 141.1 (C-5), 133.8 (C-2), 125.9 (C-3), 112.8 (C-4), 66.3 (C-6), 58.2 (6-OCH_3), 45.9 (C-1′), 31.9 (C-3′), 27.7 (C-2′)

Noraristolodione (**5**)

Yellowish amorphous powder

$C_{17}H_{11}NO_4$

$[\alpha]_D^{21}$ -16.6 (*c* 0.10, MeOH)

UV (MeOH) λ_{max} nm (logε) 314 (3.28), 302 (3.29), 241 (3.73), 206 (3.81)

IR (neat) ν_{max} 3330, 2980, 2945, 1716, 1706, 1680, 1599 cm^{-1}

HRMS (ESI-TOF) *m/z* 292.0612 $[M-H]^-$ (calcd. for $C_{17}H_{10}NO_4$, 292.0615)

^{1}H NMR (DMSO-d_6, 400 MHz) : δ 12.02 (1H, s, NH), 9.45 (1H, m, H-11), 8.10 (1H, s, H-3), 7.92 (1H, m, H-8), 7.66 (1H, m, H-9), 7.65 (1H, m, H-10), 7.49 (1H, s, H-7), 4.06 (3H, s, 1-OCH_3)

^{13}C NMR (DMSO-d_6, 100 MHz) : δ 177.0 (C-4), 155.6 (C-5), 152.9 (C-1), 151.3 (C-2), 132.4 (C-7a), 130.4 (C-6a), 128.4 (C-8), 127.8 (C-9), 127.2 (C-11), 126.6 (C-10), 126.1 (C-11a), 124.8 (C-3a), 124.0 (C-1a), 117.1 (C-1b), 117.1 (C-3), 111.9 (C-7), 59.5 (1-OCH_3)

N-Methylasimilobine (**6**)

Brown amorphous powder

$C_{18}H_{19}NO_2$

$[\alpha]_D^{21}$ -116.7 (*c* 0.10, MeOH)

UV (MeOH) λ_{max} nm (logε) 272 (4.07), 208 (4.40)

IR (neat) ν_{max} 2933, 1594, 1423, 1342, 1255 cm^{-1}

HRMS (ESI-TOF) *m/z* 282.1492 $[M+H]^+$ (calcd. for $C_{18}H_{20}NO_2$, 282.1489)

^{1}H NMR (CD_3OD, 400 MHz) : See Table 4

^{13}C NMR (CD_3OD, 100 MHz) : See Table 5

Isoboldine (**7**)

Brown amorphous powder

$C_{19}H_{21}NO_4$

$[\alpha]_D^{21}$ -10.8 (*c* 0.10, MeOH)

UV (MeOH) λ_{max} nm (logε) 306 (3.71), 280 (3.72), 218 (4.10)

IR (neat) ν_{max} 3276, 1604, 1509, 1474, 1248 cm^{-1}

HRMS (ESI-TOF) *m/z* 328.1543 $[M+H]^+$ (calcd. for $C_{19}H_{22}NO_4$, 328.1543)

^1H NMR (CD_3OD, 300 MHz) : See Table 4

^{13}C NMR (CD_3OD, 75 MHz) : See Table 5

N-Methyllaurotetanine (**8**)

White amorphous powder

$C_{20}H_{23}NO_4$

$[\alpha]_D^{21}$ +38.7 (*c* 0.10, MeOH)

UV (MeOH) λ_{max} nm (logε) 302 (3.78), 281 (3.85), 216 (4.23)

IR (neat) ν_{max} 2919, 2850, 1594, 1509, 1459 cm^{-1}

HRMS (ESI-TOF) *m/z* 342.1714 $[M+H]^+$ (calcd. for $C_{20}H_{24}NO_4$, 342.1700)

^1H NMR (CD_3OD, 400 MHz) : See Table 4

^{13}C NMR (CD_3OD, 100 MHz) : See Table 5

N-Nornuciferine (**9**)

Yellowish amorphous powder

$C_{18}H_{19}NO_2$

$[\alpha]_D^{21}$ +4.9 (*c* 0.10, MeOH)

UV (MeOH) λ_{max} nm (logε) 269 (4.17), 236 (4.22)

IR (neat) ν_{max} 2935, 1654, 1594, 1482, 1463 cm^{-1}

HRMS (ESI-TOF) *m/z* 282.1500 $[M+H]^+$ (calcd. for $C_{18}H_{20}NO_2$, 282.1489)

^1H NMR (CD_3OD, 400 MHz) : See Table 4

^{13}C NMR (CD_3OD, 100 MHz) : See Table 5

Asimilobine (**10**)

Yellowish amorphous powder

$C_{17}H_{17}NO_2$

$[\alpha]_D^{21}$ -92.0 (*c* 0.10, MeOH)

UV (MeOH) λ_{max} nm (logε) 272 (4.06)

IR (neat) ν_{max} 2934, 2836, 1588 cm^{-1}

HRMS (ESI-TOF) *m/z* 268.1333 $[M+H]^+$ (calcd. for $C_{17}H_{18}NO_2$, 268.1332)

^1H NMR (CD_3OD, 300 MHz) : See Table 4

^{13}C NMR (CD_3OD, 75 MHz) : See Table 5

Laurotetanine (**11**)

Brown amorphous powder

$C_{19}H_{21}NO_4$

$[\alpha]_D^{21}$ +33.5 (*c* 0.10, MeOH)

UV (MeOH) λ_{max} nm (logε) 303 (3.82), 281 (3.92), 216 (4.26)

IR (neat) ν_{max} 2932, 1589, 1509, 1249 cm^{-1}

HRMS (ESI-TOF) *m/z* 328.1551 $[M+H]^+$ (calcd. for $C_{19}H_{22}NO_4$, 328.1543)

^1H NMR (CD_3OD, 800 MHz) : See Table 4

^{13}C NMR (CD_3OD, 200 MHz) : See Table 5

Norisoboldine (**12**)

Brown amorphous powder

$C_{18}H_{19}NO_4$

$[\alpha]_D^{21}$ +53.8 (*c* 0.10, MeOH)

UV (MeOH) λ_{max} nm (logε) 307 (3.54), 281 (3.60)

IR (neat) ν_{max} 3324, 2922, 1595, 1032 cm^{-1}

HRMS (ESI-TOF) *m/z* 314.1385 $[M+H]^+$ (calcd. for $C_{18}H_{20}NO_4$, 314.1387)

^1H NMR (CD_3OD, 500 MHz) : See Table 4

^{13}C NMR (CD_3OD, 125 MHz) : See Table 5

Table 4. ^{13}C NMR spectroscopic data of compounds **6-12**.

	6[a]	**7**[b]	**8**[a]	**9**[a]	**10**[b]	**11**[c]	**12**[d]
1	146.1	143.5	146.1	147.3	146.0	147.2	143.7
1a	128.0	121.2	128.4	127.8	127.6	128.8	120.9
1b	123.0	122.1	124.7	123.3	122.8	128.5	126.9
2	152.2	149.5	154.4	155.1	152.2	155.8	155.8
3	116.3	109.9	111.8	113.0	116.6	112.7	110.2
3a	128.1	122.8	128.6	127.7	128.1	129.0	121.8
4	27.2	27.2	28.2	26.5	26.6	27.5	26.2
5	53.8	54.0	53.9	42.7	42.8	43.5	42.8
6a	63.6	64.0	63.8	54.4	54.4	55.3	54.8
7	33.8	33.0	33.6	35.1	35.4	35.3	34.3
7a	135.0	127.5	129.2	134.5	134.7	124.9	131.4
8	129.1	115.8	116.0	128.8	128.8	116.7	115.7
9	129.0	146.8	147.6	129.3	129.2	148.6	147.8
10	128.8	147.6	148.1	129.2	129.1	149.0	149.8
11	129.4	114.0	113.3	129.7	129.2	114.1	114.3
11a	132.9	125.0	124.2	132.7	132.9	130.0	125.1
1-OCH_3	60.5		60.5	60.7	60.5	61.3	
2-OCH3		56.6	56.4	56.5		57.2	56.5
9-OCH3							
10-OCH_3		56.5	56.6			57.4	56.7
NCH_3	41.8	41.7	42.6				

In CD_3OD, ^{13}C NMR data were measured at [a]100 MHz, [b]75 MHz, [c]200 MHz and [d]125 MHz, respectively.

Table 5. ^{1}H NMR spectroscopic data (*J* in Hz) of compounds **6-12**.

	6[a]	**7**[b]	**8**[a]	**9**[a]	**10**[b]	**11**[c]	**12**[d]
1							
1a							
1b							
2							
3	6.71 s	6.71 s	6.74 s	6.90 s	6.72 s	6.69 s	6.75 s
3a							
4	3.24 m	3.23 m	3.20 m	3.23 m	3.14 m	3.04 m	3.21 m
	2.90 d (13.1)	2.92 m	2.81 m	2.94 m	2.93 m	2.78 m	2.99 m
5	3.56 m	3.55 m	3.34 m	3.63 m	3.64 m	3.37 m	3.70 m
	3.22 m	3.22 m	2.88 m	3.26 m	3.28 m	3.04 m	3.34 m
6a	3.87 m	3.90 m	3.46 m	4.24 m	4.14 dd (4.4, 13.8)	3.78 dd (13.6, 4.4)	4.25 m
7	3.33 m	3.22 m	3.10 dd (3.6, 13.4)	3.02 m	3.02 dd (4.4, 13.7)	2.64 m	2.91 m
	2.82 t (13.7)	3.18 m	2.57 dd (13.4, 13.8)	2.89 m	2.88 dd (13.8, 13.7)	2.73 m	2.84 m
7a							
8	7.35 m	6.76 s	6.76 s	7.30 m	7.30 m	6.73 s	6.75 s
9	7.27 ddd (7.3, 7.3, 1.1)			7.28 m	7.27 m		
10	7.34 m			7.35 m	7.35 m		
11	8.34 dd (7.9, 1.1)	8.12 s	7.97 s	8.33 d (8.0)	8.35 d (8.1)	8.02 s	8.17 s
11a							
1-OCH_3	3.57 s		3.64 s	3.65 s	3.58 s	3.90 s	
2-OCH3		3.90 s	3.86 s	3.89 s		3.66 s	3.88 s
9-OCH3							
10-OCH_3		3.86 s	3.87 s			3.91 s	3.92 s
NCH_3	2.97 s	2.97 s	2.77 s				

In CD_3OD, ^{1}H NMR data were measured at [a]400 MHz, [b]300 MHz, [c]800 and [d]500 MHz, respectively.

(*S*)-Reticuline (**13**)

Brown syrup

$C_{19}H_{23}NO_4$

$[\alpha]_D^{21}$ +7.6 (*c* 0.10, MeOH)

UV (MeOH) λ_{max} nm (logε) 283 (3.74)

IR (neat) ν_{max} 3342, 2935, 2857, 1513, 1275 cm^{-1}

HRMS (ESI-TOF) *m/z* 330.1698 $[M+H]^+$ (calcd. for $C_{19}H_{24}NO_4$, 330.1700)

^{1}H NMR (CD_3OD, 600 MHz) : δ 6.88 (1H, d, *J* = 8.1 Hz, H-5′), 6.78 (1H, s, H-5), 6.67 (1H, d, *J* = 1.5 Hz, H-2′), 6.62 (1H, dd, *J* = 8.1, 1.5 Hz, H-6′), 6.23 (1H, s, H-8), 4.43 (1H, t, *J* = 6.8 Hz, H-1), 3.85 (3H, s, 6-OCH_3), 3.85 (3H, s, 4′-OCH_3), 3.64 (1H, m, H-3a), 3.28 (1H, m, H-3b), 3.20 (1H, dd, *J* = 5.5, 14.0 Hz, 1-CH_2-1′), 3.08 (1H, dd, *J* = 7.1, 10.4 Hz, H-4a), 3.03 (1H, dd, *J* = 7.6, 14.0 Hz, 1-CH_2-1′), 2.99 (1H, m, H-4b) 2.86 (3H, s, NCH_3)

^{13}C NMR (CD_3OD, 150 MHz) : δ 149.4 (C-6), 148.6 (C-3′), 148.0 (C-4′), 146.5 (C-7), 129.5 (C-1′), 124.3 (C-8a), 122.1 (C-4a), 121.9 (C-6′), 117.5 (C-2′), 115.5 (C-8), 113.0 (C-5′), 112.6 (C-5), 66.1 (C-1), 56.4 (6-OCH_3), 56.4 (4′-OCH_3), 47.1 (C-3), 41.0 (NCH_3), 40.9 (1-CH_2-1′), 23.4 (C-4)

Houttuycorine (**14**)

Yellowish amorphous powder

$C_{16}H_{14}N_2O_3$

$[\alpha]_D^{21}$ -13.3 (*c* 0.30, MeOH)

UV (MeOH) λ_{max} nm (logε) 290 (3.76), 252 (3.89), 236 (4.00), 212 (4.05)

IR (neat) ν_{max} 3308, 1630, 1604, 1425, 1363, 1157 cm^{-1}

HRMS (ESI-TOF) *m/z* 283.1093 $[M+H]^+$ (calcd. for $C_{16}H_{15}N_2O_3$, 283.1077)

^1H NMR (DMSO-d_6, 800 MHz) : See Table 6

^{13}C NMR (DMSO-d_6, 200 MHz) : See Table 6

Perlolyrine (**15**)

Yellowish amorphous powder

$C_{16}H_{12}N_2O_2$

$[\alpha]_D^{21}$ -62.6 (*c* 0.10, MeOH)

UV (MeOH) λ_{max} nm (logε) 386 (3.68), 287 (3.92), 218 (4.33)

IR (neat) ν_{max} 3360, 1723, 1317, 1129 cm^{-1}

HRMS (ESI-TOF) *m/z* 265.0975 $[M+H]^+$ (calcd. for $C_{16}H_{13}N_2O_2$, 265.0972)

^1H NMR (CD_3OD, 300 MHz) : See Table 6

^{13}C NMR (CD_3OD, 75 MHz) : See Table 6

Table 6. ^{1}H and ^{13}C NMR spectroscopic data of compounds **14** and **15**.

	14[a]		**15**[b]	
No.	δ_C	δ_H (*J* in Hz)	δ_C	δ_H (*J* in Hz)
1	142.9		134.2	
3	137.0	8.33 d (5.2)	138.4	8.28 d (4.9)
4	114.5	8.10 d (5.2)	114.9	8.02 d (4.9)
4a	128.9		132.3	
4b	120.2		122.1	
5	121.4	8.22 d (7.9)	122.6	8.18 d (7.9)
6	119.1	7.23 t (7.6)	121.2	7.29 t (7.5)
7	128.2	7.55 t (7.6)	130.0	7.58 t (7.5)
8	112.2	7.70 d (7.9)	113.3	7.71 d (8.3)
8a	140.3		143.1	
9a	132.9		132.5	
1′	37.2	2.30 dd (4.7, 12.8)		
		1.92 dd (11.6, 12.8)		
2′	64.9	3.99 dd (4.7, 11.6)	154.0	
3′	67.0	3.79 brs	111.0	6.60 d (3.0)
4′	102.6		111.1	7.23 d (3.0)
5′	64.8	4.09 d (12.1)		
		3.88 d (12.1)	157.3	
6′			57.1	4.80 s
NH		10.84 s		
OH		2.98 s		

[a]In DMSO-d_6, ^{1}H (800 MHz) and ^{13}C (200 MHz) NMR data were measured.

[b]In CD_3OD, ^{1}H (300 MHz) and ^{13}C (75 MHz) NMR data were measured.

Indole-3-carboxylic acid (**16**)

Yellowish amorphous powder

$C_9H_7NO_2$

$[\alpha]_D^{21}$ -40.6 (*c* 0.10, MeOH)

UV (MeOH) λ_{max} nm (logε) 280 (3.92), 212 (4.39)

IR (neat) ν_{max} 3301, 1660, 1533, 1441, 1190 cm^{-1}

HRMS (ESI-TOF) *m/z* 162.0553 $[M+H]^+$ (calcd. for $C_9H_8NO_2$, 162.0550)

^1H NMR (CD_3OD, 400 MHz) : δ 8.06 (1H, m, H-4), 7.93 (1H, s, H-2), 7.42 (1H, m, H-7), 7.18 (1H, m, H-6), 7.17 (1H, m, H-5)

^{13}C NMR (CD_3OD, 100 MHz) : δ 170.0 (COOH), 139.0 (C-9), 134.2 (C-2), 128.4 (C-8), 124.4 (C-4), 123.2 (C-6), 122.8 (C-7), 113.7 (C-7), 109.6 (C-3)

Nicotinamide (**17**)

Yellowish amorphous powder

$C_6H_6N_2O$

$[\alpha]_D^{21}$ –66.7 (*c* 0.05, MeOH)

UV (MeOH) λ_{max} nm (logε) 279 (3.19), 264 (4.23)

IR (neat) ν_{max} 3363, 3283, 2938, 2359, 1680, 1054, 1032 cm^{-1}

HRMS (ESI-TOF) *m/z* 123.0559 $[M+H]^+$ (calcd. for $C_6H_7N_2O$, 123.0553)

^1H NMR (CD_3OD, 600 MHz) : δ 9.03 (1H, brs, H-2), 8.69 (1H, brs, H-6), 8.28 (1H, d, *J* = 7.9 Hz, H-4), 7.53 (1H, dd, *J* = 4.5, 7.9 Hz, H-5)

^{13}C NMR (CD_3OD, 125 MHz) : δ 169.8 (C=O), 152.8 (C-6), 149.5 (C-2), 137.3 (C-4), 131.4 (C-3), 125.1 (C-5)

4-(1*H*)-Quinolinone (**18**)

Colorless syrup

C_9H_7NO

$[\alpha]_D^{21}$ +4.6 (*c* 0.10, MeOH)

UV (MeOH) λ_{max} nm (logε) 330 (3.67), 317 (4.64), 233 (3.85), 210 (3.95)

IR (neat) ν_{max} 3333, 2972, 1614, 1516, 1056 cm^{-1}

HRMS (ESI-TOF) *m/z* 146.0604 $[M+H]^+$ (calcd. for C_9H_8NO, 146.0600)

^{1}H NMR (CD_3OD, 300 MHz) : δ 8.26 (1H, dd, *J* = 1.4, 8.2 Hz, H-5), 7.98 (1H, d, *J* = 7.4 Hz, H-2), 7.70 (1H, m, H-7), 7.58 (1H, d, *J* = 8.2 Hz, H-8), 7.43 (1H, m, H-6), 6.34 (1H, d, *J* = 7.4 Hz, H-3)

^{13}C NMR (CD_3OD, 75 MHz) : δ 180.8 (C-4), 141.5 (C-9), 141.4 (C-2), 133.6 (C-7), 126.7 (C-10), 126.1 (C-5), 125.3 (C-6), 119.4 (C-8), 109.8 (C-3)

Adenosine (**19**)

White amorphous powder

$C_{10}H_{13}N_5O_4$

$[\alpha]_D^{21}$ -31.3 (*c* 0.10, MeOH)

UV (MeOH) λ_{max} nm (logε) 260 (3.84)

IR (neat) ν_{max} 3335, 2937, 1647, 1603, 1081 cm^{-1}

HRMS (ESI-TOF) *m/z* 266.0879 $[M-H]^-$ (calcd. for $C_{10}H_{12}N_5O_4$, 266.0895)

^1H NMR (DMSO-d_6, 400 MHz) : See Table 7

^{13}C NMR (DMSO-d_6, 100 MHz) : See Table 7

5′-Deoxy-5′-methylsulfinyladenosine (**20**)

White amorphous powder

$C_{11}H_{15}N_5O_4S$

$[\alpha]_D^{21}$ -19.4 (*c* 0.10, MeOH)

UV (MeOH) λ_{max} nm (logε) 260 (4.06)

IR (neat) ν_{max} 3332, 1647, 1601, 1338, 1026 cm^{-1}

ESI-MS *m/z* 314.1 $[M+H]^+$

^1H NMR (DMSO-d_6, 400 MHz) : See Table 7

^{13}C NMR (DMSO-d_6, 100 MHz) : See Table 7

Table 7. ^{1}H and ^{13}C NMR spectroscopic data of compounds **19** and **20**

	19		**20**	
No.	δ_C	δ_H (*J* in Hz)	δ_C	δ_H (*J* in Hz)
2	152.4	8.14 s	152.6	8.15 s
4	149.1		149.2	
5	119.3		119.3	
6	156.2		156.1	
8	139.9	8.34 s	140.2	8.35 s
1′	87.9	5.88 d (6.1)	88.1	5.92 d (5.1)
2′	73.4	4.61 t (6.1)	72.7	4.75 t (5.1)
3′	85.9	3.96 dd (3.1, 6.1)	77.9	4.25 m
4′	70.6	4.14 m	73.2	4.26 m
5′	61.7	3.67 dd (3.5, 12.1)	57.6	3.30 dd (10.1, 13.0)
		3.55 dd (3.1, 12.1)		3.08 dd (2.8, 13.0)
NH_2		7.32 s		7.28 s
CH_3			39.0	2.56 s

In DMSO-d_6, ^{1}H (400 MHz) and ^{13}C (100 MHz) NMR data were measured.

Uridine (**21**)

White amorphous powder

$C_9H_{12}N_2O_6$

$[\alpha]_D^{21}$ -1.0 (*c* 0.10, MeOH)

UV (MeOH) λ_{max} nm (logε) 263 (3.41)

IR (neat) ν_{max} 3305, 1688, 1599, 1057 cm^{-1}

ESI-MS *m/z* 245.1 $[M+H]^+$

^{1}H NMR (CD_3OD, 300 MHz) : δ 8.00 (1H, d, *J* = 8.1 Hz, H-4), 5.89 (1H, d, *J* = 4.6 Hz, H-1′), 5.68 (1H, d, *J* = 8.1 Hz, H-5), 4.15 (1H, m, H-2′), 4.13 (1H, m, H-3′), 3.99 (1H, m, H-4′), 3.84 (1H, dd, *J* = 2.7, 12.2 Hz, H-5′a), 3.55 (1H, dd, *J* = 3.2, 12.2 Hz, H-5′b)

^{13}C NMR (CD_3OD, 75 MHz) : δ 167.0 (C-6), 153.2 (C-2), 143.5 (C-4), 103.4 (C-5), 91.4 (C-1′), 87.1 (C-4′), 76.5 (C-2′), 72.1 (C-3′), 63.1 (C-5′)

2.2.2. Further isolation of constituents of *H. cordata*

The BuOH residue (253.1 g) was fractionated by Diaion HP-20 chromatography eluting stepwise with 20%, 40%, 60%, 80% and 100% aq. MeOH to yield 5 fractions (B1-5). A portion of fraction B2 (13.0 g) was subjected to silica gel chromatography eluting with $CHCl_3$/MeOH (15:1→0:1, step-gradient system) to give 13 fractions (B2a-B2m). B2e (645.0 mg) was separated into 10 fractions (B2e01-B2e10) on silica gel MPLC (80 g) eluting with $CHCl_3$/MeOH (12:1→0:1, step-gradient system). From B2e06, compound **46** (4.2 mg) was purified using an Inno column with the isocratic solvent of 30% aq. MeOH. B2e08 was fractionated using a Sephadex LH-20 (MeOH), followed by Luna 5u column (30% aq. MeOH) to give compound **32** (15.9 mg). From B2e09, compounds **19** (520.0 mg) and **31** (36.0 mg) were purified using a Hypersil GOLD column with the isocratic solvent of 20% aq. MeCN. B2g (1.03 g) was separated into 11 subfractions (B2g01-11) on an RP-MPLC column (120 g) eluting with aq. MeOH (5%→100%, step-gradient system). B2g03 (121.8 mg) was further fractionated by Sephadex LH-20 (50% aq. MeOH) and gave 4 subfractions (B2g03A-D). B2g03B was subsequently purified using an Inno HPLC column (10% aq. MeOH) to afford compounds **20** (4.2 mg) and **47** (5.3 mg). HPLC purification (Luna 5u, 17% aq. MeOH) of B2g04 (103.4 mg) furnished compound **45** (35.6 mg). B2k (816.8 mg) was subjected to an RP-MPLC (120 g) eluting with aq. MeOH (5%→100%, step-gradient system) to yield 8 fractions (B2k1-8). B2k2 (54.6 mg) was again subjected to an RP-MPLC this time eluting stepwise with aq. MeOH (10%→100%) to yield 8 fractions (B2k2a-h). From B2k2g, compounds **36** (93.7 mg) and **38** (201.6 mg) were isolated by HPLC

separation (Hypersil GOLD, 12% aq. MeCN).

B3 (16.6 g) was subjected to a silica gel chromatography eluting with $CHCl_3$/MeOH/ Water (70:5:1→0:1:0, step-gradient system) to yield 20 fractions (B3a-t) and compound **29** (220.0 mg). From B3m (378.7 mg), compound **56** (5.9 mg) was isolated by HPLC separation (Hypersil GOLD, 30% MeOH). B3o (892.9 mg) was subjected to silica MPLC column (80 g) eluting stepwise with $CHCl_3$/MeOH (10:1→0:1) and gave compounds **37** (5.5 mg) and **39** (3.5 mg). B3p (911.2 mg) was fractionated on two separate occasions using silica gel MPLC eluting with $CHCl_3$/MeOH (20:1→0:1, step-gradient system and 5:1, isocratic system, respectively) and further purified on Hypersil GOLD column to give compound **28** (17.0 mg, 18% aq. MeCN).

B4 (5.0 g) was subjected to an RP-MPLC (120 g) eluting with aq. MeOH (25%→100%, step-gradient system) to yield 15 fractions (B4a-o). B4g (323.4 mg) was fractionated using Sephadex LH-20 with MeOH, followed by Luna 5u HPLC (24% aq. MeOH) to give compounds **2** (1.0 mg) and **48** (19.1 mg). B4i (228.1 mg) was separated into 7 fractions (B4i1-7) on a Sephadex LH-20 eluting MeOH. From B4i2, compound **33** (2.6 mg) was isolated by HPLC separation (Luna 5u, 45% aq. MeOH).

The alkaloid-rich fractions B5A (1.71 g) was separated into 9 fractions (B5A1-9) on a silica MPLC column (80 g) eluting stepwise with $CHCl_3$/MeOH (50:1→0:1). B5A5 (300.8 mg) was subjected to an RP-MPLC column (80 g) and gave 15 fractions (B5A5a-o). B5A5e (20.0 mg) was further purified on a Luna column (40% aq. MeCN) to yield compounds **3** (15.0 mg) and **44** (5.0 mg). From B5A5h,

compound **49** (2.0 mg) was purified using an Inno column with the isocartic solvent of 25% MeCN.

A portion of BuOH fraction was subjected to silica gel chromatography eluting with $CHCl_3$/MeOH (50:1→0:1, step-gradient system) to give 18 fractions (BN01-BN18). BN12 was fractionated using silica gel MPLC eluting with $CHCl_3$/MeOH (20:1→0:1, step-gradient system), followed by Luna 5u HPLC (45% aq. MeOH) to give compound **43** (26.0 mg).

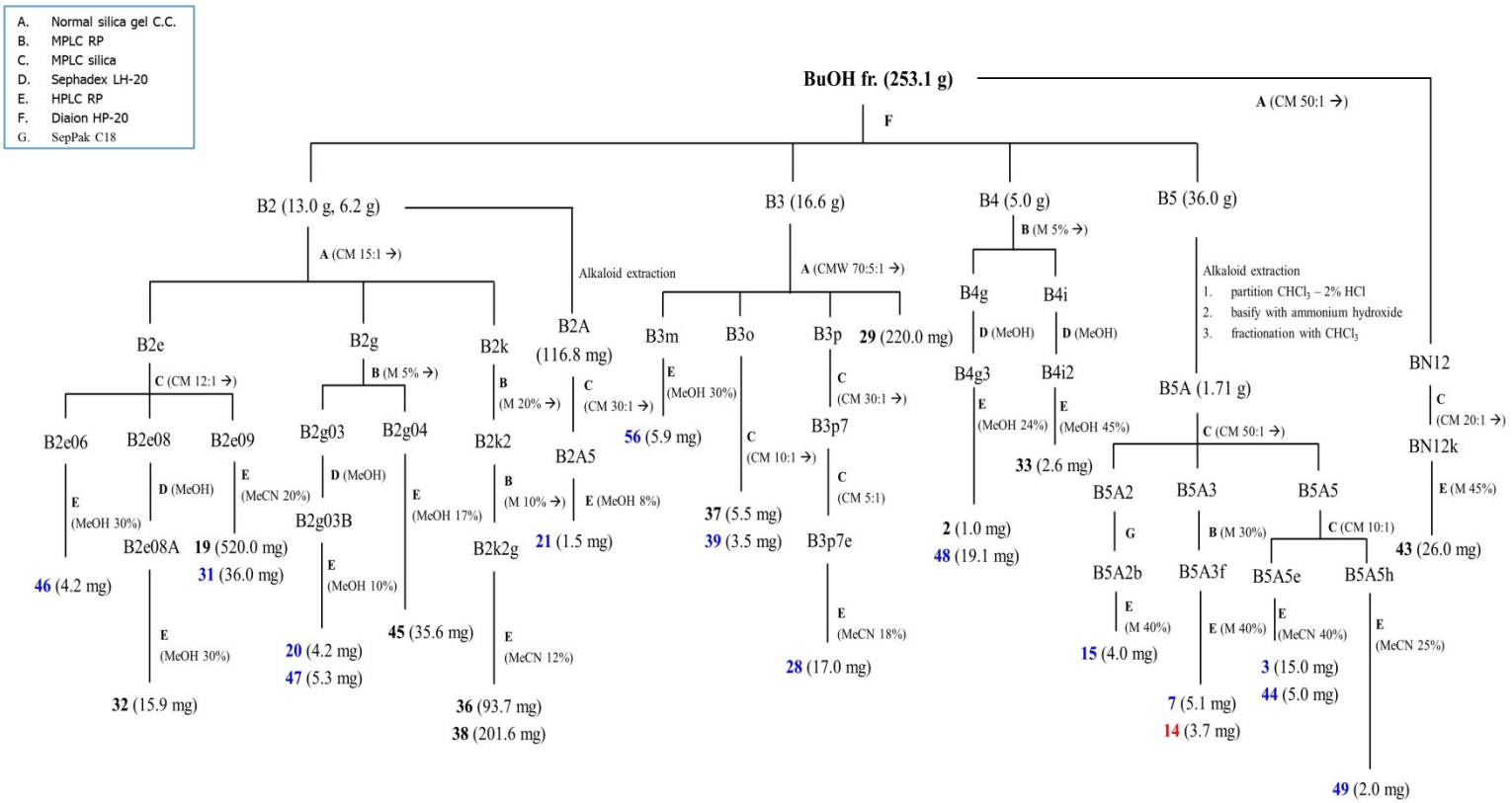

Scheme 5. Isolation of constituents from *H. cordata* (1).

The ethyl acetate residue (32.2 g) was fractionated by chromatography eluting with $CHCl_3$/MeOH (20:1→0:1, step-gradient system) to give 10 fractions (E01-12) with compounds **25** (2.0 g) and **26** (13.6 g). E04 (668.6 g) was subjected to Sephadex LH-20 eluting with MeOH to yield 9 fractions (E04a-i). From E04d (116.9 mg), compounds **1** (11.6 mg), **4** (18.3 mg) and **40** (33.0 mg) were purified by a Luna 5u column (25% aq. MeCN). E04e (98.1 mg) was chromatographed on an RP-MPLC (120 g), yielding compound **35** (12.3 mg). HPLC purification (Luna 5u, 40% aq. MeCN) of E04h (17.6 mg) furnished compounds **5** (4.0 mg) and **24** (3.1 mg). E05 (813.5 mg) was subjected to an RP-MPLC using a aq. MeOH step-gradient system (20%→100%), giving 18 fractions (E05a-r). From E05f (26.0 mg), compound **34** (9.0 mg) was purified by a Hypersil GOLD colunm (40% aq. MeOH). E05o (89.4 mg) was further purified on Luna 5u column (23% aq. MeCN) to give compounds **22** (2.0 mg) and **23** (14.0 mg). E11 (5.8 g) was fractionated using silica MPLC with $CHCl_3$/MeOH (20:1→0:1, step-gradient system), followed by Hypersil GOLD column (35% aq. MeOH) to give compound **27** (200.0 mg).

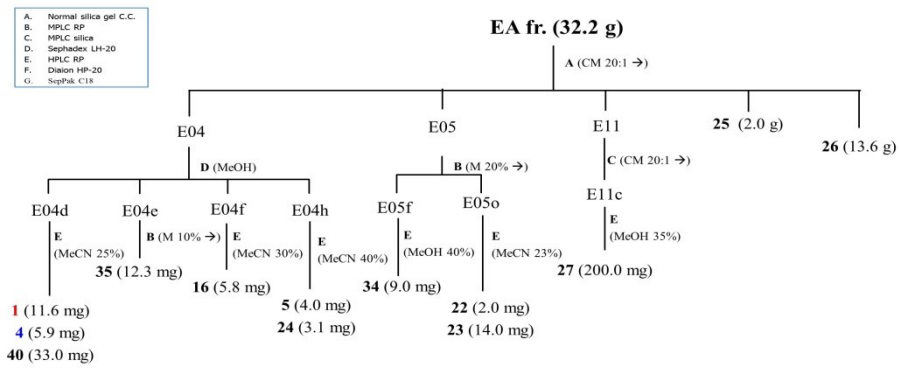

Scheme 6. Isolation of constituents from *H. cordata* (2).

Silica gel MPLC (120 g) for 1A (3.79 g) and 3A (1.12 g) were performed using step-gradient elution with $CHCl_3$/MeOH (100:1→0:1) to give 15 fractions (1A01-1A15) and 12 fractions (3A01-3A12), respectively. Compound **42** (4.7 mg) was obtained from 1A08 (27.6 mg) using a Luna 5u column (25% aq. MeOH). From 1A09 (33.4 mg), compounds **17** (29.6 mg) and **41** (2.3 mg) were isolated by HPLC separation (Inno column, 25% aq. MeOH). Fraction 3A11 (79.6 mg) was further purified on an Inno column (40% aq. MeOH) to give compounds **12** (2.4 mg) and **30** (13.5 mg).

The other total extract (0.9 kg) was suspended in H_2O, and then partitioned with $CHCl_3$. After removal of the solvent *in vacuo*, the chlorophylls were removed using HP-20 resin eluting with 90% aqueous MeOH. The chloroform fraction (85.2 g) was fractionated by silica column chromatography eluting stepwise with $CHCl_3$/MeOH (50:1→0:1) to give 15 fractions. C09 (2.5 g) was fractionated using an RP-MPLC with aq. MeOH step-gradient system (40%→100%), followed by

Luna 5u prep-column (70% aq. MeCN) to give compound **58** (163.6 mg). RP-MPLC (40 g) for C11 (1.1 g) was performed using step-gradient elution with aq. MeOH (30%→100%) to give 25 fractions (C11a-y) and compound **59** (13.6 mg). From C11b (21.4 mg), compound **57** (5.8 mg) was isolated by HPLC separation (Inno column, 20% aq. MeCN). Compound **53** (2.7 mg) was obtained from C11g (12.5 mg) using an Inno column (20% aq. MeCN). Fraction C11i (8.9 mg) was further purified on a Luna 5u column to give compounds **54** (2.0 mg) and **55** (2.1 mg). From C11k (75.2 mg), compounds **50** (3.0 mg), **51** (13.6 mg) and **52** (4.9 mg) were isolated by HPLC separation (Luna 5u, 25% aq. MeCN).

All water and solvents used for HPLC were 0.05% formic acid buffer. The common flow rate for semi-prep HPLC column, prep HPLC column and MPLC chromatography was 2, 4 and 40 ml/min, respectively.

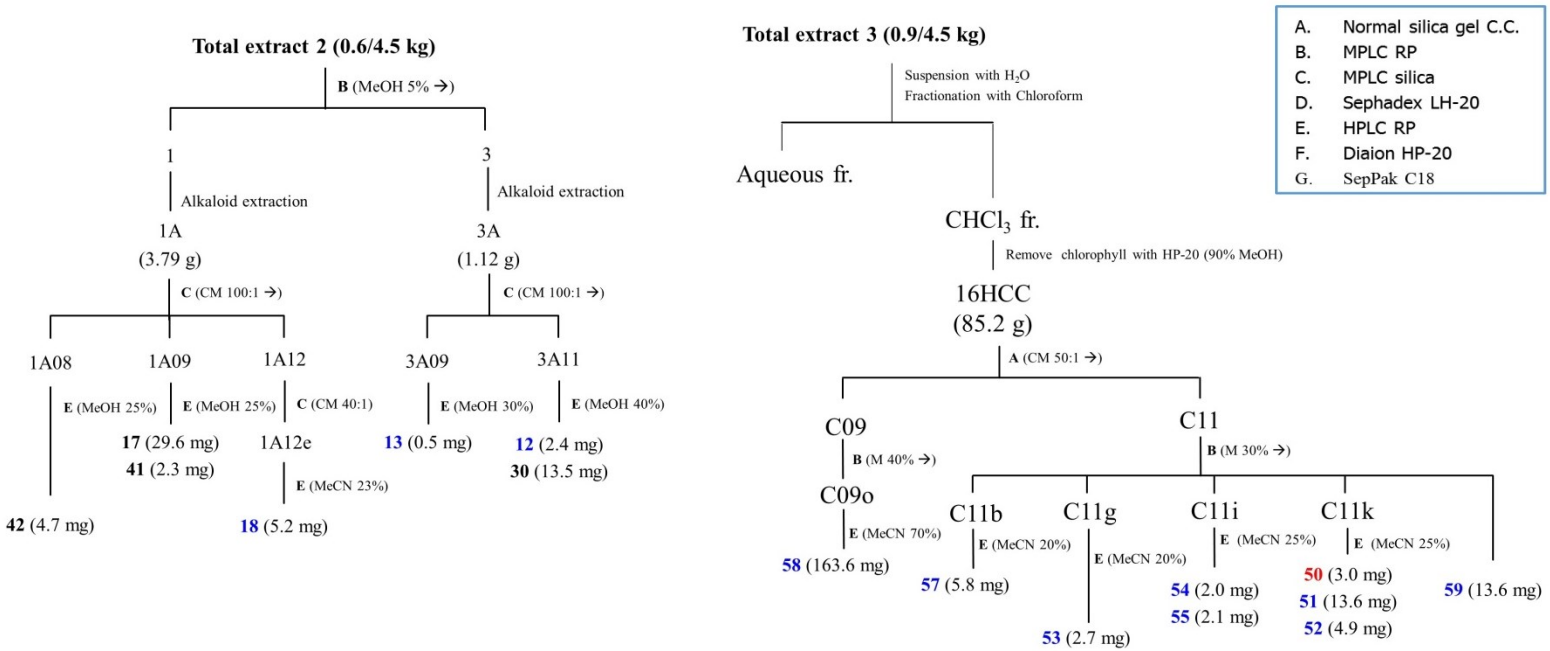

Scheme 7. Isolation of constituents from *H. cordata* (3)

Luteolin (**22**)

Yellowish amorphous powder

$C_{15}H_{10}O_6$

$[\alpha]_D^{21}$ -19.6 (*c* 0.10, MeOH)

UV (MeOH) λ_{max} nm (logε) 349 (3.76), 255 (3.78)

IR (neat) ν_{max} 2971, 1604, 1055, 1032 cm^{-1}

ESI-MS *m/z* 287.3 $[M+H]^+$

^1H NMR (DMSO-d_6, 300 MHz) : See Table 8

^{13}C NMR (DMSO-d_6, 75 MHz) : See Table 9

Quercetin (**23**)

Yellowish amorphous powder

$C_{15}H_{10}O_7$

$[\alpha]_D^{21}$ -65.6 (*c* 0.10, MeOH)

UV (MeOH) λ_{max} nm (logε) 368 (3.76), 295 (3.88), 256 (3.86)

IR (neat) ν_{max} 3384, 2970, 1642, 16604, 1163 cm^{-1}

ESI-MS *m/z* 301.0 $[M-H]^-$

^1H NMR (DMSO-d_6, 300 MHz) : See Table 8

^{13}C NMR (DMSO-d_6, 75 MHz) : See Table 9

Apigenin (**24**)

Yellowish amorphous powder

$C_{15}H_{10}O_5$

$[\alpha]_D^{21}$ -59.5 (*c* 0.10, MeOH)

UV (MeOH) λ_{max} nm (logε) 335 (3.81), 268 (3.79)

IR (neat) ν_{max} 2924, 1607, 1506, 1032 cm^{-1}

ESI-MS *m/z* 269.1 $[M-H]^-$

^1H NMR (DMSO-d_6, 400 MHz) : See Table 8

^{13}C NMR (DMSO-d_6, 100 MHz) : See Table 9

Afzelin (**25**)

Yellowish amorphous powder

$C_{21}H_{20}O_{10}$

$[\alpha]_D^{21}$ -141.4 (*c* 0.10, MeOH)

UV (MeOH) λ_{max} nm (logε) 342 (3.92), 265 (4.09)

IR (neat) ν_{max} 3385, 1657, 1609, 1361, 1176 cm^{-1}

ESI-MS *m/z* 432.8 $[M+H]^+$

^1H NMR (CD_3OD, 300 MHz) : See Table 8

^{13}C NMR (CD_3OD, 100 MHz) : See Table 9

Quercitrin (**26**)

Yellowish amorphous powder

$C_{21}H_{20}O_{11}$

$[\alpha]_D^{21}$ -154.3 (*c* 0.10, MeOH)

UV (MeOH) λ_{max} nm (logε) 350 (4.10), 256 (4.23)

IR (neat) ν_{max} 3393, 1657, 1608, 1360, 1201 cm^{-1}

ESI-MS *m/z* 448.9 $[M+H]^+$

^1H NMR (CD_3OD, 400 MHz) : See Table 8

^{13}C NMR (CD_3OD, 100 MHz) : See Table 9

Hyperoside (**27**)

Yellowish amorphous powder

$C_{21}H_{20}O_{12}$

$[\alpha]_D^{21}$ -72.4 (*c* 0.10, MeOH)

UV (MeOH) λ_{max} nm (logε) 360 (4.09), 257 (4.17)

IR (neat) ν_{max} 3287, 1657, 1606, 1360, 1202 cm^{-1}

ESI-MS *m/z* 465.0 $[M+H]^+$

^1H NMR (DMSO-d_6, 300 MHz) : See Table 8

^{13}C NMR (DMSO-d_6, 75 MHz) : See Table 9

Kaempferol-3-*O*-*α*-L-rhamnopyranosyl-7-*O*-*β*-D-glucopyranoside (**28**)

Yellowish amorphous powder

$C_{27}H_{30}O_{15}$

$[\alpha]_D^{21}$ -165.2 (*c* 0.10, MeOH)

UV (MeOH) λ_{max} nm (logε) 339 (4.05), 266 (4.15)

IR (neat) ν_{max} 3369, 1603, 1360, 1059, 1032 cm^{-1}

ESI-MS *m/z* 595.1 $[M+H]^+$

^1H NMR (DMSO-d_6, 400 MHz) : See Table 8

^{13}C NMR (DMSO-d_6, 75 MHz) : See Table 9

Quercetin-3-*O*-*α*-L-rhamnopyranosyl-7-*O*-*β*-D-glucopyranoside (**29**)

Yellowish amorphous powder

$C_{27}H_{30}O_{16}$

$[\alpha]_D^{21}$ -193.3 (*c* 0.10, MeOH)

UV (MeOH) λ_{max} nm (logε) 351 (4.03), 257 (4.19)

IR (neat) ν_{max} 3395, 1659, 1602, 1074 cm^{-1}

ESI-MS *m/z* 611.1 $[M+H]^+$

^1H NMR (DMSO-d_6, 300 MHz) : See Table 8

^{13}C NMR (DMSO-d_6, 75 MHz) : See Table 9

Table 8. ^{13}C NMR spectroscopic data of compounds **22-29**.

	22[a]	**23**[a]	**24**[b]	**25**[c]	**26**[d]	**27**[a]	**28**[b]	**29**[a]
2	161.4	146.6	164.5	159.4	159.3	156.3	157.8	157.4
3	102.7	135.9	102.7	137.0	136.2	133.5	134.4	134.4
4	181.5	175.8	181.6	180.4	179.6	177.4	177.9	177.9
5	163.8	160.6	161.2	162.4	163.2	161.2	160.9	105.7
6	98.9	98.3	98.9	100.6	122.9	98.7	99.4	99.3
7	164.5	164.3	163.6	166.7	165.8	164.1	162.9	162.9
8	93.8	93.4	94.0	95.6	94.7	93.4	94.7	94.5
9	157.4	156.1	157.3	160.1	158.5	156.2	156.1	160.9
10	103.2	102.9	103.4	106.7	105.9	103.9	105.8	156.0
1′	121.2	121.9	121.1	123.4	123.0	121.0	120.3	120.4
2′	113.2	114.9	128.4	132.7	117.0	115.1	130.7	115.7
3′	145.8	145.1	115.9	117.3	146.4	144.8	115.4	145.2
4′	150.0	147.7	161.4	164.0	149.9	148.4	160.2	148.6
5′	116.0	115.6	115.9	117.3	116.4	115.9	115.4	115.4
6′	118.9	119.9	128.4	132.7	122.9	122.0	130.7	121.1
				Rha	Rha	Gal	Rha	Rha
1″				104.3	103.5	101.8	101.8	101.8
2″				72.9	72.1	71.2	70.4	70.3
3″				72.8	72.0	73.1	70.7	70.6
4″				74.0	73.3	67.9	71.1	71.1
5″				72.7	71.9	75.8	70.1	70.0
6″				18.4	17.6	60.1	17.5	17.5
							Glc	Glc
1‴							99.9	99.8
2‴							73.1	73.1
3‴							76.4	76.3
4‴							69.6	69.5
5‴							77.2	77.1
6‴							60.6	60.6

In DMSO-d_6, ^{13}C NMR data were measured at [a]75 MHz and [b]100 MHz, respectively.

In CD_3OD, ^{13}C NMR data were measured at [c]75 MHz and [d]100 MHz, respectively.

Table 9. ^{1}H NMR spectroscopic data (*J* in Hz) of compounds **22-29**.

	22[a]	**23**[a]	**24**[b]	**25**[c]	**26**[d]	**27**[a]	**28**[b]	**29**[a]
2								
3	6.64 s		6.75 s					
4								
5								
6	6.16 brs	6.15 brs	6.17 brs	6.15 d (2.1)	6.19 d (2.0)	6.19 d (1.8)	6.45 d (2.0)	6.45 d (2.0)
7								
8	6.42 brs	6.38 brs	6.46 brs	6.31 d (2.1)	6.35 d (2.0)	6.39 d (1.8)	6.78 d (2.0)	6.74 d (2.0)
9								
10								
1′								
2′	7.37 brs	7.60 brs	7.91 d (8.2)	7.73 dt (8.8, 2.1)	7.30 d (1.9)	7.51 d (2.2)	7.77 d (8.7)	7.32 d (2.4)
3′			6.92 d (8.2)	6.89 dt (8.8, 2.1)			6.92 d (8.7)	
4′								
5′	6.86 d (8.3)	6.86 d (7.7)	6.92 d (8.2)	6.89 dt (8.8, 2.1)	6.89 d (8.5)	6.80 d (8.4)	6.92 d (8.7)	6.88 d (8.3)
6′	7.38 d (8.3)	7.54 d (7.7)	7.91 d (8.2)	7.73 dt (8.8, 2.1)	7.29 dd (8.5, 1.9)	7.66 dd (8.4, 2.2)	7.77 d (8.7)	7.26 dd (8.3, 2.4)
				Rha	Rha	Gal	Rha	Rha
1″				5.35 d (1.6)	5.33 d (1.5)	5.36 d (7.7)	5.30 brs	5.27 d (1.3)
2″				4.21 m	4.20 m	5.36 d (7.7)	3.48 m	3.48 m
3″				3.71 m	3.74 dd (3.2, 9.6)		3.88 m	3.88 m
4″				3.33 m	3.40 m	3.15~3.63 m	3.13 m	3.13 m
5″				3.34 m	3.37 m		3.99 m	3.99 m
6″				0.91 d (6.1)	0.93 d (5.8)		0.80 d (5.7)	0.82 d (6.0)
							Glc	Glc
1‴							5.10 d (7.2)	5.07 d (7.3)
2‴							3.24 m	3.26 m
3‴							3.29 m	3.29 m
4‴							3.16 m	3.16 m
5‴							3.45 m	3.45 m
6‴							3.7, 3.44 m	3.7, 3.44 m

In DMSO-d_6, ^{1}H NMR data were measured at [a]300 MHz and [b]400 MHz, respectively.

In CD_3OD, ^{1}H NMR data were measured at [c]300 MHz and [d]400 MHz, respectively.

(3*S*, 5*R*, 6*R*, 9*R*)-Megastigman-7-ene-3,5,6,9-tetrol (**30**)

Brown amorphous powder

$C_{13}H_{24}O_4$

$[\alpha]_D^{21}$ -41.1 (*c* 0.10, MeOH)

UV (MeOH) λ_{max} nm (logε) 303 (3.26), 279 (3.31)

IR (neat) ν_{max} 3382, 2971, 1595, 1040 cm^{-1}

HRMS (ESI-TOF) *m/z* 289.1645 $[M+HCOO]^-$ (calcd. for $C_{14}H_{25}O_6$, 289.1657)

^{1}H NMR (CD_3OD, 300 MHz) : See Table 10

^{13}C NMR (CD_3OD, 75 MHz) : See Table 11

Megastigman-7-ene-3,5,6,9-tetrol-9-*O*-*β*-D-glucopyranoside (**31**)

White amorphous powder

$C_{19}H_{34}O_9$

$[\alpha]_D^{21}$ -45.8 (*c* 0.10, MeOH)

UV (MeOH) λ_{max} nm (logε) 328 (3.04), 288 (3.09)

IR (neat) ν_{max} 3398, 2941 cm^{-1}

HRMS (ESI-TOF) *m/z* 405.2134 $[M-H]^-$ (calcd. for $C_{19}H_{33}O_9$, 405.2130)

^{1}H NMR (CD_3OD, 300 MHz) : See Table 10

^{13}C NMR (CD_3OD, 75 MHz) : See Table 11

(6*S*, 9*S*)-Roseoside (**32**)

White amorphous powder

$C_{19}H_{30}O_8$

$[\alpha]_D^{21}$ +67.0 (*c* 0.10, MeOH)

UV (MeOH) λ_{max} nm (logε) 321 (3.32), 236 (3.97)

IR (neat) ν_{max} 3397, 2936, 1658 cm^{-1}

ESI-MS *m/z* 385.2 $[M-H]^-$

^1H NMR (DMSO-d_6, 300 MHz) : See Table 10

^{13}C NMR (DMSO-d_6, 75 MHz) : See Table 11

3-Oxo-*α*-ionyl-*β*-D-glucopyranoside (**33**)

White amorphous powder

$C_{19}H_{30}O_7$

$[\alpha]_D^{21}$ +0.2 (*c* 0.10, MeOH)

UV (MeOH) λ_{max} nm (logε) 237 (3.86)

IR (neat) ν_{max} 3399, 2966, 2941, 1654 cm^{-1}

HRMS (ESI-TOF) *m/z* 371.2079 $[M+H]^+$ (calcd. for $C_{19}H_{31}O_7$, 371.2064)

^1H NMR (CD_3OD, 400 MHz) : See Table 10

^{13}C NMR (CD_3OD, 100 MHz) : See Table 11

Table 10. ^{13}C NMR spectroscopic data of compounds **30-33**.

	30[a]	**31**[a]	**32**[b]	**33**[c]
1	40.7	40.6	48.6	37.9
2	46.4	46.3	49.3	49.1
3	65.3	65.3	197.3	202.8
4	45.7	45.6	125.6	126.9
5	77.8	77.9	164.0	166.6
6	78.9	78.9	77.8	57.5
7	131.2	132.9	130.3	129.6
8	136.1	134.7	133.3	139.0
9	69.6	78.8	74.6	77.7
10	24.2	21.8	20.9	21.8
11	26.2	26.2	23.0	28.3
12	27.5	27.5	24.1	28.8
13	27.1	27.6	18.9	24.5
1′		102.6	100.8	103.2
2′		75.3	73.7	76.0
3′		78.1	76.9	78.9
4′		71.8	70.0	72.3
5′		77.7	76.8	78.7
6′		62.8	61.0	63.5

[a]In CD_3OD, ^{13}C NMR data were measured at 75 MHz.

[b]In DMSO-d_6, ^{13}C NMR data were measured at 75 MHz.

[c]In CD_3OD, ^{13}C NMR data were measured at 100 MHz.

Table 11. ^{1}H NMR spectroscopic data (*J* in Hz) of compounds **30-33**.

	30[a]	**31**[a]	**32**[b]	**33**[c]
1				
2	1.65 dd (12.4, 12.4)	1.63 t (12.0)	2.43 d (16.8)	2.44 d (16.8)
	1.44 dd (3.6, 12.4)	1.43 dd (12.0, 3.1)	2.05 d (16.8)	2.08 d (16.8)
3	4.05 m	4.03 m		
4	1.73 m, 1.78 m	1.76 m	5.75 s	5.92 s
5				
6				2.72 d (9.0)
7	6.06 d (15.8)	6.09 d (15.9)	5.82 d (15.5)	5.62 dd (15.5, 8.8)
8	5.78 dd (6.1, 15.8)	5.84 dd (15.9, 7.3)	5.67 dd (15.5, 8.8)	5.82 dd (15.5, 3.9)
9	4.34 m	4.40 m	4.31 m	4.46 m
10	1.27 d (6.4)	1.31 d (6.3)	1.17 d (6.3)	1.33 d (6.3)
11	1.20 s	1.16 s	0.93 s	1.03 s
12	0.84 s	0.83 s	0.92 s	1.01 s
13	1.14 s	1.15 s	1.81 s	1.98 s
1′		4.34 d (7.7)	4.16 d (7.7)	4.40 d (7.7)
2′		3.18 m	3.13 m	3.16 m
3′		3.34 m	3.23 m	3.26 m
4′		3.23 m	3.26 m	3.29 m
5′		3.22 m	3.18 m	3.21 m
6′		3.83 dd (1.2, 11.7)	3.83 dd (2.2, 11.7)	3.86 dd (2.2, 11.7)
		3.60 dd (5.1, 11.7)	3.63 dd (5.1, 11.7)	3.66 dd (5.1, 11.7)

[a]In CD_3OD, ^{1}H NMR data were measured at 300 MHz.

[b]In DMSO-d_6, ^{1}H NMR data were measured at 300 MHz.

[c]In CD_3OD, ^{1}H NMR data were measured at 400 MHz.

4-Hydroxycinnamic acid (**34**)

White amorphous powder

$C_9H_8O_3$

$[\alpha]_D^{21}$ -10.5 (*c* 0.10, MeOH)

UV (MeOH) λ_{max} nm (logε) 309 (4.20), 225 (4.00), 209 (4.04)

IR (neat) ν_{max} 2951, 1672, 1603, 1248, 1215 cm^{-1}

ESI-MS *m/z* 162.9 $[M-H]^-$

^1H NMR (CD_3OD, 300 MHz) : See Table 12

^{13}C NMR (CD_3OD, 75 MHz) : See Table 12

Methyl caffeate (**35**)

White amorphous powder

$C_{10}H_{10}O_4$

$[\alpha]_D^{21}$ -12.3 (*c* 0.10, MeOH)

UV (MeOH) λ_{max} nm (logε) 317 (3.91), 296 (3.91)

IR (neat) ν_{max} 2966, 1687, 1595, 1515, 1271 cm^{-1}

ESI-MS *m/z* 195.1 $[M+H]^+$

^1H NMR (CD_3OD, 300 MHz) : See Table 12

^{13}C NMR (CD_3OD, 75 MHz) : See Table 12

Table 12. ^{1}H and ^{13}C NMR spectroscopic data of compounds **34** and **35**.

	34		**35**	
No.	δ_C	δ_H (*J* in Hz)	δ_C	δ_H (*J* in Hz)
1	128.0		127.8	
2	131.8	7.47 d (8.5)	115.6	7.17 d (2.0)
3	117.6	6.82 d (8.5)	146.5	
4	161.9		150.3	
5	117.6	6.82 d (8.5)	116.4	6.81 d (7.9)
6	131.8	7.47 d (8.5)	123.9	7.05 dd (2.0, 7.9)
7	147.3	7.62 d (15.6)	149.3	7.57 d (15.9)
8	116.5	6.31 d (15.6)	115.8	6.31 d (15.9)
9	171.9		168.8	
OCH_3			56.4	3.89 s

In CD_3OD, ^{1}H (300 MHz) and ^{13}C (75 MHz) NMR data were measured.

Neochlorogenic acid (3-*O*-caffeoylquinic acid) (**36**)

Yellowish syrup

$C_{16}H_{18}O_9$

$[\alpha]_D^{21}$ -17.5 (*c* 0.10, MeOH)

UV (MeOH) λ_{max} nm (logε) 328 (4.03), 300 (3.94), 244 (3.84), 217 (4.03)

IR (neat) ν_{max} 3391, 2976, 1688, 1605, 1277 cm^{-1}

ESI-MS *m/z* 353.1 $[M-H]^-$

^{1}H NMR (CD_3OD, 400 MHz) : See Table 13

^{13}C NMR (CD_3OD, 100 MHz) : See Table 14

Neochlorogenic acid methyl ester (**37**)

Yellowish syrup

$C_{17}H_{20}O_9$

$[\alpha]_D^{21}$ -32.9 (*c* 0.10, MeOH)

UV (MeOH) λ_{max} nm (logε) 329 (4.05), 300 (3.96), 244 (3.88), 216 (4.05)

IR (neat) ν_{max} 3422, 1718, 1688, 1270, 1119 cm^{-1}

ESI-MS *m/z* 369.1 $[M+H]^+$

^1H NMR (CD_3OD, 400 MHz) : See Table 13

^{13}C NMR (CD_3OD, 100 MHz) : See Table 14

Cryptochlorogenic acid (4-*O*-caffeoylquinic acid) (**38**)

Colorless syrup

$C_{16}H_{18}O_9$

$[\alpha]_D^{21}$ -55.3 (*c* 0.10, MeOH)

UV (MeOH) λ_{max} nm (logε) 330 (4.09), 301 (3.98), 244 (3.87), 218 (4.05)

IR (neat) ν_{max} 3391, 2946, 1688, 1605, 1279, 1181 cm^{-1}

ESI-MS *m/z* 353.1 $[M-H]^-$

^1H NMR (CD_3OD, 400 MHz) : See Table 13

^{13}C NMR (CD_3OD, 100 MHz) : See Table 14

Cryptochlorogenic acid methyl ester (**39**)

Yellowish syrup

$C_{17}H_{20}O_9$

$[\alpha]_D^{21}$ -74.8 (*c* 0.10, MeOH)

UV (MeOH) λ_{max} nm (logε) 328 (3.83), 288 (3.76)

IR (neat) ν_{max} 3391, 2951, 1731, 1278 cm^{-1}

ESI-MS *m/z* 369.1 $[M+H]^+$

^1H NMR (CD_3OD, 400 MHz) : See Table 13

^{13}C NMR (CD_3OD, 100 MHz) : See Table 14

Table 13. ^{13}C NMR spectroscopic data of compounds **36-39**.

	36	**37**	**38**	**39**
1	75.4	76.1	76.5	76.3
2	41.4	41.6	42.6	42.1
3	68.3	69.4	65.5	65.6
4	74.7	74.7	79.2	78.5
5	73.0	73.4	69.6	68.9
6	36.7	37.2	38.3	38.3
7	178.5	177.2	177.3	175.6
1′	127.9	128.7	127.8	127.7
2′	115.1	115.9	115.2	115.2
3′	146.7	147.5	146.6	146.7
4′	149.3	150.2	149.3	149.4
5′	116.5	117.3	116.4	116.4
6′	122.9	123.7	123.0	122.9
7′	146.8	147.6	147.1	147.1
8′	115.8	116.6	115.3	115.1
9′	169.0	169.7	169.0	168.8
OCH_3		53.7		52.9

In CD_3OD, ^{13}C NMR data were measured at 100 MHz.

Table 14. ^{1}H NMR spectroscopic data (*J* in Hz) of compounds **36-39**.

	36	**37**	**38**	**39**
1				
2	2.14 m	2.08 m	2.17 m	2.17 m
	1.95 dd (12.9, 9.7)	1.98 m	2.04 m	2.03 m
3	4.16 m	4.12 m	4.30 m	4.25 m
4	3.65 dd (8.5, 3.1)	3.69 m	4.82 dd (9.3, 2.7)	4.80 m
5	5.35 m	5.35 m	4.30 m	4.25 m
6	2.19 dd (3.9, 14.5)	2.19 dd (3.9, 14.5)	2.17 m	2.17 m
	2.14 m	2.12 m	2.04 m	2.03 m
7				
1′				
2′	7.04 d (2.0)	7.04 d (1.9)	7.05 d (2.0)	7.05 d (1.6)
3′				
4′				
5′	6.77 d (8.2)	6.76 d (8.1)	6.77 d (8.2)	6.77 d (8.2)
6′	6.92 dd (8.2, 2.0)	6.93 dd (8.1, 1.9)	6.93 dd (8.2, 2.0)	6.95 dd (4.6, 8.2)
7′	7.57 d (15.9)	7.58 d (15.9)	7.62 d (15.9)	7.62 d (15.9)
8′	6.30 (15.9)	6.29 d (15.9)	6.31 d (15.9)	6.35 d (15.9)
9′				
OCH_3		3.72 s		3.72 s

In CD_3OD, ^{1}H NMR data were measured at 400 MHz.

Vanillic acid (**40**)

Brown amorphous powder

$C_8H_8O_4$

$[\alpha]_D^{21}$ +56.9 (*c* 0.10, MeOH)

UV (MeOH) λ_{max} nm (logε) 288 (3.64), 259 (3.88), 212 (4.18)

IR (neat) ν_{max} 2971, 1688, 1287 cm^{-1}

ESI-MS *m/z* 169.2 $[M+H]^+$

^1H NMR (CD_3OD, 400 MHz) : See Table 15

^{13}C NMR (CD_3OD, 100 MHz) : See Table 15

4-Hydroxybenzoic acid (**41**)

Colorless syrup

$C_7H_6O_3$

$[\alpha]_D^{21}$ +49.1 (*c* 0.10, MeOH)

UV (MeOH) λ_{max} nm (logε) 254 (3.79)

IR (neat) ν_{max} 3359, 2937, 1658, 1608, 1055, 1032 cm^{-1}

ESI-MS *m/z* 139.1 $[M+H]^+$

^1H NMR (CD_3OD, 300 MHz) : See Table 15

^{13}C NMR (CD_3OD, 75 MHz) : See Table 15

3-Hydroxybenzoic acid (**42**)

Brown syrup

$C_7H_6O_3$

$[\alpha]_D^{21}$ +11.4 (*c* 0.10, MeOH)

UV (MeOH) λ_{max} nm (logε) 293 (3.23), 203 (4.30)

IR (neat) ν_{max} 3359, 1663, 1580, 1397 cm^{-1}

ESI-MS *m/z* 139.1 $[M+H]^+$

^1H NMR (CD_3OD, 600 MHz) : See Table 15

^{13}C NMR (CD_3OD, 150 MHz) : See Table 15

Table 15. ^1H and ^{13}C NMR spectroscopic data of compounds **40**-**42**.

	40[a]		**41**[b]		**42**[c]	
No.	δ_C	δ_H (*J* in Hz)	δ_C	δ_H (*J* in Hz)	δ_C	δ_H (*J* in Hz)
1	123.3		122.9		130.6	
2	115.8	7.53 m	133.0	7.89 d (8.5)	115.6	7.28 dd (2.0, 2.0)
3	148.7		116.0	6.84 d (8.5)	158.8	
4	152.6		163.3		119.5	6.95 dd (2.0, 7.7)
5	113.8	6.82 d (8.8)	116.0	6.84 d (8.5)	136.4	7.26 dd (7.7, 7.7)
6	125.2	7.55 m	133.0	7.89 d (8.5)	119.9	7.30 dd (2.0, 7.7)
7	170.2		170.3		172.6	
OCH_3	56.3	3.88 s				

In CD_3OD, ^1H NMR data were measured at [a]400 MHz, [b]300 MHz, and [c]600 MHz, respectively.

In CD_3OD, ^{13}C NMR data were measured at [a]100 MHz, [b]75 MHz, and [c]150 MHz, respectively.

Benzyl-*β*-D-glucopyranoside (**43**)

Colorless syrup

$C_{13}H_{18}O_6$

$[\alpha]_D^{21}$ -47.5 (*c* 0.10, MeOH)

UV (MeOH) λ_{max} nm (logε) 264 (2.91), 205 (3.94)

IR (neat) ν_{max} 3391, 2931 cm^{-1}

HRMS (ESI-QTOF) *m/z* 271.1178 $[M+H]^+$ (calcd. for $C_{13}H_{19}O_6$, 271.1176)

^{1}H NMR (CD_3OD, 400 MHz) : See Table 16

^{13}C NMR (CD_3OD, 100 MHz) : See Table 17

2-Phenylethyl-*β*-D-glucopyranoside (**44**)

Brown syrup

$C_{14}H_{20}O_6$

$[\alpha]_D^{21}$ +46.1 (*c* 0.10, MeOH)

UV (MeOH) λ_{max} nm (logε) 278 (3.02)

IR (neat) ν_{max} 2935, 1054, 1033 cm^{-1}

ESI-MS *m/z* 285.1 $[M+H]^+$

^{1}H NMR (CD_3OD, 400 MHz) : See Table 16

^{13}C NMR (CD_3OD, 100 MHz) : See Table 17

Dopaol-*β*-D-glucopyranoside (**45**)

Yellowish syrup

$C_{14}H_{20}O_8$

$[\alpha]_D^{21}$ +31.2 (*c* 0.10, MeOH)

UV (MeOH) λ_{max} nm (logε) 280 (3.53)

IR (neat) ν_{max} 3361, 1508 cm^{-1}

ESI-MS *m/z* 315.1 $[M-H]^-$

^1H NMR (CD_3OD, 400 MHz) : See Table 16

^{13}C NMR (CD_3OD, 100 MHz) : See Table 17

threo-Guaiacylglycerol (**46**)

Colorless syrup

$C_{10}H_{14}O_5$

$[\alpha]_D^{21}$ +41.1 (*c* 0.10, MeOH)

UV (MeOH) λ_{max} nm (logε) 280 (3.41), 229 (3.74)

IR (neat) ν_{max} 3364, 2931, 1652, 1519, 1275 cm^{-1}

ESI-MS *m/z* 237.1 $[M+Na]^+$

^1H NMR (CD_3OD, 300 MHz) : See Table 16

^{13}C NMR (CD_3OD, 75 MHz) : See Table 17

threo-Guaiacylglycerol 8-*O*-*β*-D-glucopyranoside (**47**)

Brown oil

$C_{16}H_{24}O_{10}$

$[\alpha]_D^{21}$ +23.3 (*c* 0.10, MeOH)

UV (MeOH) λ_{max} nm (logε) 280 (3.46), 229 (3.77)

IR (neat) ν_{max} 3361, 1602, 1027 cm^{-1}

ESI-MS *m/z* 421.1 $[M+HCOO]^-$

^1H NMR (DMSO-d_6, 300 MHz) : See Table 16

^{13}C NMR (DMSO-d_6, 75 MHz) : See Table 17

Table 16. ^{13}C NMR spectroscopic data of compounds **43**-**47**.

	43[a]	**44**[a]	**45**[a]	**46**[b]	**47**[c]
1	139.0	140.0	131.5	135.6	132.5
2	129.1	130.0	117.1	112.3	111.0
3	129.2	129.3	146.1	149.6	147.1
4	128.6	127.2	144.6	147.9	145.6
5	129.2	129.3	116.3	116.6	114.8
6	129.1	130.0	121.2	121.4	119.3
7	71.7	37.2	36.5	76.2	72.2
8		71.7	72.1	78.4	86.7
9				65.5	61.3
1′	103.3	104.3	104.3		104.0
2′	75.1	75.1	75.1		73.8
3′	78.1	78.1	78.1		76.8
4′	71.7	71.6	71.6		70.1
5′	78.0	77.9	77.9		76.3
6′	62.8	62.7	62.7		61.0
OCH_3				57.1	55.5

In CD_3OD, ^{13}C NMR data were measured at [a]100 MHz and [b]75 MHz, respectively.
[c]In DMSO-d_6, ^{13}C NMR data were measured at 75 MHz.

Table 17. ^{1}H NMR spectroscopic data (*J* in Hz) of compounds **43**-**47**.

	43[a]	**44**[a]	**45**[a]	**46**[b]	**47**[c]
1					
2	7.41 m	7.25 m	6.68 d (1.8)	6.98 d (1.8)	6.94 brs
3	7.32 m	7.25 m			
4	7.26 m	7.17 m			
5	7.32 m	7.25 m	6.66 d (8.1)	6.74 d (8.1)	6.68 m
6	7.41 m	7.25 m	6.54 dd (1.8, 8.1)	6.79 dd (1.8, 8.1)	6.73 m
7	4.92 d (12.2)	2.93 m	2.76 m	4.51 d (6.4)	4.52 d (6.4)
	4.66 d (12.2)				
8		4.09 m, 3.75 m	4.01 m, 3.70 m	3.66 m	3.64 m
9				3.34 m, 3.48 m	3.35 m, 3.17 m
1′	4.36 d (7.7)	4.28 d (7.7)	4.27 d (7.8)		4.24 d (7.5)
2′	3.37~3.25 m	3.17 m	3.18 dd (7.8, 7.8)		3.04 m
3′		3.34 m	3.34 m		3.13 m
4′		3.26 m	3.26 m		3.06 m
5′		3.28 m	3.25 m		3.09 m
6′		3.85 m	3.85 dd (12.2, 1.8)		3.64 m
		3.65 m	3.67 m		3.40 m
OCH_3				3.85 s	3.74 s

In CD_3OD, ^{1}H NMR data were measured at [a]400 MHz and [b]300 MHz, respectively.
[c]In DMSO-d_6, ^{1}H NMR data were measured at 300 MHz.

Undatuside A (**48**)

Yellowish oil

$C_{19}H_{26}O_{10}$

$[\alpha]_D^{21}$ -10.5 (*c* 0.10, MeOH)

UV (MeOH) λ_{max} nm (logε) 280 (3.27), 260 (3.30)

IR (neat) ν_{max} 3396, 2972, 1731 cm^{-1}

HRMS (ESI-QTOF) *m/z* 437.1407 $[M+Na]^+$ (calcd. for $C_{19}H_{26}O_{10}Na$, 437.1418)

^{1}H NMR (DMSO-d_6, 400 MHz) : δ 7.36 (2H, m, H-2, 6), 7.34 (2H, m, H-3, 5), 7.28 (1H, m, H-4), 4.76 (1H, d, *J* = 12.3 Hz, H-7a), 4.54 (1H, d, *J* = 12.3 Hz, H-7b), 4.35 (1H, d, *J* = 11.4 Hz, H-6′a), 4.26 (1H, d, *J* = 7.5 Hz, H-1′), 4.06 (1H, dd, *J* = 11.4, 6.8 Hz, H-6′b), 3.35 (1H, m, H-5′), 3.15 (1H, m, H-3′), 3.09 (1H, m, H-4′), 3.05 (1H, m, H-2′), 2.64 (2H, m, H-2″), 2.48 (2H, m, H-4″), 1.29 (3H, s, 3″-CH_3)

^{13}C NMR (DMSO-d_6, 100 MHz) : δ 172.6 (C-5″), 170.4 (C-1″), 137.9 (C-1), 128.1 (C-2, 6), 127.7 (C-3,5), 127.4 (C-4), 102.1 (C-1′), 76.3 (C-3′), 73.7 (C-5′), 73.3 (C-2′), 70.1 (C-4′), 69.7 (C-7), 68.9 (C-3″), 63.5 (C-6′), 45.6 (C-2″), 45.3 (C-4″), 27.5 (3″-CH_3)

(*E*)-3-Hexenyl-*β*-D-glucopyranoside (**49**)

Yellowish oil

$C_{12}H_{22}O_6$

$[\alpha]_D^{21}$ -4.7 (*c* 0.10, MeOH)

UV (MeOH) λ_{max} nm (logε) 280 (3.19)

IR (neat) ν_{max} 3404, 2927, 1372 cm^{-1}

ESI-MS *m/z* 307.1 $[M+HCOO]^-$

^1H NMR (CD_3OD, 300 MHz) : δ 5.75 (1H, m, H-4), 5.58 (1H, m, H-3), 4.31 (1H, m, H-1a), 4.18 (1H, d, *J* = 7.9 Hz, H-1′), 4.08 (1H, m, H-1b), 3.85 (1H, m, H-6′a), 3.67 (1H, m, H-6′b), 3.34 (1H, m, H-3′), 3.26 (1H, m, H-4′), 3.25 (1H, m, H-5′), 3.17 (1H, m, H-2′), 2.04 (2H, m, H-2), 1.42 (2H, m, H-5), 0.93 (3H, t, *J* = 7.5 Hz, H-6)

^{13}C NMR (CD_3OD, 75 MHz) : δ 135.8 (C-3), 127.3 (C-4), 102.9 (C-1′), 78.1 (C-3′), 78.0 (C-5′), 75.0 (C-2′), 71.6 (C-4′), 70.8 (C-1), 62.7 (C-6′), 35.5 (C-2), 23.4 (C-5), 14.0 (C-6)

Houttuylignan (**50**)

Colorless oil

$C_{20}H_{24}O_7$

$[\alpha]_D^{21}$ +32.2 (*c* 0.10, MeOH)

UV (MeOH) λ_{max} nm (logε) 309 (3.79), 280 (3.89), 231 (4.11)

IR (neat) ν_{max} 3400, 2936, 2867, 1674, 1590, 1514, 1273 cm^{-1}

HRMS (ESI-QTOF) *m/z* 399.1428 $[M+Na]^+$ (calcd. for $C_{20}H_{24}O_7Na$, 399.1414)

^1H NMR (CD_3OD, 500 MHz) : See Table 18

^{13}C NMR (CD_3OD, 125 MHz) : See Table 19

(7*S*, 8*R*)-Dihydrodehydrodiconiferyl alcohol (**51**)

Colorless oil

$C_{20}H_{24}O_6$

$[\alpha]_D^{21}$ +6.4 (*c* 0.10, MeOH)

UV (MeOH) λ_{max} nm (logε) 281 (3.87), 230 (4.22), 205 (4.84)

IR (neat) ν_{max} 3352, 2937, 1517, 1276, 1211 cm^{-1}

HRMS (ESI-QTOF) *m/z* 383.1470 $[M+Na]^+$ (calcd. for $C_{20}H_{24}O_6Na$, 383.1465)

^1H NMR (CD_3OD, 400 MHz) : See Table 18

^{13}C NMR (CD_3OD, 100 MHz) : See Table 19

(7*S*, 8*R*)-Dehydrodiconiferyl alcohol (**52**)

Yellowish oil

$C_{20}H_{22}O_6$

$[\alpha]_D^{21}$ -1.5 (*c* 0.10, MeOH)

UV (MeOH) λ_{max} nm (logε) 277 (4.11)

IR (neat) ν_{max} 3423, 2926, 1603, 1518, 1496, 1144 cm^{-1}

HRMS (ESI-QTOF) *m/z* 359.1493 $[M+H]^+$ (calcd. for $C_{20}H_{23}O_6$, 359.1489)

^{1}H NMR (CD_3OD, 300 MHz) : See Table 18

^{13}C NMR (CD_3OD, 75 MHz) : See Table 19

(7*R*, 8*S*, 8′*S*)-Isolariciresinol (**53**)

Colorless oil

$C_{20}H_{24}O_6$

$[\alpha]_D^{21}$ +3.0 (*c* 0.10, MeOH)

UV (MeOH) λ_{max} nm (logε) 284 (3.66), 224 (4.04), 202 (4.56)

IR (neat) ν_{max} 3365, 2933, 1602, 1513, 1273 cm^{-1}

HRMS (ESI-QTOF) *m/z* 383.1472 $[M+Na]^+$ (calcd. for $C_{20}H_{24}O_6Na$, 383.1465)

^{1}H NMR (CD_3OD, 800 MHz) : See Table 18

^{13}C NMR (CD_3OD, 200 MHz) : See Table 19

(+)-(8*S*,8′*S*)-Secoisolariciresinol (**54**)

Colorless oil

$C_{20}H_{26}O_6$

$[\alpha]_D^{21}$ +27.3 (*c* 0.10, MeOH)

UV (MeOH) λ_{max} nm (logε) 280 (3.58), 229 (4.10), 202 (4.69)

IR (neat) ν_{max} 3364, 2932, 1601, 1515, 1272 cm^{-1}

HRMS (ESI-QTOF) *m/z* 385.1608 $[M+Na]^+$ (calcd. for $C_{20}H_{26}O_6Na$, 385.1622)

^1H NMR (CD_3OD, 800 MHz) : See Table 18

^{13}C NMR (CD_3OD, 200 MHz) : See Table 19

erythro-1-(4-hydroxy-3-methoxyphenyl)-2-[4-(3-hydroxypropyl)-2,6-dimethoxyphenoxy] -propane-1,3-diol (**55**)

Colorless oil

$C_{21}H_{28}O_8$

$[\alpha]_D^{21}$ +0.4 (*c* 0.10, MeOH)

UV (MeOH) λ_{max} nm (logε) 280 (3.78), 229 (4.10)

IR (neat) ν_{max} 3421, 2938, 1590, 1124 cm^{-1}

HRMS (ESI-QTOF) *m/z* 431.1683 $[M+Na]^+$ (calcd. for $C_{21}H_{28}O_8Na$, 431.1676)

^1H NMR (CD_3OD, 300 MHz) : See Table 18

^{13}C NMR (CD_3OD, 75 MHz) : See Table 19

erythro-(7*S*,8*R*)-4,7,9-trihydroxy-3,3'-dimethoxy-8-*O*-4'-neolignan-9'-*O*-*β*-D-glucopyranoside (**56**)

Brown oil

$C_{26}H_{36}O_{12}$

$[\alpha]_D^{21}$ +8.1 (*c* 0.10, MeOH)

UV (MeOH) λ_{max} nm (logε) 280 (3.72), 229 (4.07)

IR (neat) ν_{max} 3393, 2935, 1512, 1273 cm^{-1}

HRMS (ESI-QTOF) *m/z* 539.2136 $[M-H]^-$ (calcd. for $C_{26}H_{35}O_{12}$, 539.2134)

^{1}H NMR (DMSO-d_6, 300 MHz) : See Table 18

^{13}C NMR (DMSO-d_6, 75 MHz) : See Table 19

Table 18. ^{13}C NMR spectroscopic data of compounds **50-56**.

	50[c]	**51**[b]	**52**[a]	**53**[d]	**54**[d]	**55**[a]	**56**[e]
1	138.1	134.8	134.5	138.6	133.8	133.7	133.3
2	114.0	110.5	110.5	113.8	113.3	111.3	111.4
3	151.0	149.1	149.1	149.0	148.8	148.7	146.9
4	146.6	147.5	147.5	146.0	145.4	146.8	145.4
5	117.5	116.1	116.1	116.0	115.7	115.7	114.6
6	121.6	119.7	119.7	123.2	122.7	120.5	119.4
7	32.6	89.0	89.3	48.1	36.0	74.0	71.6
8	35.5	55.4	55.2	48.0	44.1	87.5	83.9
9	62.1	65.0	64.9	62.2	62.1	61.5	60.1
1′	128.6	136.9	132.5	134.2	133.8	139.9	134.7
2′	112.6	114.1	112.0	112.4	113.3	106.8	113.0
3′	149.1	145.2	145.5	147.2	148.8	154.3	149.5
4′	153.9	147.5	149.2	145.3	145.4	134.7	146.0
5′	115.9	129.9	129.9	117.4	115.7	154.3	116.0
6′	125.2	117.9	116.5	129.0	122.7	106.8	120.1
7′	197.4	32.9	132.0	33.6	36.0	33.4	31.1
8′	84.1	35.8	127.5	40.0	44.1	35.5	31.2
9′	64.4	62.2	63.9	65.9	62.1	62.1	67.9
3-OCH_3	56.3	56.4	56.3	56.3	56.1	56.3	55.4
3′-OCH_3	56.4	56.7	56.7	56.4	56.1	56.6	55.6
5′-OCH_3						56.6	
							Glc
1″							103.0
2″							73.5
3″							76.8
4″							70.1
5″							76.7
6″							61.1

In CD_3OD, ^{13}C NMR data were measured at [a]75 MHz, [b]100 MHz, [c]125 MHz and [d]200 MHz.

[e]In DMSO-d_6, ^{13}C NMR data was measured at 75 MHz.

Table 19. ^{1}H NMR spectroscopic data (*J* in Hz) of compounds **50-56**.

	50[c]	**51**[b]	**52**[a]	**53**[d]	**54**[d]	**55**[a]	**56**[c]
1							
2	6.82 d (1.8)	6.94 d (1.8)	6.95 m	6.65 d (1.9)	6.58 d (1.8)	6.98 d (1.7)	6.98 d (1.7)
3							
4							
5	6.75 d (8.2)	6.75 d (8.1)	6.77 d (8.1)	6.72 d (8.0)	6.65 d (7.9)	6.73 d (8.1)	6.67 d (8.1)
6	6.63 dd (1.8, 8.2)	6.81 dd (1.8, 8.1)	6.83 dd (1.8, 8.1)	6.59 dd (1.9, 8.0)	6.54 dd (1.8, 7.9)	6.78 dd (1.7, 8.1)	6.76 dd (8.1, 1.7)
7	2.59 m	5.48 d (6.2)	5.52 d (6.3)	3.78 d (5.1)	2.65 dd (7.1, 13.7)	4.91 d (4.9)	4.70 d (5.3)
					2.57 dd (7.8, 13.7)		
8	1.77 m	3.45 m	3.49 dd (6.3, 12.4)	1.74 m	1.89 m	4.16 m	4.21 m
9	3.52 t (6.5)	3.81 m	3.81 m	3.66 m	3.58 dd (5.0, 11.1)	3.87 dd (5.6, 12.0)	3.57 m
		3.74 dd (7.0, 11.0)		3.37 dd (4.1, 11.3)	3.54 dd (4.5, 11.1)	3.52 dd (3.6, 12.0)	
1′							
2′	7.61 d (2.0)	6.72 brs	6.94 m	6.63 s	6.58 d (1.8)	6.53 s	6.76 d (1.7)
3′							
4′							
5′	6.86 d (8.4)			6.16 s	6.65 d (7.9)		6.85 d (8.3)
6′	7.68 dd (2.0, 8.4)	6.72 brs	6.97 m		6.54 dd (1.8, 7.9)	6.53 s	6.65 dd (1.7, 8.3)
7′		2.62 t (7.6)	6.54 d (15.8)	2.75 d (7.7)	2.65 dd (7.1, 13.7)	2.63 dd (7.0, 8.5)	2.55 t (8.1)
8′	5.50 dd (4.3, 5.5)	1.80 m	6.23 dt (15.8, 5.9)	1.98 m	2.57 dd (7.8, 13.7)	1.81 m	1.77 m
9′	4.01 m	3.56 t (6.4)	4.21 d (5.9)	3.71 dd (4.9, 11.0)	1.89 m	3.56 t (6.5)	3.77 m
			4.20 d (5.9)	3.65 m	3.58 dd (5.0, 11.1)		3.40 m
3-OCH_3	3.77 s	3.80 s	3.82 s	3.75 s	3.54 dd (4.5, 11.1)	3.83 s	3.72 s
3′-OCH_3	3.87 s	3.84 s	3.88 s	3.79 s	3.73 s	3.80 s	3.69 s
5′-OCH_3					3.73 s	3.80 s	
1″							4.10 d (7.6)
2″							2.95 t (8.1)
3″							3.13 m
4″							3.04 m
5″							3.06 m
6″							3.66 m, 3.44 m

In CD_3OD, ^{1}H NMR data were measured at [a]300 MHz, [b]400 MHz, [c]500 MHz and [d]800 MHz.

[e]In DMSO-*d*$_6$, ^{1}H NMR data was measured at 300 MHz.

1,2-Bis-(4-hydroxy-3methoxyphenyl)propane-1,3-diol (**57**)

Colorless oil

$C_{17}H_{20}O_6$

$[\alpha]_D^{21}$ +15.6 (*c* 0.10, MeOH)

UV (MeOH) λ_{max} nm (logε) 280 (3.79), 226 (4.11)

IR (neat) ν_{max} 3395, 2936, 1517, 1273 cm^{-1}

HRMS (ESI-QTOF) *m/z* 319.1190 $[M-H]^-$ (calcd. for $C_{17}H_{19}O_6$, 319.1187)

^{1}H NMR (CD_3OD, 300 MHz) : δ 6.70 (1H, m, H-5′), 6.67 (1H, m, H-6′), 6.66 (1H, m, H-2″), 6.63 (1H, m, H-2′), 6.62 (1H, m, H-6″), 6.61 (1H, m, H-5″), 4.92 (1H, d, *J* = 5.7 Hz, H-1), 3.84 (1H, dd, *J* = 10.8, 6.5 Hz, H-3a), 3.76 (3H, s, OCH_3), 3.70 (3H, s, OCH_3), 3.68 (1H, m, H-3b), 2.91 (1H, m, H-2)

^{13}C NMR (CD_3OD, 75 MHz) : δ 148.4 (C-3′), 148.3 (C-3″), 146.5 (C-4′), 146.1 (C-4″), 136.4 (C-1′), 132.2 (C-1″), 123.1 (C-6″), 120.3 (C-6′), 115.6 (C-5′), 115.4 (C-5″), 114.5 (C-2″), 111.5 (C-2′), 75.5 (C-1), 64.4 (C-3), 56.8 (C-2), 56.3 (OCH_3), 56.2 (OCH_3)

(9*Z*, 11*E*, 13*S*, 15*Z*)-Octadeca-9,11,15-trien-13-olide (**58**)

Colorless oil

$C_{18}H_{28}O_2$

$[\alpha]_D^{21}$ +20.7 (*c* 0.10, MeOH)

UV (MeOH) λ_{max} nm (logε) 280 (3.29), 229 (4.76)

IR (neat) ν_{max} 2931, 2858, 1711 cm^{-1}

HRMS (ESI-QTOF) *m/z* 277.2158 $[M+H]^+$ (calcd. for $C_{18}H_{29}O_2$, 277.2162)

^1H NMR (CD_3OD, 300 MHz) : See Table 20

^{13}C NMR (CD_3OD, 75 MHz) : See Table 20

(*S*)-Coriolide (**59**)

Colorless oil

$C_{18}H_{30}O_2$

$[\alpha]_D^{21}$ +13.1 (*c* 0.10, MeOH)

UV (MeOH) λ_{max} nm (logε) 280 (3.37), 233 (4.21)

IR (neat) ν_{max} 2930, 2857, 1712 cm^{-1}

HRMS (ESI-QTOF) *m/z* 279.2326 $[M+H]^+$ (calcd. for $C_{18}H_{31}O_2$, 279.2319)

^1H NMR (CD_3OD, 300 MHz) : See Table 20

^{13}C NMR (CD_3OD, 75 MHz) : See Table 20

Table 20. ^{1}H and ^{13}C NMR spectroscopic data of compounds **58**-**59**.

No.	**58**		**59**	
	δ_C	δ_H (*J* in Hz)	δ_C	δ_H (*J* in Hz)
1	177.6		177.9	
2	35.0	2.27 t (7.4)	35.1	2.27 t (7.4)
3	26.1	1.59 m	26.1	1.59 m
4~7	30.7	~1.33 m	30.6	1.42~1.29
	30.3	~1.33 m	30.5	1.42~1.29
	30.2	~1.33 m	30.4	1.42~1.29
	30.1	~1.33 m	30.2	1.42~1.29
8	28.6	2.18 dd (6.6, 13.2)	28.6	2.19 tdd (7.3, 7.3, 1.3)
9	133.0	5.40 m	132.9	5.41 dt (7.3, 11.1)
10	129.3	5.96 t (11.2)	129.3	5.98 t (11.1)
11	126.6	6.50 dd (11.2, 15.2)	126.5	6.50 dd (11.1, 15.1)
12	136.6	5.63 dd (6.6, 15.2)	137.2	5.62 dd (6.3, 15.1)
13	73.2	4.11 m	73.4	4.07 m
14	36.3	2.31 m	38.4	1.50 m
15	125.5	5.36 ddd (1.4, 7.1, 10.9)	26.6	1.42 m, 1.34 m
16	134.5	5.47 ddd (1.3, 7.1, 10.9)	32.6	1.30 m
17	21.7	2.05 m	23.6	1.32 m
18	14.6	0.95 t (7.5)	14.4	0.91 dd (4.7, 9.1)

In CD_3OD, ^{1}H NMR (300 MHz) and ^{13}C NMR (75 MHz) data were measured.

2.2.3. Preparation of (*S*)-MTPA ester and (*R*)-MTPA ester

Compounds **1** and **30** (0.5 mg, each) were transferred into two 4 ml vials and dried. Anhydrous pyridine (600 μL), 4-(*N*,*N*-dimethylamino)pyridine (DMAP) (10 mg) and (*R*)-(-)-α-methoxy-α-(trifluoromethyl)phenylacetyl chloride (MTPA-Cl) (10 μL) were added into the vial. The vial was shaken carefully to mix the reactant. After 12 h, the (*S*)-MTPA esters was obtained from the mixture using HPLC column. Similarly, another portions of **1** and **30** (0.5 mg, each) were reacted with (*S*)-MTPA-Cl to afford the (*R*)-MTPA ester.

2.2.4. Determination of absolute configuation of sugar

Compounds **2**, **25**-**32**, **43**-**45**, **47**-**49**, **56** (0.1 mg) was hydrolyzed using 1 N H_2SO_4 (100 μL) heated with a water bath at 90 °C for 2 h, then neutralized with saturated aqueous Na_2CO_3 solution. After the solution was dried under a stream of N_2, the products and standard sugars (D- and L-galactose, D- and L-glucose and L-rhamnose) were dissolved in pyridine (100 μl) containing L-cysteine methyl ester hydrochloride (1.0 mg). An L-rhamnose was dissolved in pyridine (100 μl) containing D-cysteine methyl ester hydrochloride (0.5 mg). After that, they were heated at 60 °C for 1 h. The solutions were treated with 1 μL (1.11 mg) of *o*-tolylisothiocyanate, which were heated again at 60 °C for 1 h. Each final mixtures were directly analyzed by analytical RP-HPLC (Hypersil^{TM} BDS C18 column, 17% aq. MeCN, 0.8 ml/min, 40 min, 35 °C). The t_R of the peak at 18.5, 21.5 and 36.0

min coincided with those of the thiocarbamoyl thiazolidine derivative of D-galactose, D-glucose and L-rhamnose, respectively.

2.2.5. ECD Calculation

The absolute configuration of **14** was established by the calculated ECD spectra using the time-dependent density functional theory (TDDFT) method.(Jiao et al. 2015) A conformational search using molecular mechanics force field in Conflex 7. The ECD spectra of the optimized conformers were calculated at the B_3LYP/def-SV(P) level with the COSMO model in MeOH and computed as Boltzmann-weighted averages.

The ECD spectra were simulated using Gaussian functions overlapping each transition, where σ is the width of the band at 1/*e* height and ΔE_i and R_i are the excitation energies and rotatory strengths for transition *i*, respectively. The value of σ was 0.10 eV and *R* was R_{len} in this work.

$$\Delta\epsilon(\mathrm{E}) = \frac{1}{2.297 \times 10^{-39}} \frac{1}{\sqrt{2\pi\sigma}} \sum_{i}^{A} \Delta E_i R_i e^{\left[-(E-\Delta E_i)^2/(2\sigma)^2\right]}$$

2.2.6. Evaluation of anti-inflammatory effects

2.2.6.1. Cell culture

Murine macrophages, RAW264.7, were obtained from the Korean Research Institute of Bioscience and Biotechnology (Korea), and grown in RPMI medium containing 10% fetal bovine serum and 100 U/mL penicillin/streptomycin sulfate. Cells were incubated in a humidified 5% CO_2 atmosphere at 37 °C.

2.2.6.2. Measurement of NO production

The nitrite concentration in the culture medium was measured as an indicator of NO production according to the Griess reaction. RAW 264.7 cells (2×10^5 cells/well) were cultured in 96-well plates using RPMI without phenol red, and pretreated with samples for 0.5 h. Cellular NO production was induced by the addition of 500 ng/mL final concentration LPS and a 24 h incubation. Following incubation, 100 μL of conditioned media was mixed with the same volume of Griess reagent and incubated for 15 min. The absorbance of the mixture at 540 nm was measured with an ELISA microplate reader (Benchmark, Bio-Rad Laboratories, USA). The values obtained were compared with those of standard concentrations of sodium nitrite dissolved in RPMI, and the concentrations of nitrite in the conditioned media of sample-treated cells were calculated.

2.2.6.3. MTT assay

Cells were seeded into 96-well plates at a density of 5×10^4 cells/well and incubated with serum-free media in the presence of samples. Following incubation for 24 h, 10 μL MTT (5 mg/mL in saline) was added and incubation was continued for further 4 h. Mitochondrial succinate dehydrogenase in live cells converts MTT into visible formazan crystals during incubation. The formazan crystals were then solubilized in dimethyl sulfoxide and the absorbance was measured at 540 nm using an ELISA microplate reader (Benchmark, Bio-Rad Laboratories, USA). Relative cell viability was calculated compared with the absorbance of the untreated control group. All experiments were performed in triplicate.

3. Results and Discussion

3.1. Structural elucidation of alkaloids from *H. cordata*

3.1.1. Compounds **1**-**3**

Compound **1**, a yellowish amorphous powder, was determined to have a molecular formula of $C_{15}H_{15}NO_3$ by the positive mode high resolution ESI-QTOF-MS, which showed the parent ion at *m/z* 258.1117 $[M+H]^+$ (calcd. for $C_{15}H_{16}NO_3$, 258.1130). The IR spectrum displayed absorptions characteristic of an amide group (3307 and 1641 cm^{-1}). The ^1H NMR spectrum showed an 1,4-disubstituted benzene ring at δ_H 7.68 (2H, d, *J*=8.7 Hz, H-2,6) and 6.80 (2H, d, *J*=8.7 Hz, H-3,5) and a mono-substituted benzene ring at δ_H 7.42 (2H, d, *J*=7.2 Hz, H-2″,6″), 7.34 (2H, t, *J*=7.2 Hz, H-3″,5″) and 7.25 (1H, t, *J*=7.2 Hz, H-4″) (Figure 7). The HMBC correlation of a carbonyl carbon at δ_C 170.4 and H-2 suggested an 1,4-disubstituted benzene ring attached to a carbonyl group. A hydroxylated ethylamine group was confirmed by the chemical shifts and splitting patterns of hydrogen signals at δ_H 4.88 (1H, dd, *J*=4.7, 7.9 Hz, H-2′), 3.62 (1H, dd, *J*=13.5, 4.7 Hz, H-1′a) and 3.50 (1H, dd, *J*=13.5, 7.9 Hz, H-1′b). From the HMBC spectrum, a carbonyl carbon showed long range coupling with two protons of C-1′ involved in hydroxylated ethylamine group. The oxygenated methine proton (H-2′) was coupled to carbon atoms of a mono-substituted aromatic ring, at δ_C 127.2 (C-2″,6″). These data suggested 4-hydroxy-*N*-(2-hydroxy-2-phenylethyl) benzamide.

The configuration of C-2′ was identified as *S* by the application of Mosher's rule (Seco et al. 2004), using *α*-methoxy-*α*-(trifluoromethyl)phenylacetyl chloride (MTPA-Cl) (Figure 10). Therefore, compound **1** was determined as (*S*)-(-)-4-hydroxy-*N*-(2-hydroxy-2-phenylethyl)benzamide and named houttynamide B. This compound was isolated firstly from nature.

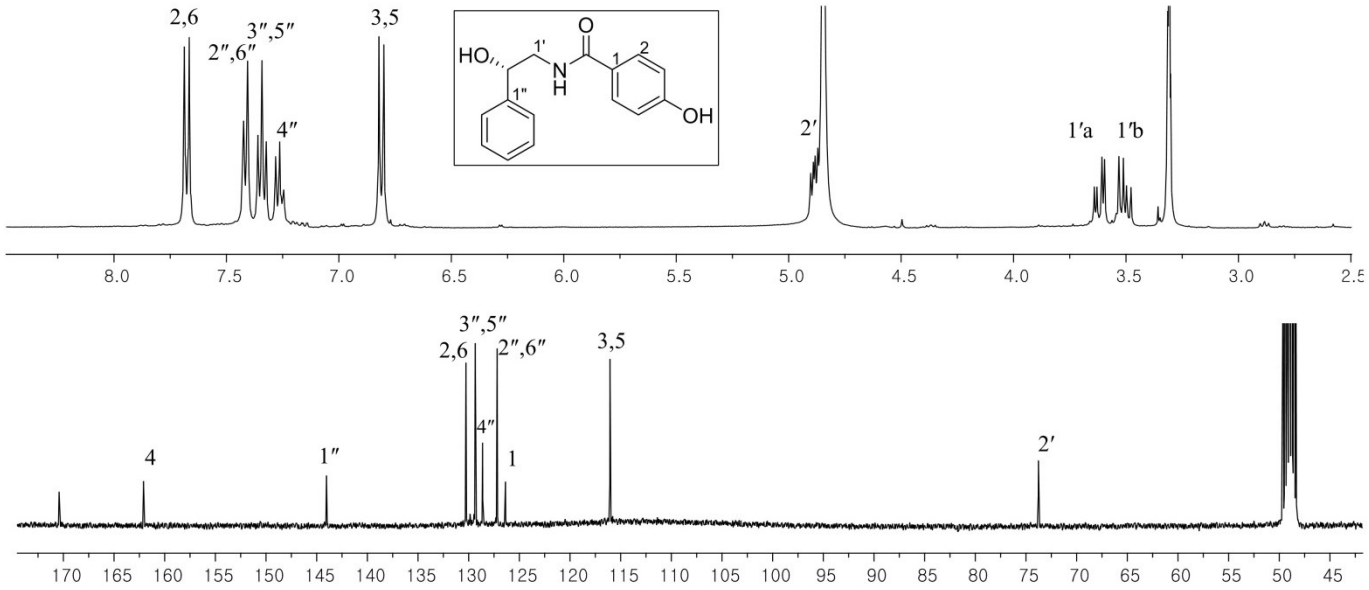

Figure 7. ^{1}H and ^{13}C NMR spectra of compound **1** (CD_3OD, 400/100 MHz)

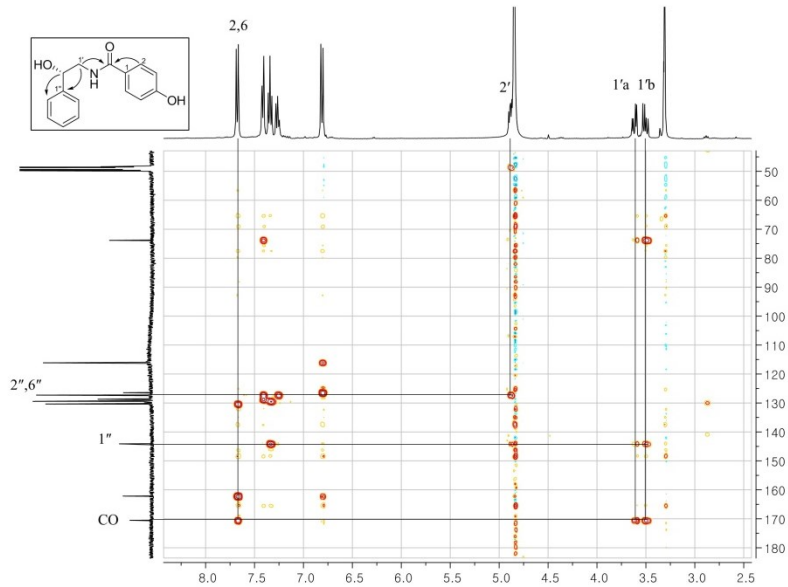

Figure 8. The HMBC spectrum of compound **1** (400 MHz, CD_3OD)

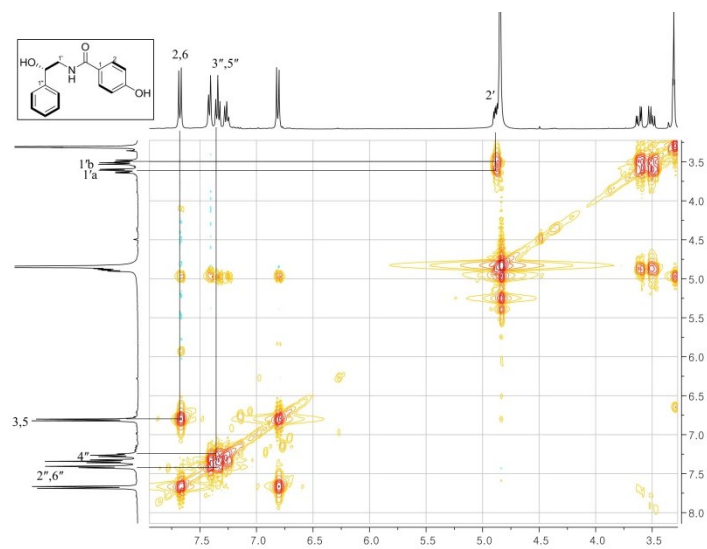

Figure 9. The COSY spectrum of compound **1** (400 MHz, CD_3OD)

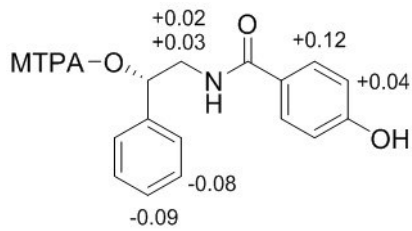

Figure 10. $\Delta\delta_H^{SR}$ values for the MTPA esters of compound **1**

Compound **2** was obtained as a white amorphous powder. Its molecular formula was determined to be $C_{21}H_{25}NO_8$ by ESI-QTOF-MS based on the protonated ion peak at *m/z* 420.1645 $[M+H]^+$ (calcd. for $C_{21}H_{26}NO_8$, 420.1658). In the IR spectrum, absorption bands indicative of an amide group (3335 and 1641 cm^{-1}) were observed.

The ^{13}C NMR spectrum showed 21 carbon signals including a carbonyl carbon, twelve carbons in aromatic groups, a sugar unit and two carbons in a hydroxylated ethylamine. The 1D NMR spectra (Figure 11) were similar to those of compound **1** except for the signals corresponding to a sugar and one of the aromatic ring moieties. An 1,3-disubstituted aromatic group signals at δ_H 7.21 (1H, m, H-5), 7.20 (1H, m, H-6), 7.17 (1H, dd, *J*=1.9, 1.5 Hz, H-2) and 6.89 (1H, ddd, *J*=7.5, 1.9, 1.5 Hz, H-4) were appeared instead of 1,4-disubstituted aromatic ring. From the HMBC spectrum, the correlations of a carbonyl carbon at δ_C 166.3 with H-2 and H-6 suggested a 3-hydroxybenzamide substructure. Compared to **1**, these data suggested a 3-hydroxy-*N*-(2-hydroxy-2-phenylethyl)benzamide moiety.

A sugar unit was confirmed to be D-glucose by HPLC analysis of the acid hydrolysate of **2** (Tanaka et al. 2007). A *β*-glucopyranosyl moiety was clearly observed in the ^{13}C NMR spectrum (δ_C 102.9, 76.9, 76.5, 73.9, 69.9 and 60.9) and the coupling constant of anomeric proton (δ_H 4.44, d, *J*=7.6 Hz). The anomeric proton showed a HMBC correlation with C-2′ (δc 79.0). Based on the above data, the structure of **2** was determined as 3-hydroxy-*N*-(2-*β*-D-glucopyranosyl-2-phenylethyl)benzamide.

The configuration of C-2′ was identified as *S* by comparison with the CD spectra of compounds **1** and literature (Liu et al. 2015). The CD spectrum of **2** showed a negative Cotton effect at 240 nm, similar to those of **1** (Figure 14). According to literature, the CD spectrum of (*S*)-tembamide exhibited negative Cotton effect at 235 nm, whereas (*R*)-tembamide showed positive Cotton effect at 235 nm. The positive Cotton effect at approximately 210 nm could be ascribed to the positive rotatory strength, which were cause by the π→π* transition in the benzene moiety. The negative rotatory strength at approximately 240 nm contributed to the negative Cotton effect, which was associated with the π→π* transition of beazamide group. Based on these data, compound **2** was defined as (*S*)-(-)-3-hydroxy-*N*-(2-*β*-D-glucopyranosyl-2-phenylethyl)benzamide and named houttuynamide C. This compound was isolated from nature for the first time.

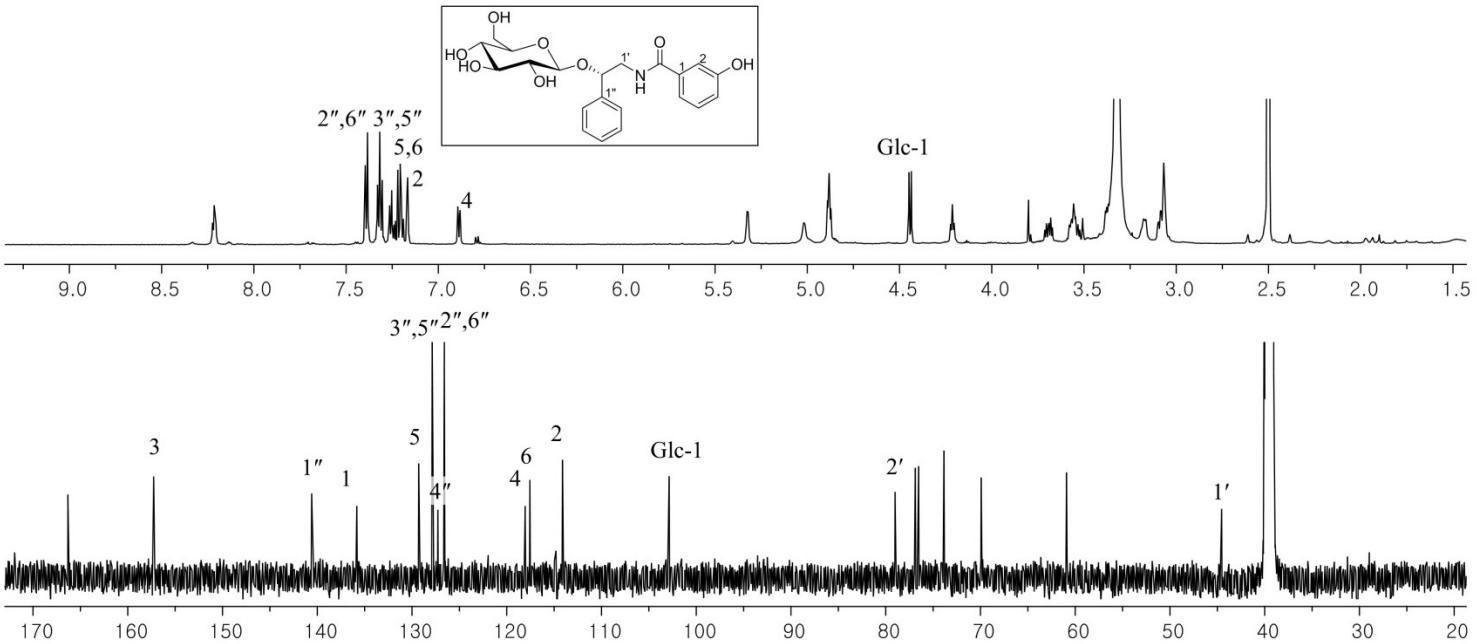

Figure 11. ^{1}H and ^{13}C NMR spectra of compound **2** (DMSO-d_6, 600/150 MHz)

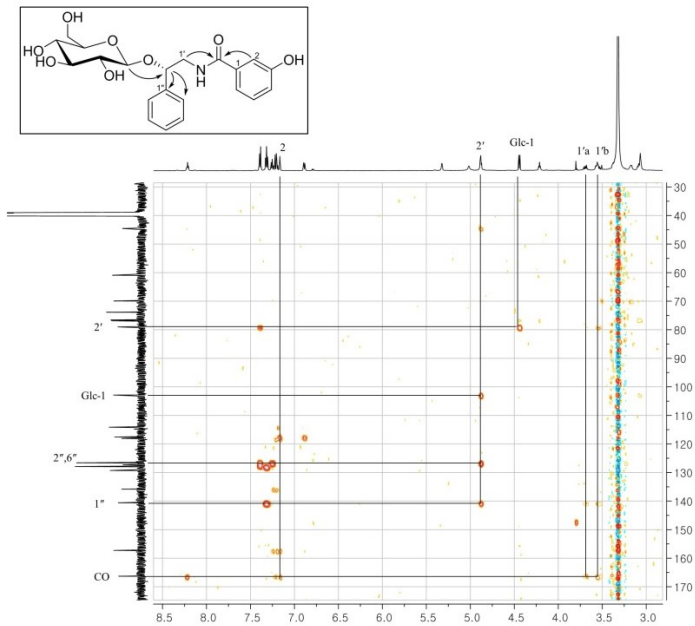

Figure 12. The HMBC spectrum of compound **2** (400 MHz, DMSO-d_6)

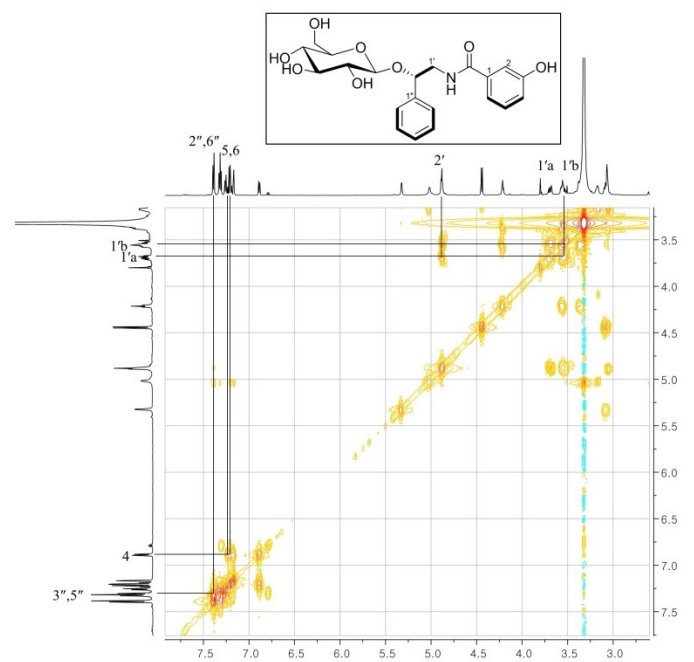

Figure 13. The COSY spectrum of compound **2** (400 MHz, DMSO-d_6)

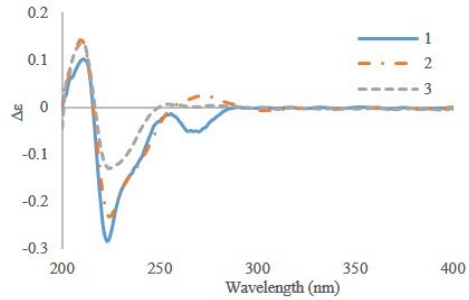

Figure 14. The experimental CD spectra of **1**, **2** and **3**.

Compound **3**, a white amorphous powder, was determined to have a molecular formula of $C_{21}H_{25}NO_7$ by ESI-QTOF-MS, which showed an adduct ion at *m/z* 426.1524 $[M+Na]^+$ (calcd. for $C_{21}H_{25}NO_7Na$, 426.1658). The 1D NMR spectra (Figure 15) were similar to those of compound **2**, but two mono-substituted benzene rings were observed. Two mono-substituted aromatic group signals at [δ_H 7.78 (2H, m, H-2,6), 7.51 (1H, dd, J=7.4, 7.4 Hz, H-4) and 7.44 (2H, m, H-3,5)] and [δ_H 7.44 (2H, m, H-2″,6″), 7.30 (2H, t, *J*=7.1 Hz, H-3″,5″) and 7.27 (1H, t, *J*=7.1 Hz, H-4″)].

A sugar moiety was identified as D-glucose by HPLC analysis of the acid hydrolysate of **3** (Tanaka et al. 2007). A *β*-glucopyranosyl moiety was clearly observed in the ^{13}C NMR spectrum (δ_C 104.8, 78.0, 77.8, 75.4, 71.4 and 62.5) and the coupling constant of anomeric proton (δ_H 4.55, d, *J*=7.2 Hz). The anomeric proton showed a HMBC correlation with C-2′ (δc 81.9). The CD spectrum of **3** was identical with those of compounds **1** and **2** (Figure 14). Based on these spectral data and comparison with literature (Liu et al. 2015), compound **3** was identified as *N*-(2-*β*-D-glucosidyl-2-phenylethyl)benzamide.

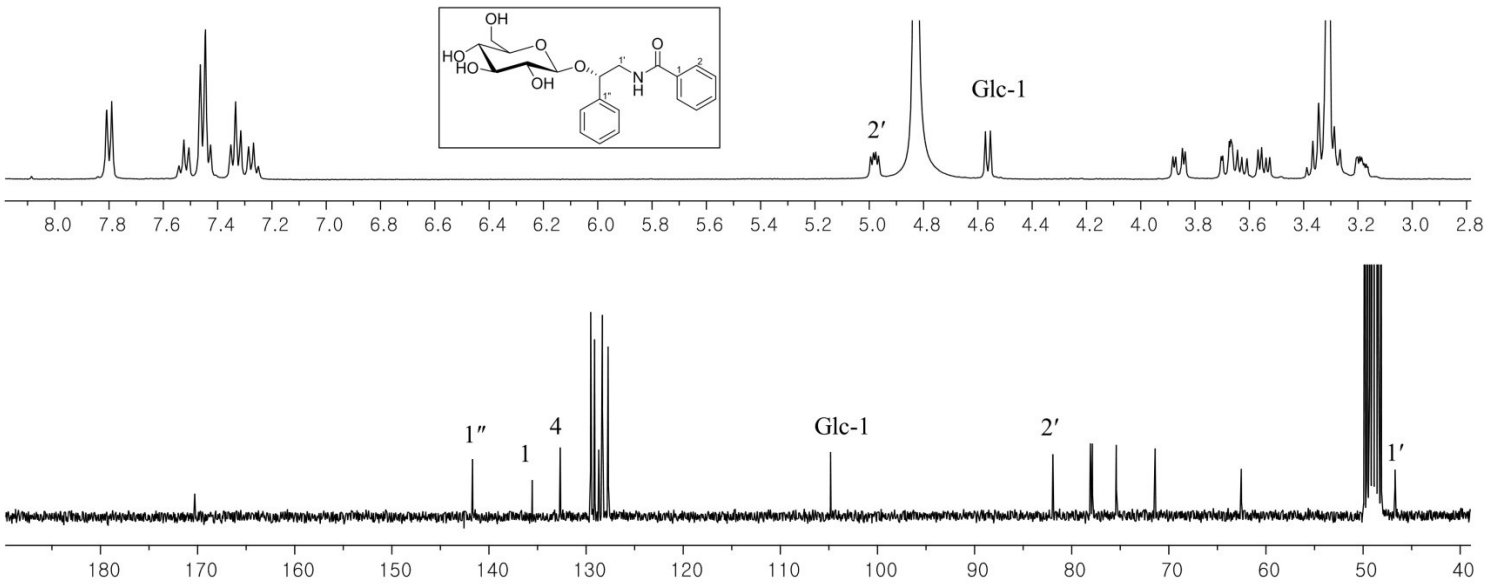

Figure 15. ^{1}H and ^{13}C NMR spectra of compound **3** (CD_3OD, 300/75 MHz)

3.1.2. Compound **4**

Compound **4**, a yellowish amorphous powder, was determined to have a molecular formula of $C_{11}H_{15}NO_4$ by the negative mode high resolution ESI-QTOF-MS, which showed the pseudo-molecular peak at *m/z* 224.0917 $[M-H]^-$, (calcd. for $C_{11}H_{14}NO_4$, 224.0928).

The ^1H NMR and HSQC spectra showed a aldehyde proton at δ_H 9.45 (1H, s, CHO), a methoxy group at δ_H 3.36 (3H, s, 6-OCH_3), four methylene protons at δ_H 4.50 (2H, s, H-6), 4.37 (2H, m, H-1′), 2.32 (2H, t, *J*=7.2 Hz, H-3′) and 2.00 (2H, m, H-2′) and a pyrrole ring at δ_H 6.99 (1H, d, *J*=4.0 Hz, H-3) and 6.28 (1H, d, *J*=4.0 Hz, H-4) (Figure 16). A 2,5-disubstituted pyrrole ring was suggested by chemical shifts and coupling constants of H-3 and H-4. The carbon atoms in a pyrrole group were assigned by the HMBC correlations of H-3 with C-5 (δ_C 141.1) and C-2 (δ_C 133.8) and of H-4 with C-5 and C-2. The HMBC correlations between H-6 and C-5 and between H-6 and methoxy group (δ_C 58.2) and between aldehyde proton and C-2 suggested 2-formyl-5-(methoxymethyl)pyrrole group.

The sequential COSY correlations from H-1′ to H-3′ confirmed a propyl group. The HMBC spectrum showed long range coupling of a proton (H-1′) in propyl group with C-2 and C-5 as well as coupling of H-3′ with carbonyl carbon at δ_C 176.8. These data indicated that a butanoic acid moiety was attached to nitrogen atom of the pyrrole ring. On the basis of these data, the structure of **4** was determined as 4-[Formyl-5-(methoxymethyl)-1*H*-pyrrol-1-yl] butanoic acid and confirmed by comparison with literature (Chin et al. 2003).

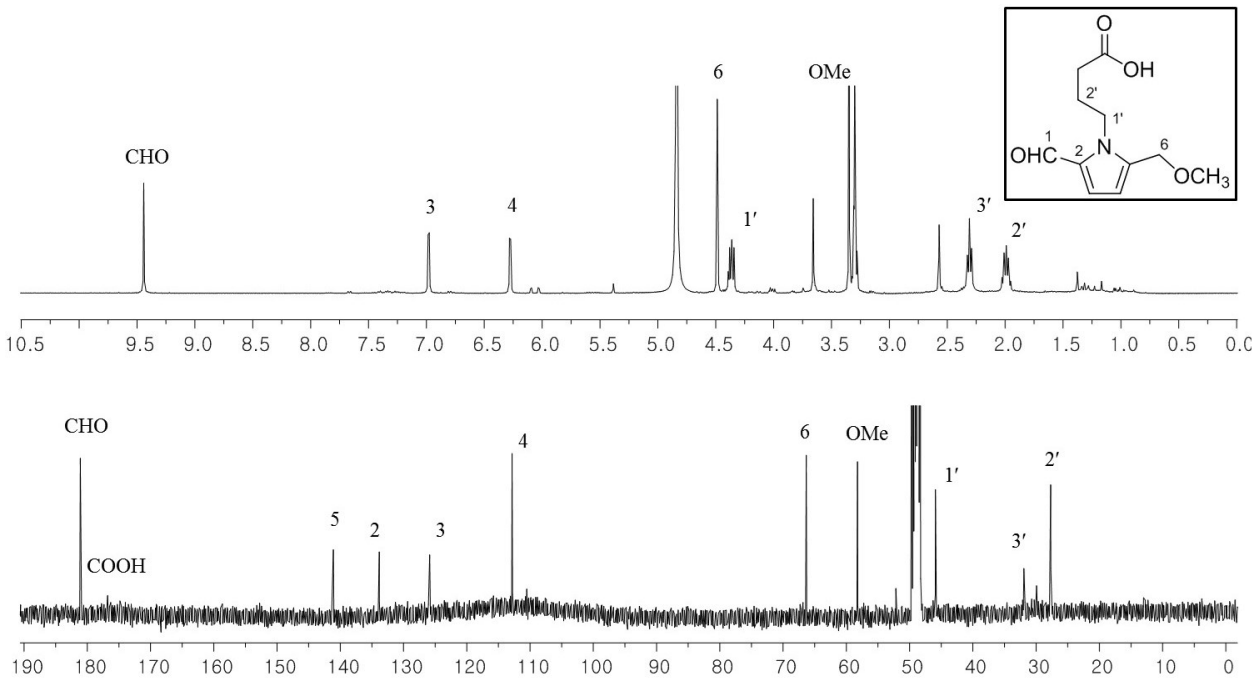

Figure 16. ^{1}H and ^{13}C NMR spectra of compound **4** (CD_3OD, 400/100 MHz)

3.1.3. Compound **5**

Compound **5** was obtained as a yellowish amorphous powder with molecular formula $C_{17}H_{11}NO_4$, indicated by pseudo-molecular peak at *m/z* 292.0612 $[M-H]^-$ (calcd. for $C_{17}H_{10}NO_4$, 292.0615) in ESI-QTOF-MS. In the IR spectrum, absorption bands indicative of an amide group (3330 and 1680 cm^{-1}) and an 1,2-diketone group (1716 and 1706 cm^{-1}) were observed. ^{13}C and HSQC spectra showed a methoxy group at δ_C 59.5/δ_H 4.06 (3H, s, 1-OCH_3), two carbonyl group at δ_C 177.0 (C-4) and 155.6 (C-5) and aromatic carbons (Figure 17). ^1H and HMBC spectra implied the presence of two penta-substituted benzene ring. The sequential COSY correlations between H-8 (δ_H 7.92, m), H-9 (δ_H 7.66, m), H-10 (δ_H 7.65, m) and H-11 (δ_H 9.45, m) confirmed an 1,2-disubstituted benzene ring. Considered by these spectral data and comparison with literature, compound **5** was identified as noraristolodione (Jiang et al. 2014).

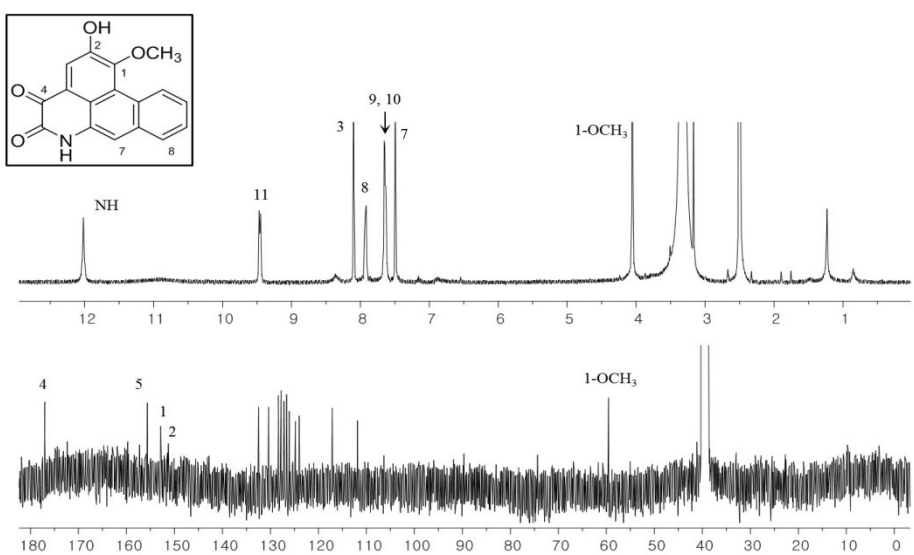

Figure 17. ^1H and ^{13}C NMR spectra of compound **5** (DMSO-d_6, 400/100 MHz)

3.1.4. Compound **6**

Compound **6** was obtained as a brown amorphous powder. Its molecular formula was determined to be $C_{18}H_{19}NO_2$ by ESI-QTOF-MS based on the protonated molecular ion peak at *m/z* 282.1492 $[M+H]^+$ (calcd. for $C_{18}H_{20}NO_2$, 282.1489). A characteristic fragment ion of $[M+H-31]^+$ suggested to be an aporphine alkaloid with methyl group at the *N* atom (Zhang et al. 2015). ^1H and HSQC spectra showed a methylamine group at δ_H 2.97 (3H, s, NCH_3), a methoxy group at δ_H 3.57 (3H, s, 1-OCH_3), a penta-substituted benzene ring at δ_H 6.71 (1H, s, H-3), an 1,2-disubstituted benzene ring at δ_H 8.34 (1H, dd, *J*=7.9, 1.1 Hz, H-11), 7.35 (1H, m, H-8), 7.34 (1H, m, H-10) and 7.27 (1H, ddd, *J*=7.3, 7.3, 1.1 Hz, H-9), a methine proton at δ_H 3.87 (1H, m, H-6a) and three methylene groups (Figure 18).

An 1,2-disubstituted benzene ring was confirmed by the sequential COSY correlations from H-8 to H-11 and the HMBC correlations of H-8 with C-11a (δ_C 132.9) and H-11 with C-7a (δ_C 135.0). A penta-substituted benzene ring was suggested by the HMBC correlations of H-3 with C-1 (δ_C 146.1), C-1b (δ_C 123.0), C-2 (δ_C 152.2) and C-3a (δ_C 128.1). From the COSY spectrum, the correlations between H-4 and H-5 and between H-6a and H-7 were observed. The HMBC correlations between H-8 and C-7 (δ_C 33.8) and between H-3 and C-4 (δ_C 27.2) suggested the presence of two phenylethyl moieties. In the HMBC spectrum, the methylamine proton was coupled to C-5 (δ_C 53.8) and C-6a (δ_C 63.6). In addition, the HMBC correlations between H-7 and C-1b and between H-11 and C-1a (δ_C 128.0) were observed. These spectral data suggested an aporphine moiety.

The position of methoxy group was suggested by the HMBC and NOESY

spectra. From the HMBC spectrum, the correlation between a methoxy proton (δ_H 3.57) and C-1 (δ_C 146.1) was observed. The methoxy-substituted position (C-1) was further proved by NOESY spectrum, which had a cross peak of methoxy proton with H-11. On the basis of these data, compound **6** was identified as *N*-methylasimilobine and confirmed by comparison with literature (Ma et al. 2014).

The absolute configuration of compound **6** was assigned to be (*S*) configuration based on CD spectrum (Craig & Roy 1965). In which, the Cotton effect at 245 nm was positive.

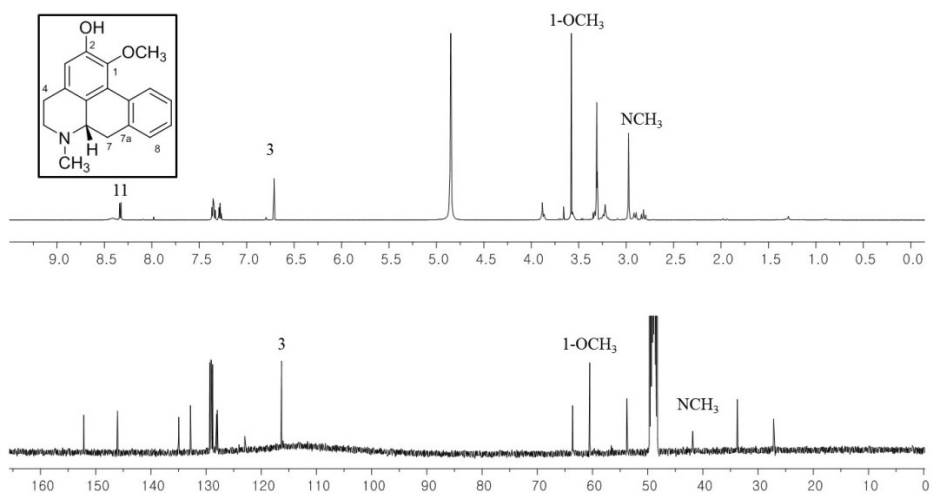

Figure 18. ^{1}H and ^{13}C NMR spectra of compound **6** (CD_3OD, 400/100 MHz)

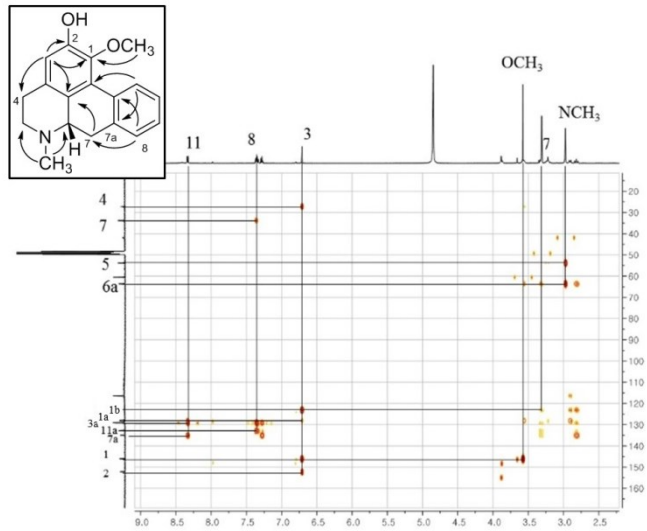

Figure 19. The HMBC spectrum of compound **6** (CD_3OD, 600 MHz)

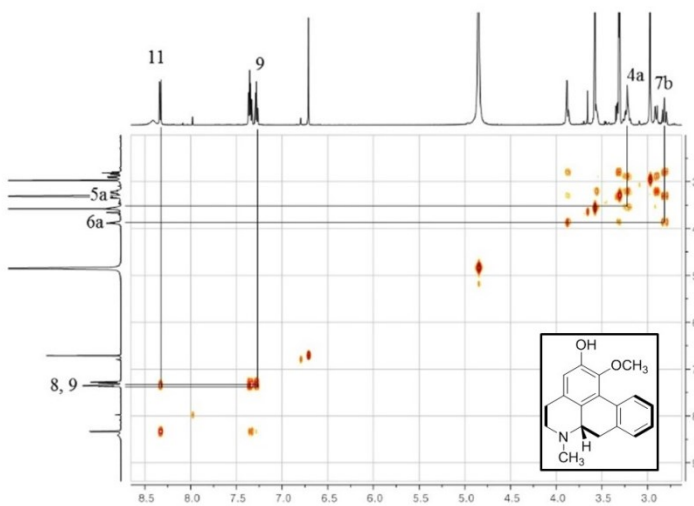

Figure 20. The COSY spectrum of compound **6** (CD_3OD, 600 MHz)

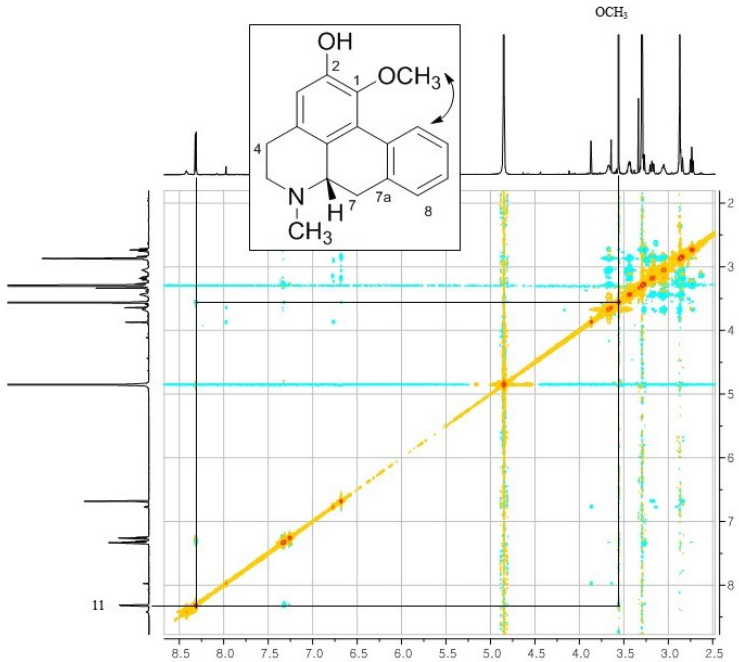

Figure 21. The NOESY spectrum of compound **6** (CD_3OD, 800 MHz)

3.1.5. Compounds **7**-**12**

Compound **7** was isolated as an amorphous brown powder. Its molecular formula was established as $C_{19}H_{21}NO_4$ on the basis of positive mode ESI-QTOF-MS data with a protonated molecular ion peak at *m/z* 328.1543 $[M+H]^+$ (calcd. for $C_{19}H_{21}NO_4$, 328.1543). A characteristic fragment ion of $[M+H-31]^+$ suggested to be an aporphine alkaloid with methyl group at the *N* atom (Zhang et al. 2015). ^{13}C NMR spectrum (Figure 22) showed 19 carbon signals including two aromatic rings, two paraffinic carbons at δ_C 33.0 (C-7) and 27.2 (C-4) and five hetero atom-substituted carbons at δ_C 64.0 (C-6a), 56.6 (2-OCH_3), 56.5 (10-OCH_3), 54.0 (C-5)

and 41.7 (NCH_3). The ^1H and HSQC spectra showed a methylamine group at δ_H 2.97 (3H, s, NCH_3), two methoxy group at δ_H 3.90 (3H, s, 2-OCH_3) and 3.86 (3H, s, 10-OCH_3), three singlet aromatic protons at δ_H 8.12 (1H, s, H-11), 6.76 (1H, s, H-8) and 6.71 (1H, s, H-3), a methine proton at δ_H 3.90 (1H, m, H-6a) and three methylene groups. An 1,2,4,5-tetrasubstituted benzene ring was confirmed by the HMBC correlations of H-8 with C-10 (δ_C 147.6), C-9 (δ_C 146.8) and C-11a (δ_C 125.0) and H-11 with C-9, C-10, C-11a and C-7a (δ_C 127.5).

1D NMR spectra of compound **7** were similar to those of compound **6** except for the signals corresponding to benzene rings and two methoxy groups. The position of methoxy groups were suggested by the HMBC and NOESY spectra. From the HMBC spectrum, the correlations between δ_H 3.90 (2-OCH_3) and δ_C 149.5 (C-2) and between δ_H 3.86 (10-OCH_3) and δ_C 147.6 (C-10) were observed. A methoxy group on C-2 was further proved by NOESY spectrum, which showed the correlation of a methoxy proton on C-2 with H-3. A methoxy group on C-10 was confirmed by the NOESY correlation with H-11. On the basis of these data, compound **7** was identified as isoboldine and confirmed by comparison with the literature (Ndi et al. 2016).

The absolute configuration of compound **7** was assigned to be (*S*) configuration based on CD spectrum (Craig & Roy 1965). In which, the Cotton effect at 240 nm was positive.

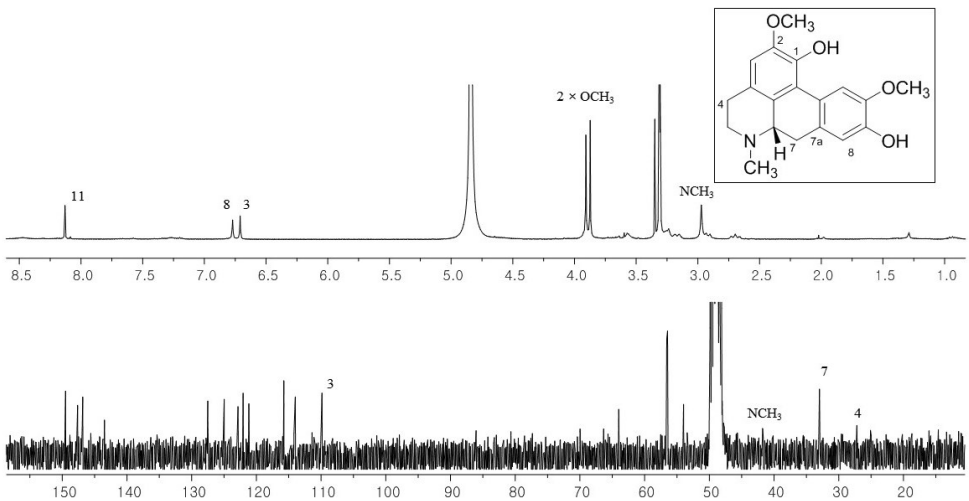

Figure 22. ^{1}H and ^{13}C NMR spectra of compound **7** (CD_3OD, 300/75 MHz)

Compound **8** was isolated as a white amorphous powder. Its molecular formula was determined to be $C_{20}H_{23}NO_4$ by ESI-QTOF-MS based on the protonated molecular ion peak at *m/z* 342.1714 $[M+H]^+$ (calcd. for $C_{20}H_{23}NO_4$, 342.1700). A characteristic fragment ion of $[M+H-31]^+$ assigned to be an aporphine alkaloid with methyl group at the *N* atom. ^{13}C NMR spectrum (Figure 23) showed 20 carbon signals including two aromatic ring, two paraffinic carbons at δ_C 33.6 (C-7) and 28.2 (C-4) and six hetero atom-substituted carbons at δ_C 63.8 (C-6a), 60.5 (1-OCH_3), 56.6 (10-OCH_3), 56.4 (2-OCH_3), 53.9 (C-5) and 42.6 (NCH_3). The NMR spectra of compound **8** were similar to those of compound **7** except for the signals corresponding to C-1 (δ_C 146.1) and one more methoxy groups (δ_C 60.5/δ_H 3.64). By comparison with the spectral data of compound **7** and the literature (Ndi et al. 2016), compound **8** was identified as *N*-methyllaurotetanine.

The absolute configuration of compound **8** was assigned to be (*S*) configuration based on the positive Cotton effect at 240 nm in the CD spectrum (Craig & Roy 1965).

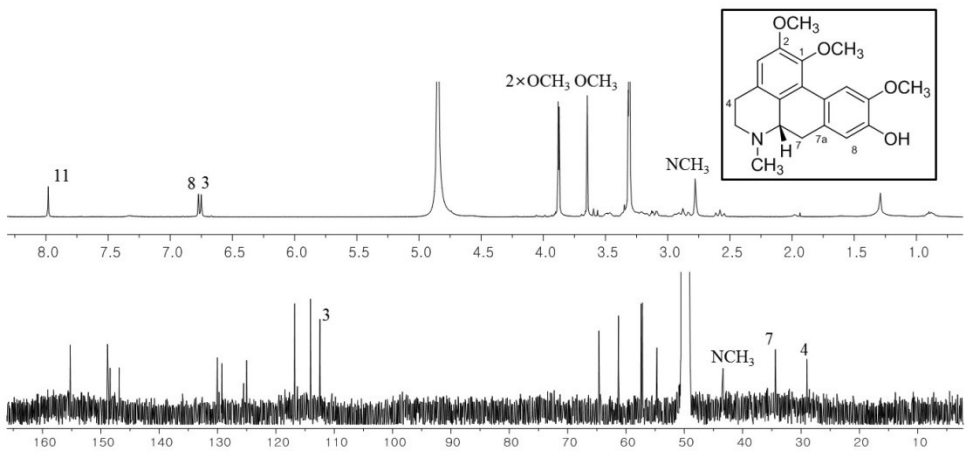

Figure 23. ^{1}H and ^{13}C NMR spectra of compound **8** (CD_3OD, 400/100 MHz)

Compound **9** was obtained as a yellowish amorphous powder with molecular formula $C_{18}H_{19}NO_2$, indicated by the protonated molecular ion peak at *m/z* 282.1500 $[M+H]^+$ (calcd. for $C_{18}H_{20}NO_2$, 282.1489). A characteristic fragment ion of $[M+H-17]^+$ suggested to be an aporphine alkaloid with no substituent at the *N* atom (Zhang et al. 2015).

^{13}C NMR spectrum (Figure 24) showed 18 carbon signals including two aromatic ring, two paraffinic carbons at δ_C 35.1 (C-7) and 26.5 (C-4) and four hetero atom-substituted carbons at δ_C 60.7 (1-OCH_3), 56.5 (2-OCH_3), 54.4 (C-6a) and 42.7 (C-5). The NMR spectra of compound **9** were similar to those of compound **6** except for the signals corresponding to the A ring, a methoxy group

(δ_C 60.7) and nitrogen-adjancent atom peaks at δ_C 42.7 (C-5) and 54.4 (C-6a). By comparison with the spectral data of other aporphine alkaloids and the literature (Rossini et al. 2015), compound **9** was identified as *N*-nornuciferine.

The absolute configuration of compound **9** was assigned to be (*R*) configuration based on the negative Cotton effect at 245 nm in the CD spectrum (Craig & Roy 1965).

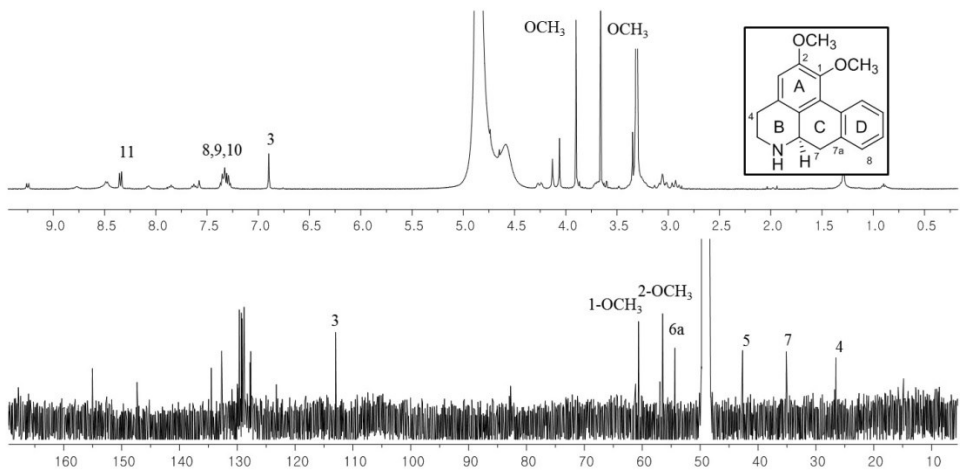

Figure 24. ^{1}H and ^{13}C NMR spectra of compound **9** (CD_3OD, 400/100 MHz)

Compound **10** was isolated as a yellowish amorphous powder. Its molecular formula was established as $C_{17}H_{17}NO_2$ on the basis of positive mode ESI-QTOF-MS data with a protonated molecular ion peak at *m/z* 268.1333 $[M+H]^+$ (calcd. for $C_{17}H_{18}NO_2$, 268.1332). An aporphine alkaloid with no substituent at the *N* atom was suggested by a characteristic fragment ion of $[M+H-17]^+$. ^{13}C NMR spectrum (Figure 25) showed 17 carbon signals including an aporphine moiety and a methoxy group at δ_C 60.5 (1-OCH_3). Compound **10** was identified and confirmed

as asimilobine by comparison with other aporphine alkaloids and the literature (Guinaudeau et al. 1979).

The absolute configuration of compound **10** was assigned to be (*S*) configuration based on CD spectrum (Craig & Roy 1965). In which, the Cotton effect at 245 nm was positive.

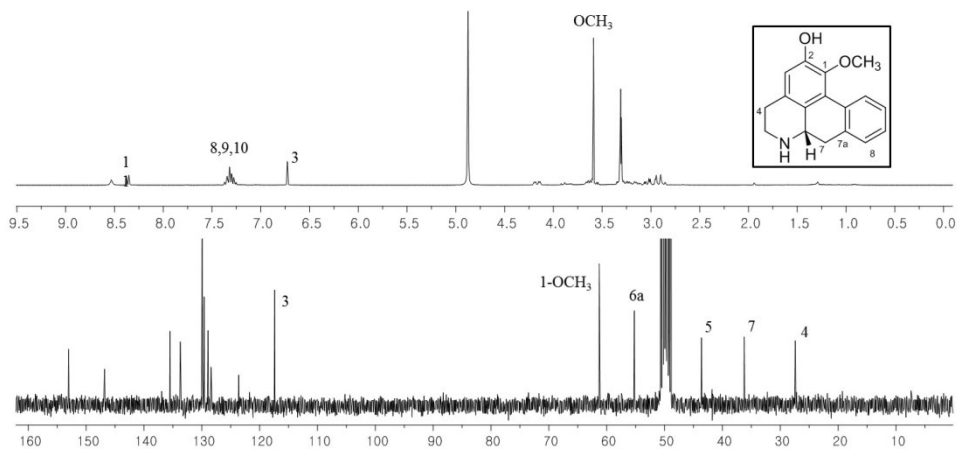

Figure 25. ^{1}H and ^{13}C NMR spectra of compound **10** (CD_3OD, 300/75 MHz)

Compound **11** was isolated as an amorphous brown powder. Its molecular formula was determined to be $C_{19}H_{21}NO_4$ by ESI-QTOF-MS based on the protonated molecular ion peak at *m/z* 328.1551 $[M+H]^+$ (calcd. for $C_{19}H_{22}NO_4$, 328.1543). A characteristic fragment ion of $[M+H-17]^+$ was shown, suggesting an aporphine alkaloid with no substituent at the *N* atom. ^{1}H NMR spectrum (Figure 26) showed three singlet aromatic protons at δ_H 8.02 (1H, s, H-11), 6.73 (1H, s, H-8) and 6.69 (1H, s, H-3) and three methoxy groups at 3.90 (3H, s, 1-OCH_3), 3.91 (3H, s, 10-OCH_3) and 3.66 (3H, s, 2-OCH_3). Compound **11** was identified and

confirmed as laurotetanine by comparison with other aporphine alkaloids and the literature (Cebrián-Torrejón et al. 2015). The positive Cotton effect at 240 nm confirmed the (*S*) configuration of compound **11**.

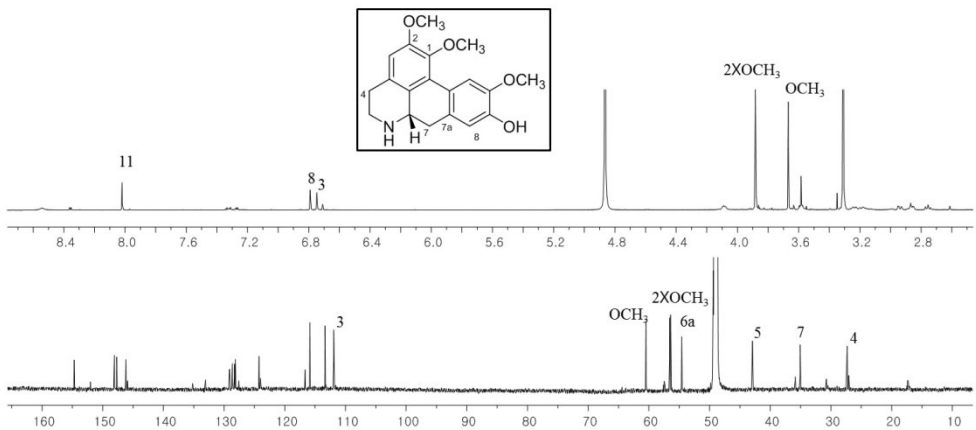

Figure 26. ^{1}H and ^{13}C NMR spectra of compound **11** (CD_3OD, 800/200 MHz)

Compound **12** was obtained as a brown amorphous powder with molecular formula $C_{18}H_{19}NO_4$, indicated by the protonated molecular ion peak at *m/z* 314.1385 $[M+H]^+$ (calcd. for $C_{18}H_{20}NO_4$, 314.1387). A characteristic fragment ion of $[M+H-17]^+$ suggested to be an aporphine alkaloid with no substituent at the *N* atom.

^{13}C NMR spectrum (Figure 27) showed 18 carbon signals including two aromatic rings, two paraffinic carbons at δ_C 34.3 (C-7) and 26.2 (C-4) and four hetero atom-substituted carbons at δ_C 56.7 (10-OCH_3), 56.5 (2-OCH_3), 54.8 (C-6a) and 42.8 (C-5). By comparison with the spectral data of other aporphine alkaloids and the literature (Vilegas et al. 1989), compound **12** was identified as

norisoboldine. The absolute configuration of compound **12** was assigned to be (*S*) configuration based on the positive Cotton effect at 240 nm in the CD spectrum (Craig & Roy 1965).

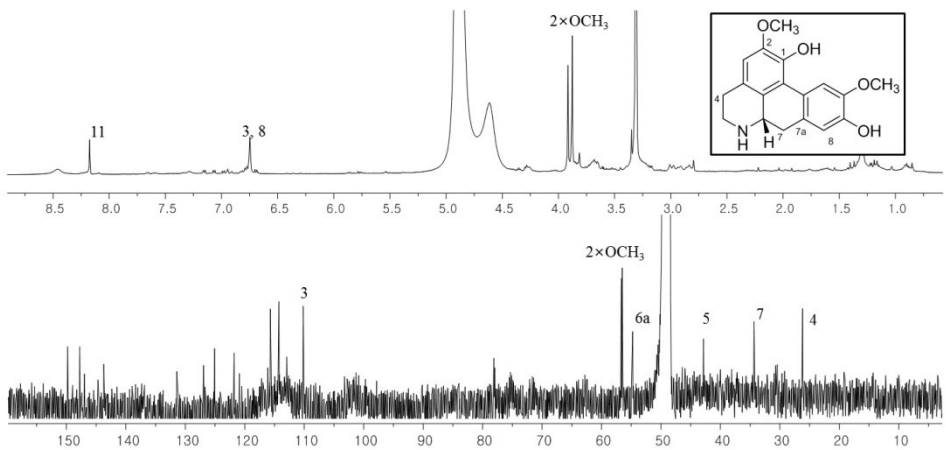

Figure 27. ^{1}H and ^{13}C NMR spectra of compound **12** (CD_3OD, 500/125 MHz)

3.1.6. Compound **13**

Compound **13** was isolated as a brown syrup. Its molecular formula was established as $C_{19}H_{23}NO_4$ on the basis of ESI-QTOF-MS data with a protonated molecular ion peak at *m/z* 330.1698 $[M+H]^+$ (calcd. for $C_{19}H_{24}NO_4$, 330.1700). ^{13}C NMR spectrum (Figure 28) showed 19 carbon signals including two aromatic rings, two paraffinic carbons at δ_C 40.9 (1-CH_2-1′) and 23.4 (C-4) and five hetero atom-substituted carbons at δ_C 66.1 (C-1), 56.4 (6-OCH_3), 56.4 (4′-OCH_3), 47.1 (C-3) and 41.0 (NCH_3). The ^{1}H and HSQC spectra showed a methylamine group at δ_H 2.86 (3H, s, NCH_3), two methoxy groups at δ_H 3.85 (3H, s, 6-OCH_3) and 3.85 (3H, s, 4′-OCH_3), two *para*-coupled aromatic protons at δ_H 6.78 (1H, s, H-5) and 6.23

(1H, s, H-8), an 1,3,4-trisubstituted benzene ring at δ_H 6.88 (1H, d, *J*=8.1 Hz, H-5′), 6.67 (1H, d, *J*=1.5 Hz, H-2′) and 6.62 (1H, dd, *J*=8.1, 1.5 Hz, H-6′), a methine proton at δ_H 4.43 (1H, t, *J*=6.8 Hz, H-1) and three methylene groups.

An 1,2,4,5-tetrasubstituted benzene ring was confirmed by the HMBC correlations of H-5 with C-6 (δ_C 149.4), C-7 (δ_C 146.5) and C-8a (δ_C 124.3) and H-8 with C-6, C-7, C-4a (δ_C 122.1). From the COSY spectrum, the correlations between δ_H 3.64 (H-3a) and δ_H 3.08 (H-4a) and between δ_H 4.43 (H-1) and δ_H 3.20 (1-CH_2a-1′) were observed. The HMBC correlations between δ_H 3.20 (1-CH_2a-1′) and δ_C 129.5 (C-1′) and between δ_H 6.78 (H-5) and δ_C 23.4 (C-4) suggested the presence of two phenylethyl moieties. From the HMBC spectrum, the correlations of methylamine proton with C-3 and C-1 and H-1 with C-8a and C-8 were observed.

The position of methoxy groups were suggested by the HMBC and NOESY spectra. From the HMBC spectrum, the correlations between a methoxy proton and C-6 and between another methoxy proton and C-4′ (δ_C 148.0) were observed. A methoxy group on C-6 was further proved by NOESY spectrum, which showed the correlation with H-5. A methoxy group on C-4′ was confirmed by the NOESY correlation with H-5′. The absolute stereochemistry of **13** was found to be *S* from the identical appearance of its CD spectrum (positive at 290 nm, positive at 238 nm and positive at 210 nm) with that of previously reported data (Lee & Doskotch 1999). On the basis of these data, compound **13** was identified as (*S*)-reticuline.

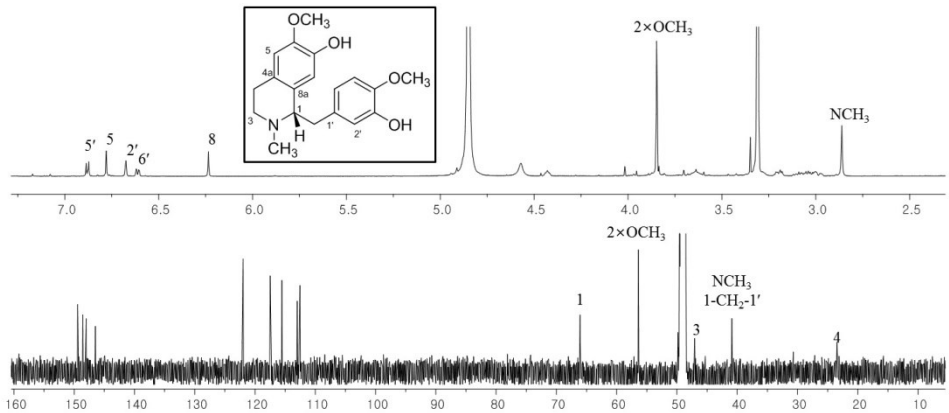

Figure 28. ^{1}H and ^{13}C NMR spectra of compound **13** (CD_3OD, 600/150 MHz)

3.1.7. Compound **14**

Compound **14** was isolated as an amorphous white powder. Its molecular formula was established as $C_{16}H_{14}N_2O_3$ on the basis of ESI-QTOF-MS data with a parent ion peak at *m/z* 283.1093 $[M+H]^+$ (calcd. for $C_{16}H_{15}N_2O_3$, 283.1083). The IR spectrum displayed absorptions characteristic of hydroxy and amine groups (approximately 3308 cm^{-1}), an imine (1630 cm^{-1}), aromatic rings (1604 cm^{-1}) and an amine (1363 cm^{-1}) group.

Peaks indicative of an 1,2-disubstituted aromatic ring at δ_H 8.22 (1H, d, *J*=7.9 Hz, H-5), 7.70 (1H, d, *J*=7.9 Hz, H-8), 7.55 (1H, t, *J*=7.9 Hz, H-7) and 7.23 (1H, t, *J*=7.9 Hz, H-6) were observed in the ^{1}H NMR and COSY spectra (Figure 29 and Figrue 30). A 2,3,4-trisubstituted pyridine ring was confirmed by the HMBC correlations of H-3 (δ_H 8.33, d, *J*=5.2 Hz) with C-1 (δ_C 142.9) and C-4a (δ_C 128.9) and H-4 (δ_H 8.10, d, *J*=5.2 Hz) with C-9a (δ_C 132.9). A proton on an amino group

at δ_H 10.84 (1H, s, NH) was coupled with the carbons of the 1,2-disubstituted benzene ring at δ_C 120.2 (C-4b) and 140.3 (C-8a) and the 2,3,4-trisubstituted pyridine carbons at δ_C 128.9 (C-4a) and 132.9 (C-9a). These spectroscopic data confirmed the 1-substituted *β*-carboline substructure (Rajemiarimoelisoa et al. 2016).

The COSY corrleations and the splitting patterns of the aliphatic protons at δ_H 3.99 (1H, dd, *J*=4.7, 11.6 Hz, H-2′), 3.79 (1H, brs, H-3′), 2.30 (1H, dd, *J*=4.7, 11.6 Hz, H-1′a) and 1.92 (1H, dd, *J*=11.6, 12.8 Hz, H-1′b) led to the identification of an 1,2-dioxygenated propyl group. Based on the HMBC spectra, the oxygenated methylene protons at δ_H 4.09 (1H, d, *J*=12.1 Hz, H-5′a) was coupled to the dioxygenated quaternary carbon at δc 102.6 (C-4′). In the HMBC spectrum, correlations of H-5′a with C-2′ (δc 64.9) and C-3′ (δc 67.0) suggested a 2,3,4,4-tetrasubstituted tetrahydrofuran ring. The hydroxy proton at δ_H 2.98 (1H, s, OH) was coupled to the dioxygenated quaternary carbon at C-4′. The HMBC correlation between H-1′b and C-1 suggested a connection between C-1 and C-1′. Based on the above spectral data, the structure of **14** was determined to be (3,4-epoxy-4-hydroxytetrahydrofuranyl)-harmane.

It was suggested that the hydrogen atom at C-2′, C-3′ and the hydroxy group at C-4′ were in the same orientation according to NOE correlation of δ_H 2.98 (4′-OH) with δ_H 3.88 (H-5′b) and of δ_H 3.99 (H-2′) with δ_H 3.79 (H-3′) and 3.88 (H-5′b). Therefore, there were only two possible structures for **14** with absolute configurations of **14A** (2′*S*, 3′*R*, 4′*S*) or **14B** (2′*R*, 3′*S*, 4′*R*). The absolute configuration was established by the calculated ECD spectra using the time-

dependent density funbctional theory (TDDFT) method. A conformational search using molecular mechanics force field yielded two possible conformers of each configuration. The ECD spectra of the optimized conformers were calculated at the B_3LYP/def-SV(P) level with the COSMO model in MeOH (Won et al. 2012) and computed as Boltzmann-weighted averages. The experimental CD spectrum of **14**, with the positive Cotton effects at 240 and 287 nm, correspinded with computed ECD spectrum of **14A**. Thus, compound **14** was established to be (2′*S*, 3′*R*, 4′*S*)-(3,4-epoxy-4-hydroxytetrahydrofuranyl)-harmane and named houttycorine. This compound was isolated for the first time from nature.

MS fragmentation prediction was suggested as Figure 35. Biosynthetically, compound **14** might rationally be generated from a tryptamine and a galactose, as seen in Figure 36 (Dewick 2009).

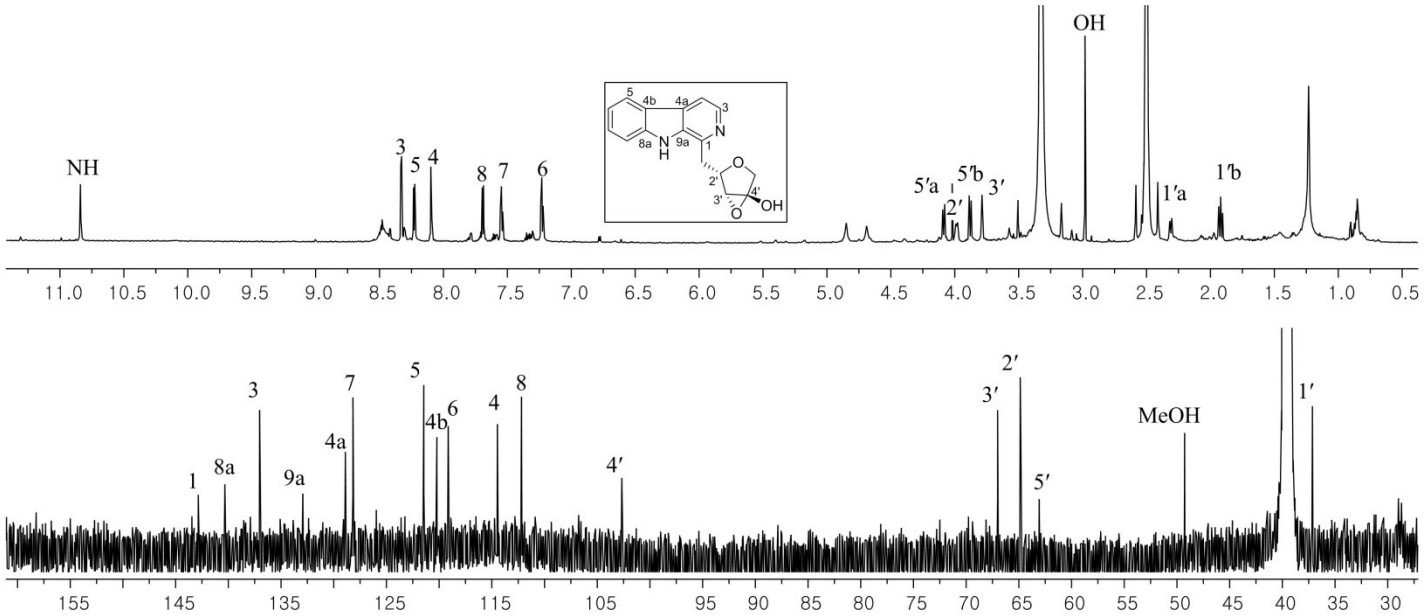

Figure 29. ^{1}H and ^{13}C NMR spectra of compound **14** (DMSO-d_6, 800/200 MHz)

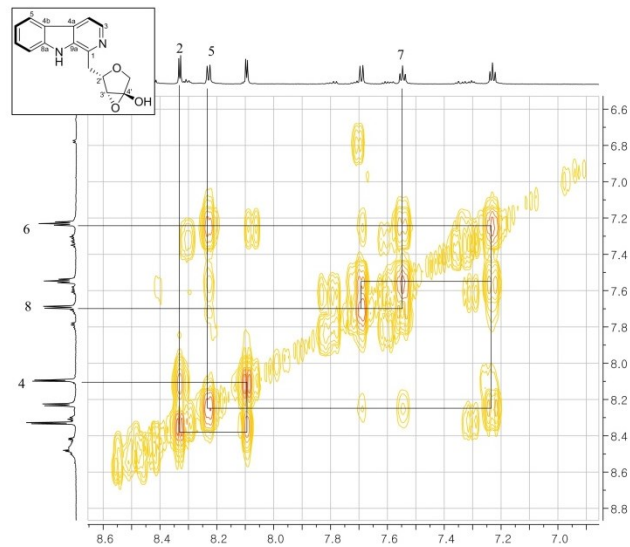

Figure 30. The COSY spectrum of compound **14** (DMSO-d_6, 600 MHz) (1)

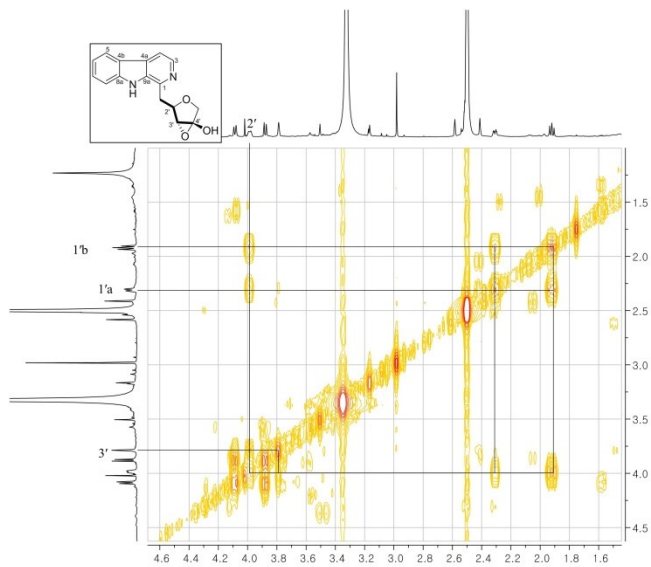

Figure 31. The COSY spectrum of compound **14** (DMSO-d_6, 600 MHz) (2)

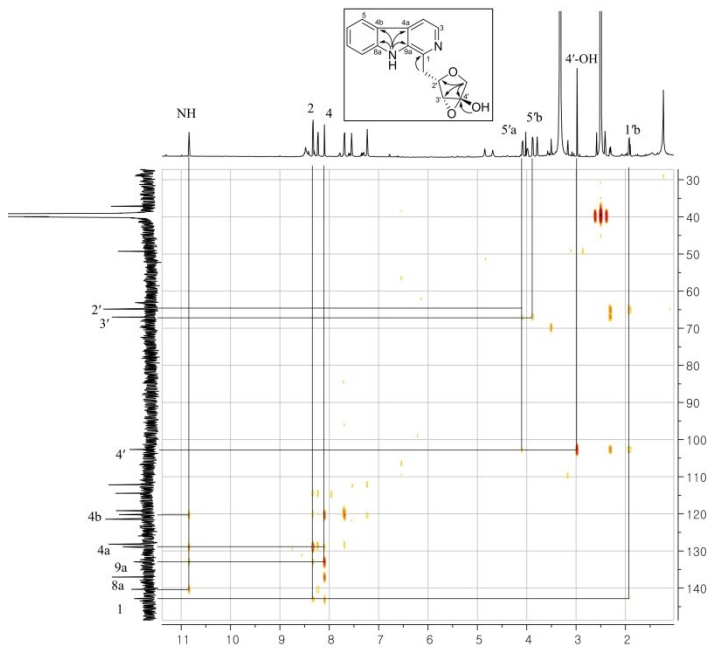

Figure 32. The HMBC spectrum of compound **14** (DMSO-d_6, 600 MHz)

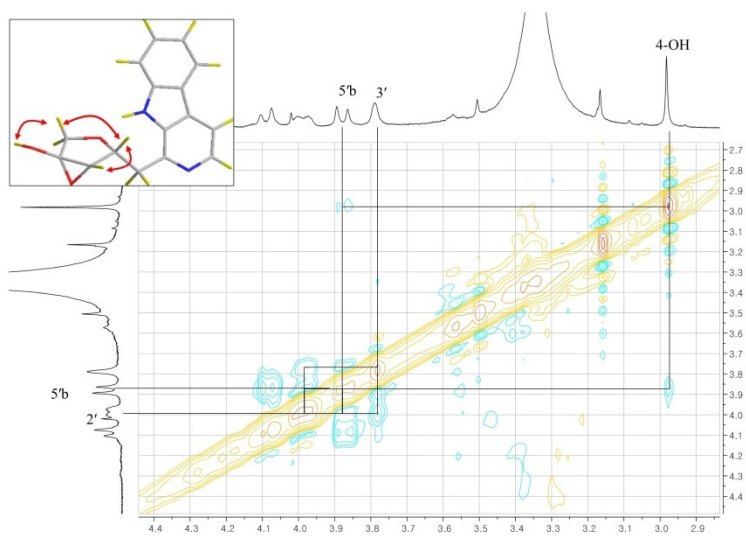

Figure 33. The NOESY spectrum of compound **14** (DMSO-d_6, 400 MHz)

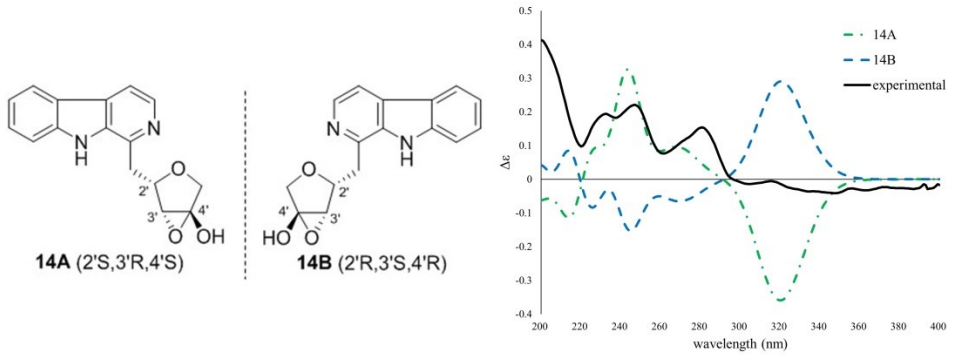

Figure 34. Structures of model compounds and the ECD spectra of **14** (experimental), **14A** and **14B** (calculated)

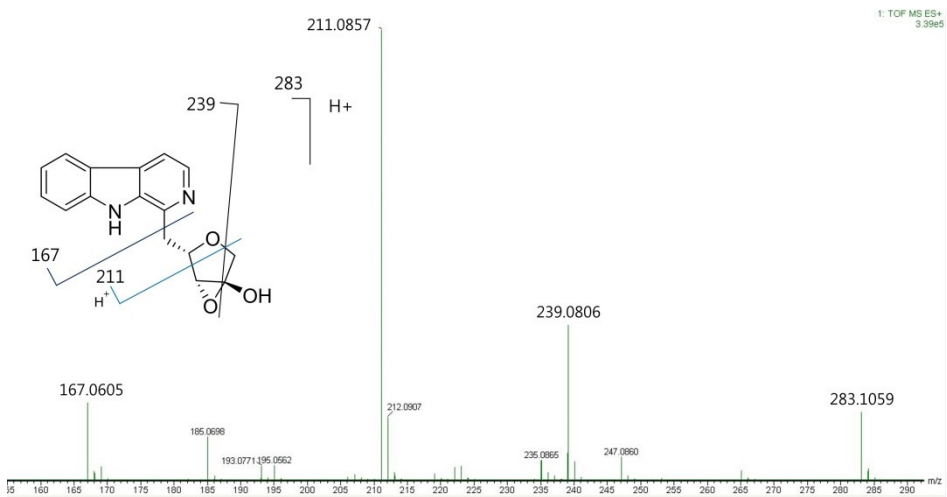

Figure 35. MS fragmentation prediction of compound **14**

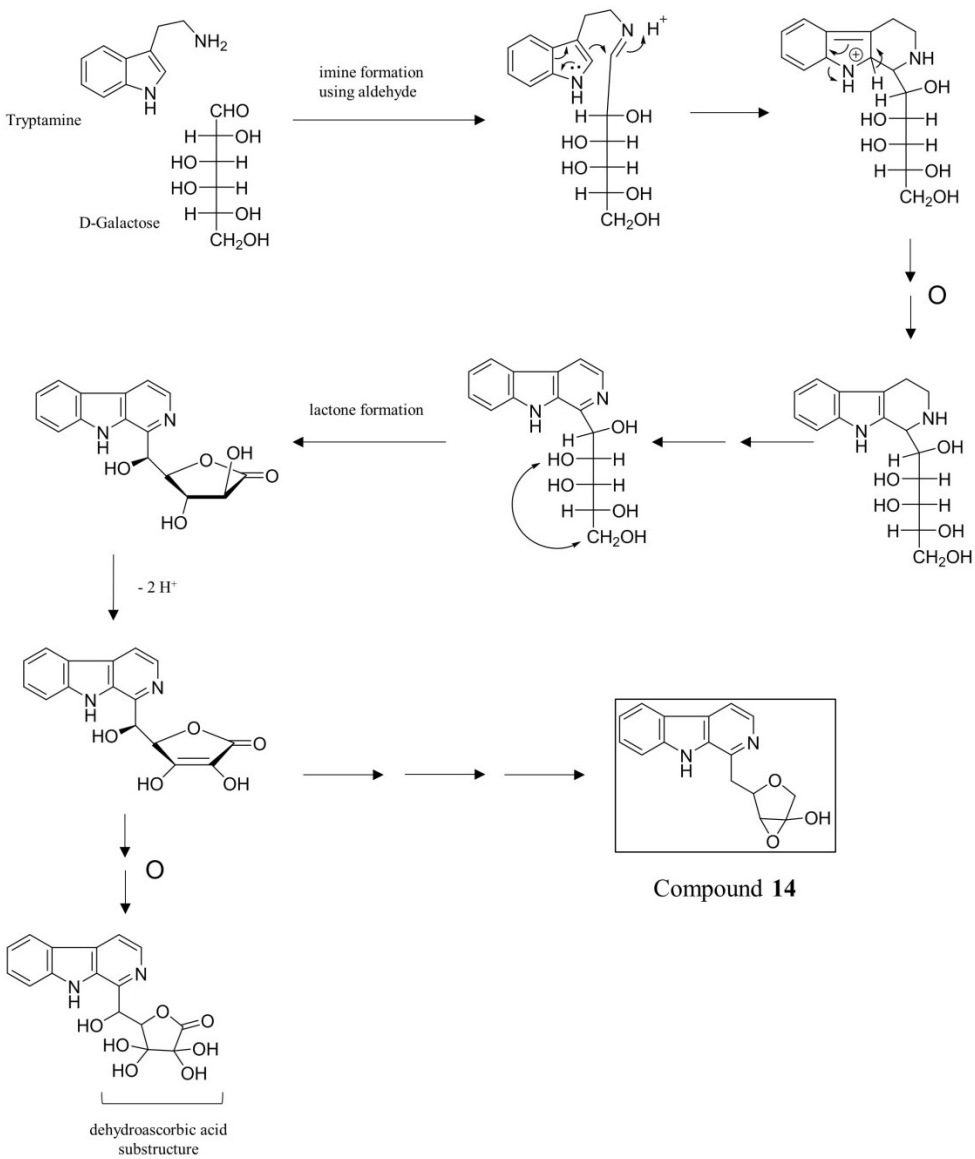

Figure 36. Possible biosynthetic pathways of compound **14**

3.1.8. Compound **15**

Compound **15** was isolated as a yellow amorphous powder. Its molecular formula was determined to be $C_{16}H_{12}N_2O_2$ by ESI-QTOF-MS based on the protonated molecular ion peak at *m/z* 265.0975 $[M+H]^+$ (calcd. for $C_{16}H_{13}N_2O_2$, 265.0972). ^{13}C NMR (Figure 37) and HSQC spectra showed 16 carbons including a *β*-carboline moiety, four olefinic carbons at δ_C 157.3, 154.0, 111.1 and 111.0 and an oxygenated methylene carbon at δ_C 57.1. The chemical shifts and splitting patterns of olefinic protons at δ_H 7.23 (1H, d, *J*=3.0 Hz, H-4′) and 6.60 (1H, d, *J*=3.0 Hz, H-3′) suggested an 1,4-disubstituted furan ring. Compound **15** was identified and confirmed as perlolyrine by comparison with the literature (Ying et al. 2013).

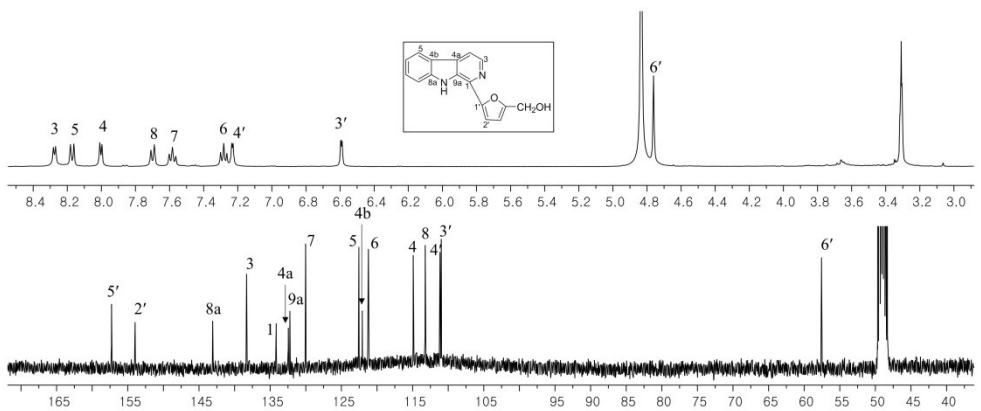

Figure 37. ^1H and ^{13}C NMR spectra of compound **15** (CD_3OD, 300/75 MHz)

3.1.9. Compound **16**

Compound **16** was isolated as a yellow amorphous powder. Its molecular formula was determined to be $C_9H_7NO_2$ by ESI-QTOF-MS based on the protonated molecular ion peak at *m/z* 162.0553 $[M+H]^+$ (calcd. for $C_9H_8NO_2$, 162.0550). ^{13}C NMR spectrum (Figure 38) showed a carbonyl carbon at δ_C 170.0 and aromatic carbons at δ_C 139.0 (C-9), 134.2 (C-2), 128.4 (C-8), 124.4 (C-4), 123.2 (C-6), 122.8 (C-7), 113.7 (C-7) and 109.6 (C-3). Compound **16** was identified and confirmed as indole-3-carboxylic acid by comparison with the literature (Nemoto et al. 2016).

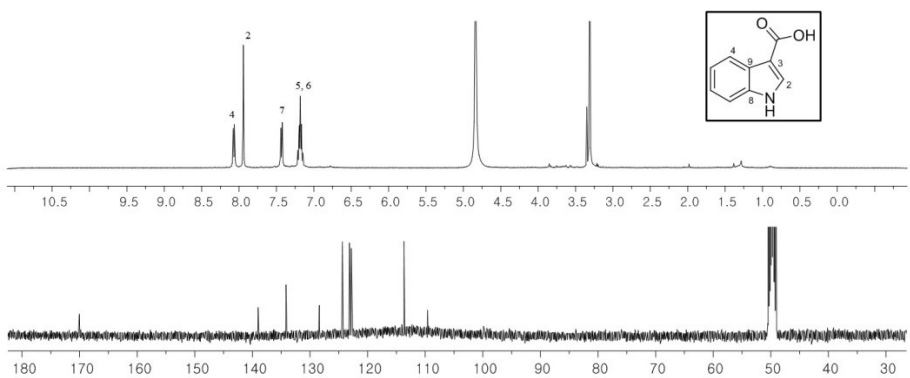

Figure 38. ^1H and ^{13}C NMR spectra of compound **16** (CD_3OD, 400/100 MHz)

3.1.10. Compound **17**

Compound **17** was obtained as a yellowish amorphous powder. Its molecular formula was determined to be $C_6H_6N_2O$ by ESI-QTOF-MS based on the protonated molecular ion peak at *m/z* 123.0559 $[M+H]^+$ (calcd. for $C_6H_7N_2O$, 123.0553). In the IR spectrum, absorption bands indicative of a primary amide group (3363, 3283 and 1680 cm^{-1}) were observed. The 3-substituted heteroaromatic protons at δ_H 9.03 (1H, brs, H-2), 8.69 (1H, brs, H-6), 8.28 (1H, d, *J* = 7.9 Hz, H-4) and 7.53 (1H, dd, *J* = 4.5, 7.9 Hz, H-5) were observed in the ^1H NMR spectrum (Figure 39). The HMBC spectrum showed the correlations of δ_C 169.8 (C=O) with H-2, H-4 and H-5. Compound **17** was identified and confirmed as nicotinamide by comparison with the literature (Kumar & Das 2013).

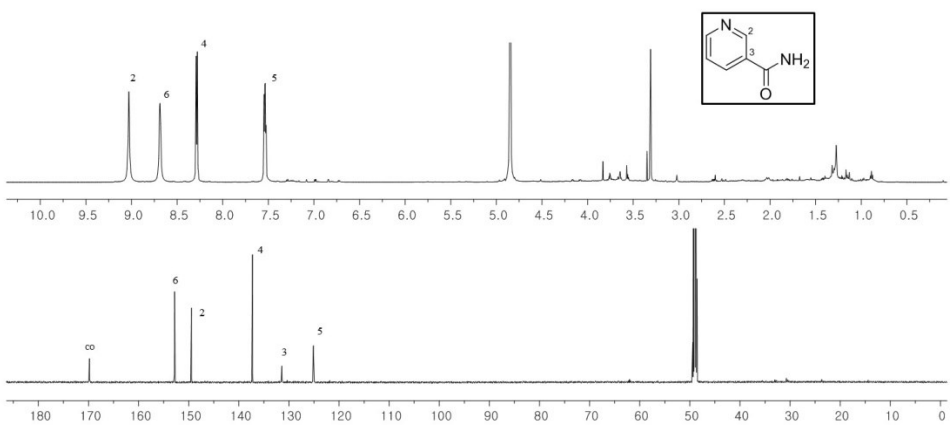

Figure 39. ^1H and ^{13}C NMR spectra of compound **17** (CD_3OD, 600/125 MHz)

3.1.11. Compound **18**

Compound **18**, a colorless syrup, was determined to have a molecular formula of C_9H_7NO by the ESI-QTOF-MS, which showed the protonated ion at *m/z* 146.0604 $[M+H]^+$ (calcd. for C_9H_8NO, 146.0600). ^1H NMR spectrum showed an 1,2-substituted benzene ring at δ_H 8.26 (1H, dd, *J* = 1.4, 8.2 Hz, H-5), 7.70 (1H, m, H-7), 7.58 (1H, d, *J* = 8.2 Hz, H-8), 7.43 (1H, m, H-6) and *cis*-olefinic protons at δ_H 7.98 (1H, d, *J* = 7.4 Hz, H-2), 6.34 (1H, d, *J* = 7.4 Hz, H-3) (Figure 40). The HMBC correlations of H-2 between a carbonyl carbon (δ_C 180.8) and C-9 (δ_C 141.5) and between H-5 and a carbonyl carbon and between H-3 and C-10 (δ_C 126.7) were observed. Based on these data, compound **18** was identified as 4-(1*H*)-quinolinone and confirmed by comparison with the literature (Almeida et al. 2010).

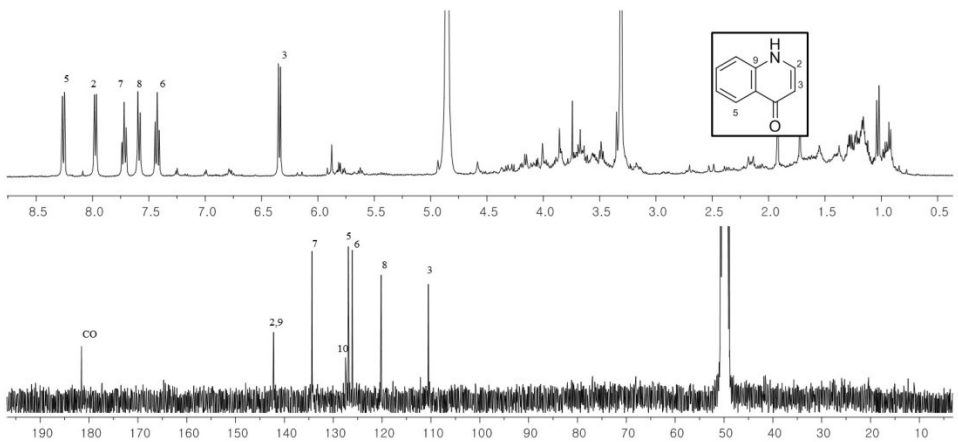

Figure 40. ^1H and ^{13}C NMR spectra of compound **18** (CD_3OD, 300/75 MHz)

3.1.12. Compounds **19**, **20**

Compound **19** was obtained as an amorphous white powder. Its molecular formula was determined to be $C_{10}H_{13}N_5O_4$ by ESI-QTOF-MS based on the pseudo-molecular ion peak at *m/z* 266.0879 $[M-H]^-$ (calcd. for $C_{10}H_{12}N_5O_4$, 266.0895). ^1H NMR spectrum showed two olefinic singlets at δ_H 8.34 (1H, s, H-8) and 8.14 (1H, s, H-2), amine protons at δ_H 7.32 (2H, s, NH_2) and an anomeric proton at δ_H 5.88 (1H, d, *J*=6.1 Hz, H-1′) (Figure 41). By analysis of the spectral data, compound **19** was identified as adenosine (Xia et al. 2014).

Compound **20** was isolated as a white amorphous powder. Its molecular formula was $C_{11}H_{15}N_5O_4S$ based on the ESI-MS (*m/z* 314.1, $[M+H]^+$) and ^{13}C NMR data. 1D NMR spectra of compound **20** (Figure 42) were similar to those of compound **19**. By comparison with compound **19**, a deshielded singlet methyl group (δ_C 39.0/ δ_H 2.56) was observed. In addition, C-3′ and C-5′ in the upfield region and C-4′ in the downfield region were observed under the influence of a methylsulfinyl group. In MS spectrum, a characteristic feature of sulfur compounds, significant M+2 peak, was observed. This peak arises from the presence of the heavy isotope, ^{34}S, which has a natural abundance of 4.4%. With above observed spectral data and literature (Kawagishi et al. 1993), compound **20** was identified and confirmed as 5′-deoxy-5′-methylsulfinyladenosine.

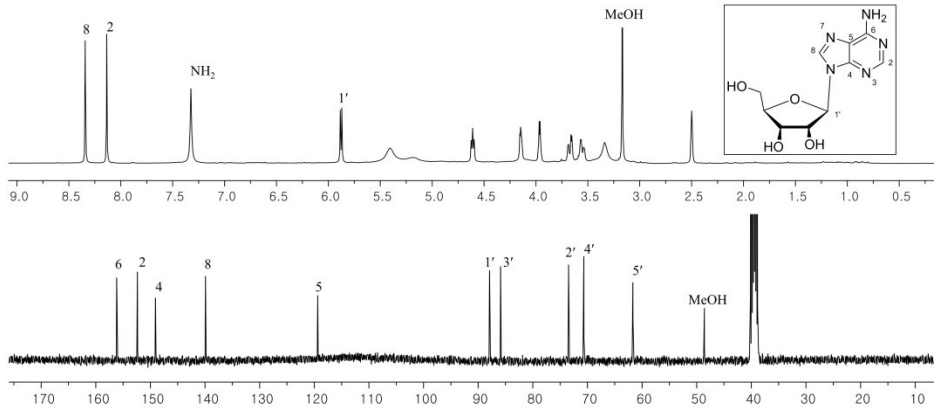

Figure 41. ^{1}H and ^{13}C NMR spectra of compound **19** (DMSO-d_6, 400/100 MHz)

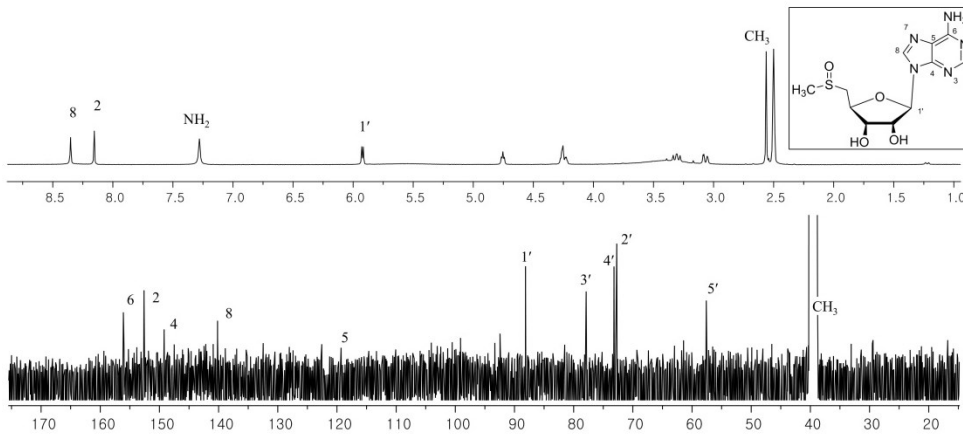

Figure 42. ^{1}H and ^{13}C NMR spectra of compound **20** (DMSO-d_6, 400/100 MHz)

3.1.13. Compound **21**

Compound **21** was obtained as an amorphous white powder. Its molecular formula was determined to be $C_9H_{12}N_2O_6$ by ESI-MS at *m/z* 245.1 $[M+H]^+$ and ^{13}C NMR data. ^{13}C NMR spectrum showed 9 carbons at δ_C 167.0 (C-6), 153.2 (C-2), 143.5 (C-4), 103.4 (C-5), 91.4 (C-1′), 87.1 (C-4′), 76.5 (C-2′), 72.1 (C-3′) and 63.1 (C-5′). The *cis*-olefinic protons at δ_H 8.00 (1H, d, *J*=8.1 Hz, H-4) and 5.68 (1H, d, *J*=8.1 Hz, H-5) and an anomeric proton at δ_H 5.89 (1H, d, *J*=4.6 Hz, H-1′) were observed in the ^1H NMR spectrum (Figure 43). Based on these data and comparison with the previously reported reference (Kumar et al. 2014), compound **21** was identified as uridine.

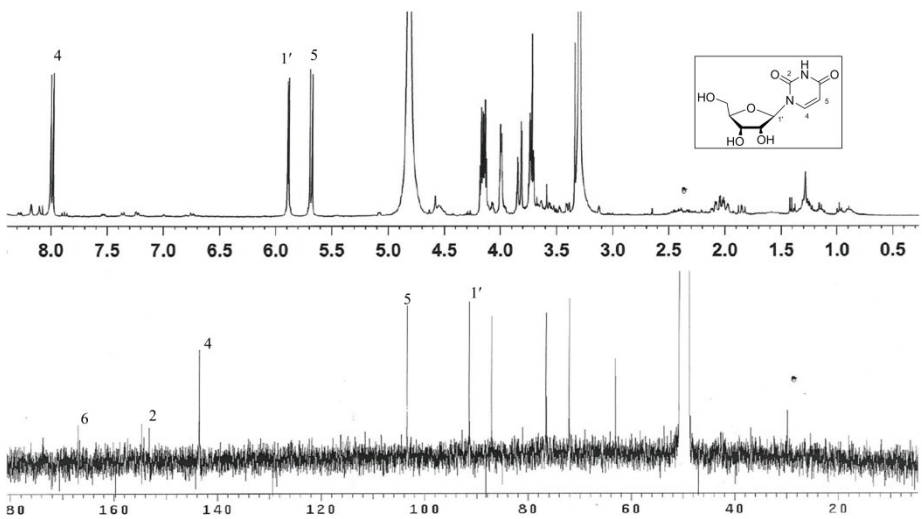

Figure 43. ^1H and ^{13}C NMR spectra of compound **21** (DMSO-d_6, 300/75 MHz)

3.2. Inhibitory activity of alkaloids isolated from *H. cordata* on NO production in LPS-stimulated RAW264.7 cells

The alkaloids from aerial parts of *H. cordata* were tested for their inhibitory effects on LPS-induced NO production in RAW 264.7 cells. Dexamethasone was used as a positive control and its IC_{50} was 7.0 μM. Of the tested compounds, compound **15**, one of *β*-carboline alkaloids, showed significant inhibitory activity on NO production with IC_{50} values of 8.7 μM. Cell viability was measured by MTT assay.

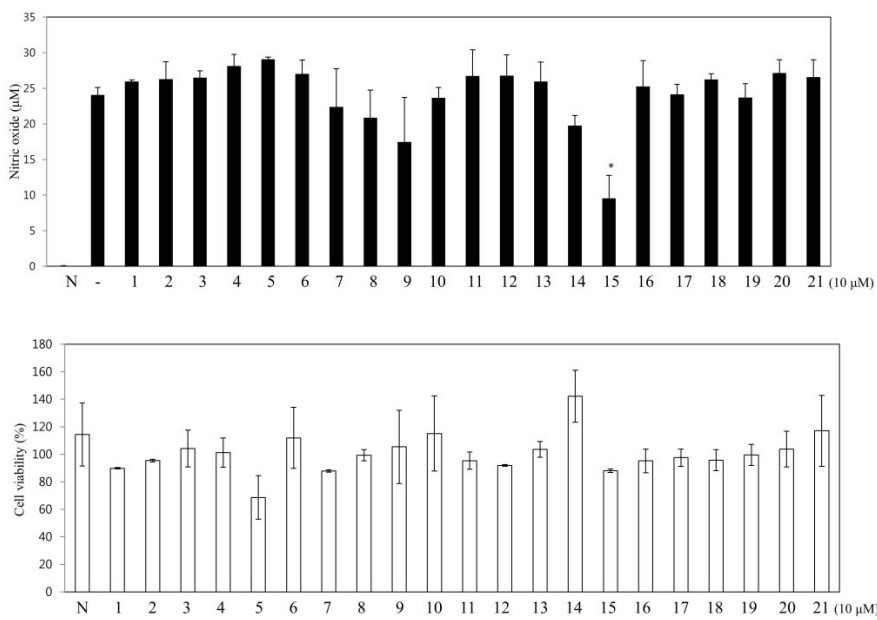

Figure 44. The inhibitory activity of the alkaloids from aerial parts of *H. cordata* on NO production in LPS-stimulated RAW 264.7 cells. The values are presented as the mean ± S.E.M. Results differ significantly from LPS alone, **P*<0.01, ***P*<0.001

3.3. Structural elucidation of further isolated constituents from *H. cordata*

3.3.1. Compounds **22-24**

Compound **22** was obtained as an amorphous yellowish powder. Its molecular formula was determined to be $C_{15}H_{10}O_6$ by ESI-MS at *m/z* 287.3 $[M+H]^+$ and ^{13}C NMR data. ^1H NMR spectrum showed two *meta*-coupled aromatic protons at δ_H 6.42 (1H, brs, H-8) and 6.16 (1H, brs, H-6), three 1,3,4-trisubstituted aromatic protons at δ_H 7.38 (1H, d, *J*=8.3 Hz, H-6′), 7.37 (1H, brs, H-2′) and 6.86 (1H, d, *J*=8.3 Hz, H-5′) and an olefinic siglet at δ_H 6.64 (1H, s, H-3), which indicated that compound **22** had a flavone moiety (Figure 45). Based on these spectral data, compound **22** was identified as luteolin (Xu et al. 2009).

Compound **23** was isolated as yellowish amorphous powder. Its molecular formula was $C_{15}H_{10}O_7$ based on the ESI-MS at *m/z* 301.0 $[M-H]^-$ and ^{13}C NMR data. ^1H NMR spectrum (Figure 46) was similar to compound **22** except for absence of H-3, which implied a flavonol moiety. With these spectral data and literature (Jung & Park 2007), compound **23** was identified and confirmed as quercetin.

Compound **24**, a yellowish amorphous powder, was determined to have a molecular formula of $C_{15}H_{10}O_5$ by the ^{13}C NMR and ESI-MS (*m/z* 269.1 $[M-H]^-$). 1D NMR spectra (Figure 47) were similar to compound **22**, but the B ring showed difference. The B ring was suggested to be an 1,4-disubstituted aromatic ring at δ_H 7.91 (2H, d, *J*=8.2 Hz, H-2′, 6′) and 6.92 (2H, d, *J*=8.2 Hz, H-3′, 5′). Based on these data, compound **24** was identified as apigenin and confirmed by comparison

with the literature (Wu-Bao et al. 2005).

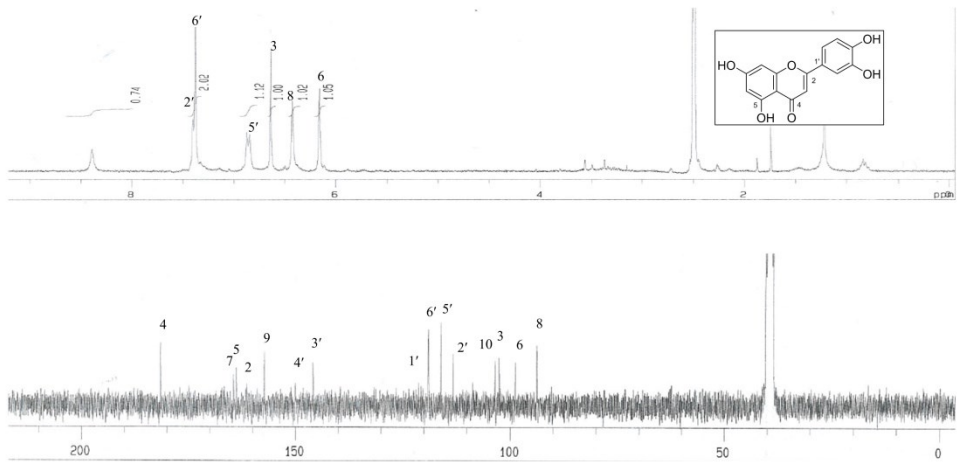

Figure 45. ^{1}H and ^{13}C NMR spectra of compound **22** (DMSO-d_6, 300/75 MHz)

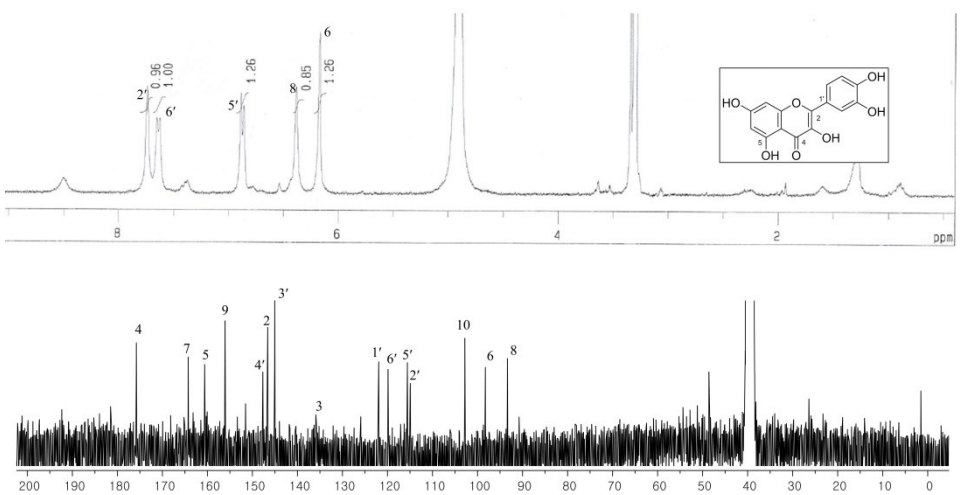

Figure 46. ^{1}H and ^{13}C NMR spectra of compound **23** (DMSO-d_6, 300/75 MHz)

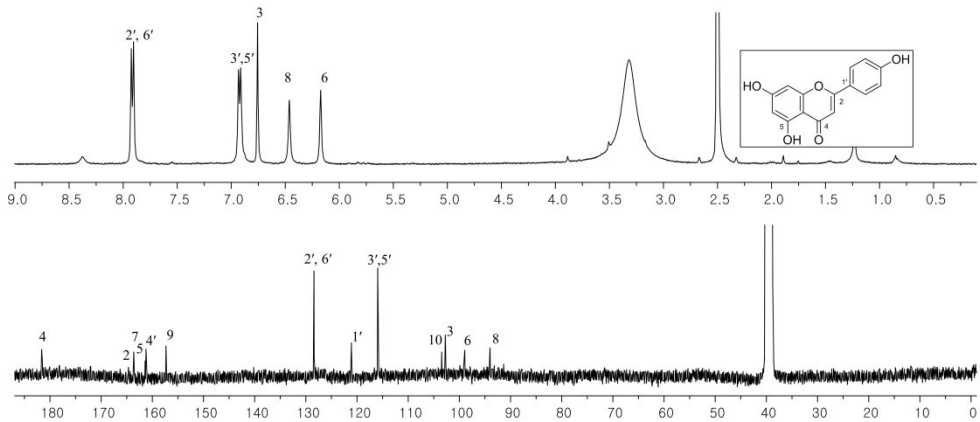

Figure 47. ^{1}H and ^{13}C NMR spectra of compound **24** (DMSO-d_6, 400/100 MHz)

3.3.2. Compounds **25**-**27**

Compound **25** was obtained as an amorphous yellowish powder. Its molecular formula was determined to be $C_{21}H_{20}O_{10}$ by ESI-MS at *m/z* 432.8 $[M+H]^+$ and ^{13}C NMR data. ^{1}H NMR spectrum (Figure 48) showed two *meta*-coupled aromatic protons at δ_H 6.31 (1H, d, *J*=2.1 Hz, H-8) and 6.15 (1H, d, *J*=2.1 Hz, H-6), an 1,4-disubstituted aromatic ring at δ_H 7.73 (2H, dt, *J*=8.8, 2.1 Hz, H-2′, 6′) and 6.89 (2H, dt, *J*=8.8, 2.1 Hz, H-3′, 5′) and an anomeric proton at δ_H 5.35 (1H, d, *J*=1.6 Hz, H-1″), suggesting the sugar-substituted kaempferol. The sugar moiety was established by the HPLC spectrum of the acid hydrolysate, with analysis of 1D NMR spectra. A rhamnopyranosyl moiety (δ_C 104.3, 74.0, 72.9, 72.8, 72.7 and 18.4) was observed in the ^{13}C NMR spectrum. The absolute stereochemistry of the sugar was determined to be L-rhamnose using HPLC analysis of the acid hydrolysate (Tanaka

et al. 2007). The sugar moiety were defined as an *α*-rhamnose by coupling constants of the anomeric protons. Based on these spectral data and comparison with literature, compound **25** was identified as afzelin (Jiang et al. 2014).

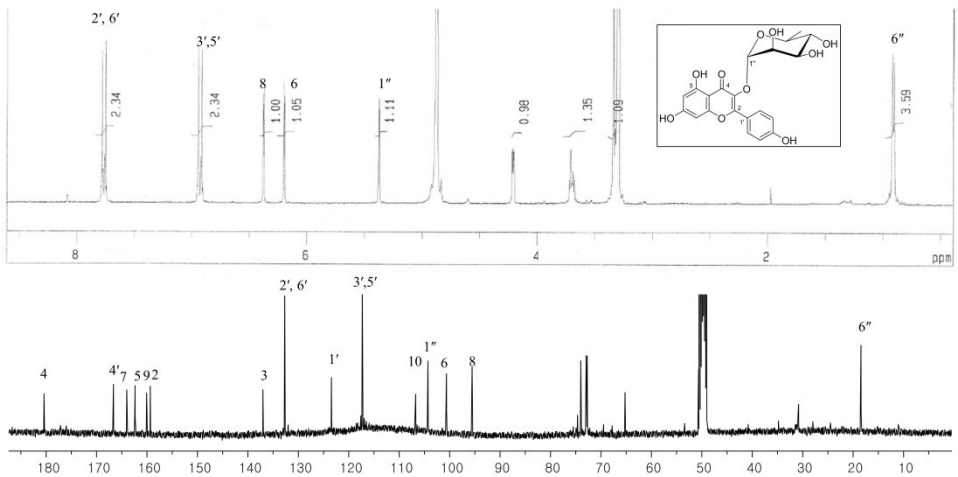

Figure 48. ^{1}H and ^{13}C NMR spectra of compound **25** (CD_3OD, 300/100 MHz)

Compound **26** was isolated as a yellowish amorphous powder. Its molecular formula was $C_{21}H_{20}O_{11}$ based on the ESI-MS at *m/z* 448.9 $[M+H]^+$ and ^{13}C NMR data. ^{1}H NMR spectrum was similar to compound **25** except for the B ring, which was suggested to be an 1,3,4-trisubstituted benzene ring at δ_H 7.30 (1H, d, *J*=1.9 Hz, H-2′), 7.29 (1H, dd, *J*=8.5, 1.9 Hz, H-6′) and 6.89 (1H, d, *J*=8.5 Hz, H-5′) (Figure 49). The absolute stereochemistry of the sugar was assigned to be L-rhamnose using HPLC analysis of the acid hydrolysate (Tanaka et al. 2007). With these spectral data and literature (Lee et al. 2014), compound **26** was identified and confirmed as quercitrin.

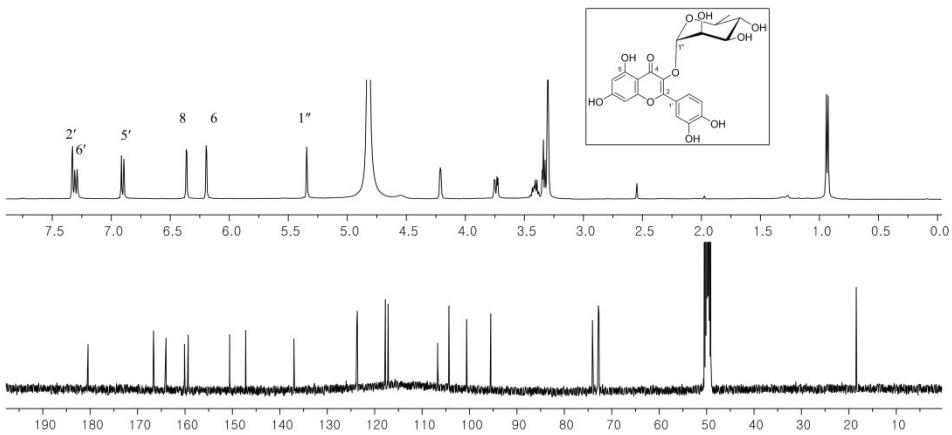

Figure 49. ^{1}H and ^{13}C NMR spectra of compound **26** (CD_3OD, 400/100 MHz)

Compound **27** was obtained as a yellowish amorphous powder. Its molecular formula was $C_{21}H_{20}O_{12}$ based on the ESI-MS at *m/z* 465.0 $[M+H]^+$ and ^{13}C NMR data. ^{1}H NMR spectrum was similar to compound **26** except for the signals corresponding to a sugar moiety. A galactopyranosyl moiety (δ_C 101.8, 75.8, 73.1, 71.2, 67.9 and 60.1) was observed in the ^{13}C NMR spectrum (Figure 50). The absolute stereochemistry of the sugar was assigned to be D-galactose using HPLC analysis of the acid hydrolysate (Tanaka et al. 2007). With these spectral data and literature (Jiang et al. 2014), compound **27** was identified and confirmed as hyperoside.

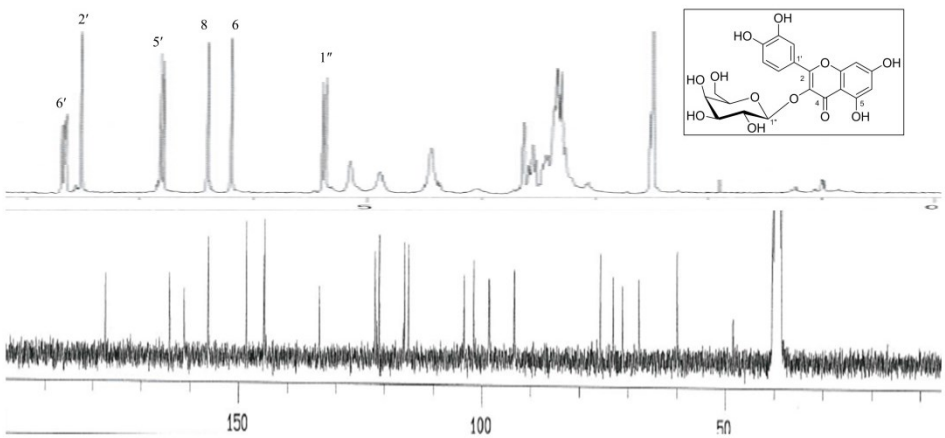

Figure 50. ^{1}H and ^{13}C NMR spectra of compound **27** (DMSO-d_6, 300/75 MHz)

3.3.3. Compounds **28**, **29**

Compound **28** was obtained as an amorphous yellowish powder. Its molecular formula was determined to be $C_{27}H_{30}O_{15}$ by ESI-MS at *m/z* 595.1 $[M+H]^+$ and ^{13}C NMR data. ^{1}H NMR spectrum (Figure 51) showed a kaempferol moiety and two anomeric proton at δ_H 5.30 (1H, brs, H-1″) and 5.10 (1H, d, *J*=7.2 Hz, H-1‴). The sugar moieties were established by the HPLC spectra of the acid hydrolysate, with analysis of 1D NMR spectra. A rhamnopyranosyl moiety (δ_C 101.8, 71.1, 70.7, 70.4, 70.1 and 17.5) and a glucopyranosyl moiety (δ_C 99.9, 77.2, 76.4, 73.1, 69.6 and 60.6) were observed in the ^{13}C NMR spectrum. The absolute stereochemistry of the sugars were determined to be L-rhamnose and D-glucose using HPLC analysis of the acid hydrolysate (Tanaka et al. 2007). The sugar moieties were defined as an *α*-rhamnose and *β*-glucose by coupling constants of the anomeric protons. From HMBC spectrum, the correlation between H-1″ and C-3 (δ_C 134.4) and between H-1‴ and C-7 (δ_C 162.9) suggested position of sugars in kaempferol

moiety. Based on these spectral data and comparison with literature (Sharaf et al. 1997), compound **28** was identified as kaempferol-3-*O*-*α*-L-rhamnopyranosyl-7-*O*-*β*-D-glucopyranoside.

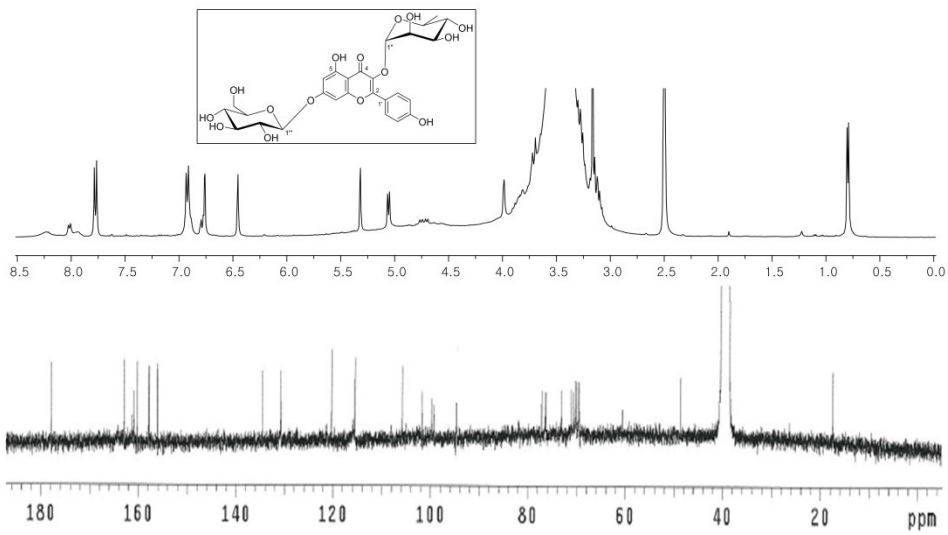

Figure 51. ^{1}H and ^{13}C NMR spectra of compound **28** (DMSO-d_6, 400/75 MHz)

Compound **29** was obtained as a yellowish amorphous powder. Its molecular formula was $C_{27}H_{30}O_{16}$ based on the ESI-MS at *m/z* 611.1 $[M+H]^+$ and ^{13}C NMR data. 1D NMR spectra were similar to compound **28** except for the B ring. The B ring was suggested to be an 1,3,4-trisubstituted aromatic ring at δ_H 7.32 (1H, d, *J*=2.4 Hz, H-2′), 7.26 (1H, dd, *J*=8.3, 2.4 Hz, H-6′) and 6.88 (1H, d, *J*=8.3 Hz, H-5′) (Figure 52). The absolute stereochemistry of the sugars was assigned to be L-rhamnose and D-glucose using HPLC analysis of the acid hydrolysate (Tanaka et al. 2007). The HMBC correlation of H-1″ with C-3 (δ_C 134.4) and H-1‴ with C-7 (δ_C 162.9) suggested position of sugars in quercetin moiety. With these spectral data

and literature (Lee et al. 2014), compound **29** was identified and confirmed as quercetin-3-*O*-*α*-L-rhamnopyranosyl-7-*O*-*β*-D-glucopyranoside.

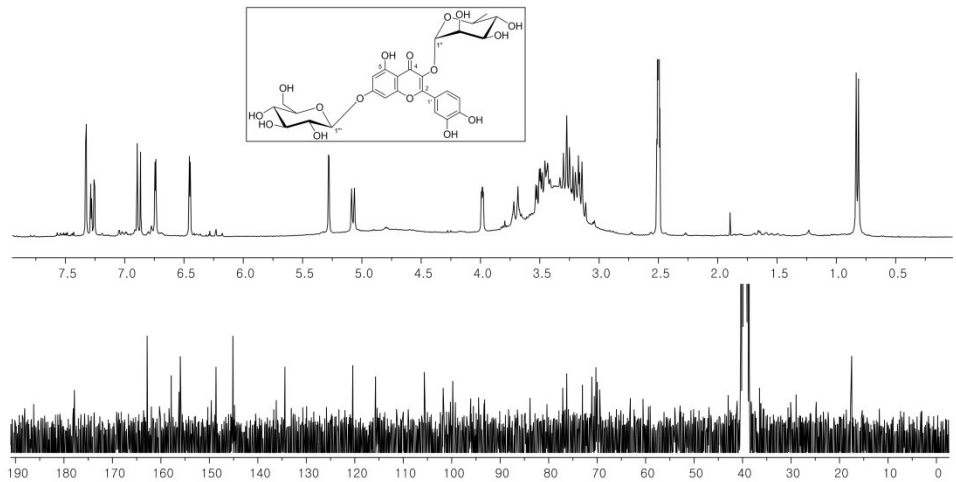

Figure 52. ^{1}H and ^{13}C NMR spectra of compound **29** (DMSO-*d*$_6$, 300/75 MHz)

3.3.4. Compounds **30**, **31**

Compound **30** was isolated as an amorphous brown powder. Its molecular formula was established as $C_{13}H_{24}O_4$ on the basis of ESI-QTOF-MS data with an adduct ion at *m/z* 289.1645 $[M+HCOO]^-$ (calcd. for $C_{14}H_{25}O_6$, 289.1657).

^{1}H NMR and HSQC spectra showed two (*E*)-olefinic protons at δ_H 6.06 (1H, d, *J*=15.8 Hz, H-7) and 5.78 (1H, dd, *J*=15.8, 6.1 Hz, H-8), two oxygenated methine protons at δ_H 4.34 (1H, m, H-9) and 4.05 (1H, m, H-3), two methylene groups at δ_H 1.78 (1H, m, H-4a), 1.73 (1H, m, H-4b), 1.65 (1H, dd, *J*=12.4, 12.4 Hz, H-2a) and 1.44 (1H, dd, *J*=12.4, 3.6 Hz, H-2b) and four methyl groups at δ_H 1.27 (3H, d, *J*=6.4 Hz, H-10), 1.20 (3H, s, H-11), 1.14 (3H, s, H-13), 0.84 (3H, s, H-12) (Figure 53).

The sequential COSY correlation of H-7, H-8, H-9 and H-10 suggested a 3-hydroxybutenyl group. In the HMBC spectrum, H-7 was coupled with an oxygenated quaternary carbon at δ_C 78.9 (C-6). The COSY correlation between H-3 and hydrogens of C-2 and C-4 suggested the presence of 2-hydroxypropyl group. From the HMBC spectrum, the correlations of geminal dimethyl protons (H-11 and H-12) with C-1 (δ_C 40.7), C-2 (δ_C 46.4) and C-6 and another methyl proton (H-13) with C-4 (δ_C 45.7), C-5 (δ_C 77.8) and C-6 were observed. With these spectral data and literature (Otsuka et al. 2003), compound **30** was identified and confirmed as megastigman-7-ene-3,5,6,9-tetrol.

In the ^{1}H NMR spectrum, the magnitude of interaction between H-2a and H-3 and between H-3 and H-4b were approximately 12 Hz, indicating that the hydrogen atom at the C-3 position must be in the axial orientation in the megastigmane skeleton. From NOESY spectrum, no cross-signal between H-3 and H-13 indicated that a methyl group at the 5-position was in the equatorial orientation. The side chain at the C-6 was confirmed to be in equatorial orientation by the NOESY correlation of H-3 with H-11 and of H-11 (axial methyl group) with H-7. From compound **30**, (*R*)- and (*S*)-MTPA esters were prepared. Based on ^{1}H NMR spectral analysis, the abolute configuration was established to be 3*S*, 5*R*, 6*R*, 9*R*. Accordingly, compound **30** was established as (3*S*, 5*R*, 6*R*, 9*R*)-megastigman-7-ene-3,5,6,9-tetrol.

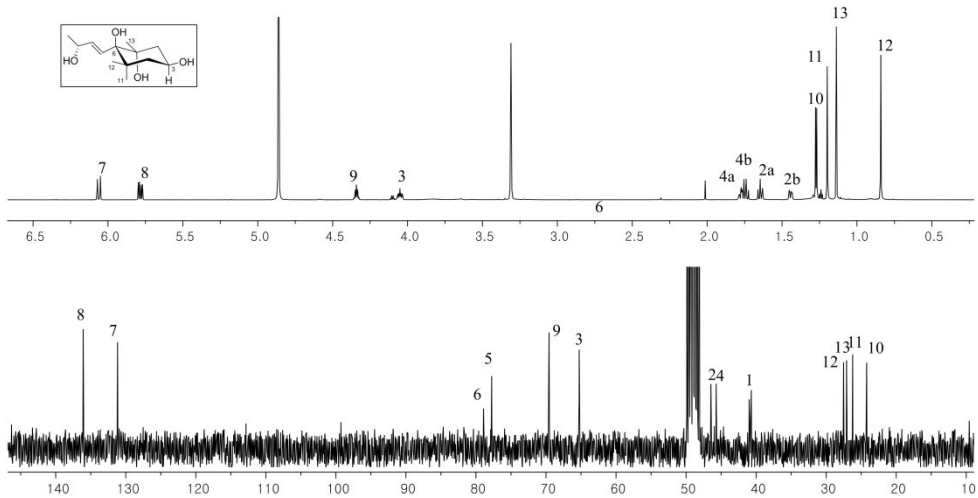

Figure 53. ^{1}H and ^{13}C NMR spectra of compound **30** (CD_3OD, 300/75 MHz)

Compound **31** was obtained as an amorphous white powder. Its molecular formula was established as $C_{19}H_{34}O_9$ on the basis of ESI-QTOF-MS data with a pseudo-molecular ion peak at *m/z* 405.2134 $[M-H]^-$ (calcd. for $C_{19}H_{33}O_9$, 405.2130). The ^{13}C NMR spectrum (Figure 54) was similar to those of **30**, but six more signal indicative of a sugar moiety was observed. The HPLC analysis of the acid hydrolysate and splitting pattern of an anomeric proton at δ_H 4.34 (1H, d, *J*=7.7 Hz, H-1′) confirmed that a sugar in **31** was a *β*-D-glucopyranoside. Based on these spectral data, compound **31** was determined to be megastigman-7-ene-3,5,6,9-tetrol-9-*O*-*β*-D-glucopyranoside (Otsuka et al. 2003).

An upfield shift of C-9 (approximately 74 ppm) is indicative for the (9*S*)-configuration whereas a signal at downfield (approximately 79 ppm) suggest (9*R*)-configuration (Calis et al. 2002). The chemical shift of C-9 of this compound was

δ_C 78.8, indicating (9*R*)-configuration.

^{1}H NMR and NOESY spectra suggested relative configuration of compound **31**. In ^{1}H NMR spectrum, coupling constants (*J*=12.0 and 3.1 Hz, each) between protons at C-2 and H-3 indicated that the hydrogen atom at the C-3 must be in the axial orientation in the megastigmane skeleton. From NOESY spectrum, no cross-signal between H-3 and H-13 indicated that a methyl group at C-5 was in the equatorial orientation. The side chain at the C-6 was confirmed to be in equatorial orientation by the NOESY correlation of H-3 with H-11 (axial methyl group) and of H-11 with H-7. By comparison with the CD spectrum of **30**, compound **31** was suggested to be mixture of diastereomer.

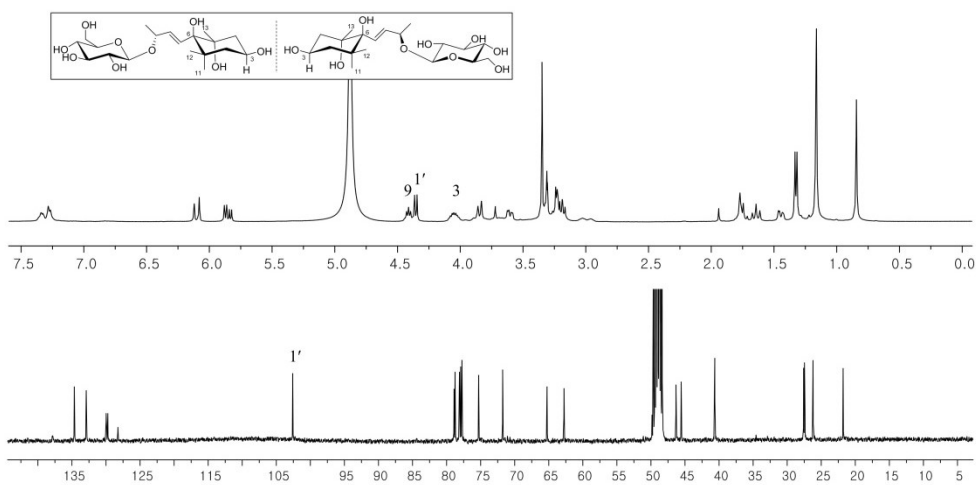

Figure 54. ^{1}H and ^{13}C NMR spectra of compound **31** (CD_3OD, 300/75 MHz)

3.3.5. Compounds **32**, **33**

Compound **32** was isolated as a white amorphous powder. Its molecular formula was established as $C_{19}H_{30}O_8$ from the ESI-MS with an pseudo-molecular ion peak at *m/z* 385.2 $[M-H]^-$ and ^{13}C NMR. The ^{13}C NMR and HSQC spectra showed the presence of 19 carbons including a sugar unit at δ_C 100.8, 76.9, 76.8, 73.7, 70.0 and 61.0, a carbonyl carbon at δ_C 197.3, four olefinic carbons at δ_C 164.0, 133.3, 130.3 and 125.6, a methylene carbon at δ_C 49.3, an oxymethine carbon at δ_C 74.6, two quaternary carbon at δ_C 77.8 and 48.6, a secondary methyl group at δ_C 20.9, three tertiary methyl groups at δ_C 24.1, 23.0 and 18.9 (Figure 55). 1D NMR spectra were similar with compounds **30** and **31**, but compound **32** had an *α*,*β*-unsaturated ketone. An *α*,*β*-unsaturated ketone was indicated by the chemical shifts of the olefinic and a carbonyl carbon at δ_C 197.3, 164.0 and 125.6. The HPLC analysis of the acid hydrolysate and splitting pattern of an anomeric proton at δ_H 4.16 (1H, d, *J*=7.7 Hz, H-1′) confirmed a *β*-D-glucopyranoside moiety. Based on the above spectroscopic data and literature (Calis et al. 2002), compound **32** was identified as roseoside.

The chemical shift of C-9 of this compound was δ_C 74.6, indicating (9*S*)-configuration. The configuration of C-6 was identified as *S* by comparison with the CD spectra of previously reported reference (Calis et al. 2002). The CD spectrum of **32** showed a positive Cotton effect at 240 nm and a negative at 320 nm. Thus, compound **32** was determined to be (6*S*, 9*S*)-roseoside.

Compound **33** was obtained as a white amorphous powder. Its molecular formula was $C_{19}H_{30}O_7$ by the ESI-QTOF-MS based on the protonated ion peak at

m/z 371.2079 $[M+H]^+$ (calcd. for $C_{19}H_{31}O_7$, 371.2064). 1D NMR spectra (Figure 56) were similar to compound **32** except for a methine group [δ_C 57.5 (C-6)/ δ_H 2.72 (1H, d, *J*=9.0 Hz, H-6)] instead of an oxygenated quaternary carbon. The ^{13}C chemical shift of C-9 (δ_C 77.7) deduced that the absolute configuration was (9*R*)-configuration. The CD spectrum of **33** was identical with literature, identifying (6*R*, 9*R*)-configuration (Matsunami et al. 2009). Accordingly, compound **33** was established as (6*R*, 9*R*)-3-oxo-*α*-ionyl-*β*-D-glucopyranoside.

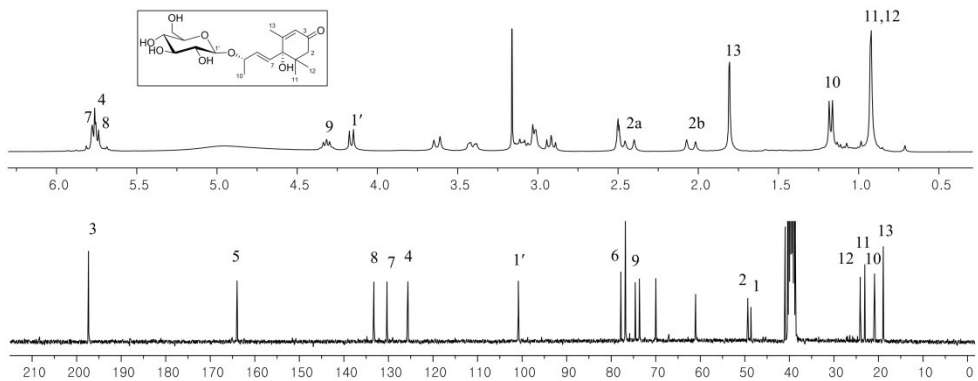

Figure 55. ^1H and ^{13}C NMR spectra of compound **32** (DMSO-d_6, 300/75 MHz)

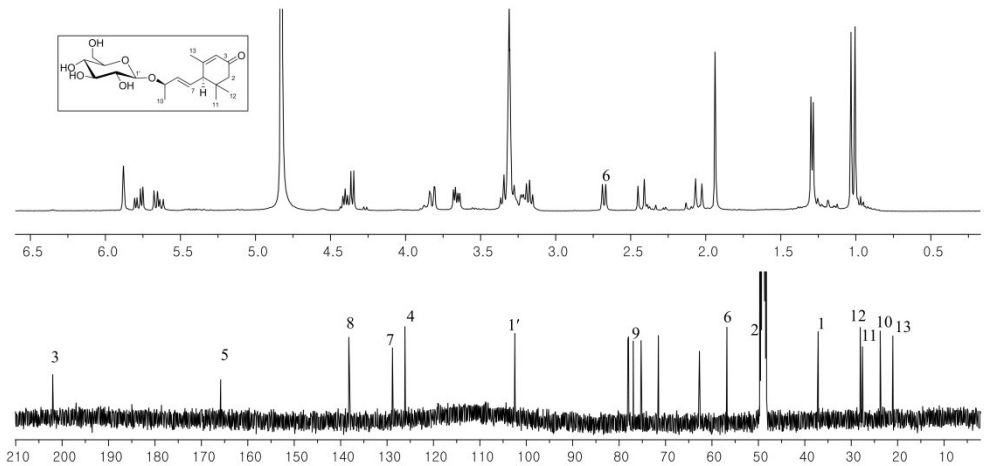

Figure 56. ^{1}H and ^{13}C NMR spectra of compound **33** (CD_3OD, 400/100 MHz)

3.3.6. Compounds **34**, **35**

Compound **34** was obtained as an amorphous white powder. Its molecular formula was determined to be $C_9H_8O_3$ by ESI-MS at *m/z* 162.9 $[M-H]^-$ and ^{13}C NMR data. ^{1}H NMR spectrum showed a mono-substituted aromatic protons at δ_H 7.47 (2H, d, *J*=8.5 Hz, H-2, 6) and 6.82 (2H, d, *J*=8.5 Hz, H-3, 5) and a (*E*)-olefin group at δ_H 7.62 (1H, d, *J*=15.6 Hz, H-7) and 6.31 (1H, d, *J*=15.6 Hz, H-8) (Figure 57). Based on these spectral data and comparison with literature, compound **34** was identified as 4-hydroxycinnamic acid (Yuan et al. 2017).

Compound **35** was obtained as a white amorphous powder. Its molecular formula was $C_{10}H_{10}O_4$ based on the ESI-MS at *m/z* 195.1 $[M+H]^+$ and ^{13}C NMR data. 1D NMR spectra (Figure 57) were similar to compound **34**, but an 1,3,4-trisubstituted benzene ring and a methoxy group was present. An 1,3,4-trisubstituted aromatic ring was suggested by ^{1}H NMR signals at δ_H 7.17 (1H, d,

J=2.0 Hz, H-2), 7.05 (1H, dd, *J*=7.9, 2.0 Hz, H-6) and 6.81 (1H, d, *J*=7.9 Hz, H-5). With these spectral data and literature (Lee et al. 2014), compound **35** was identified and confirmed as methyl caffeate.

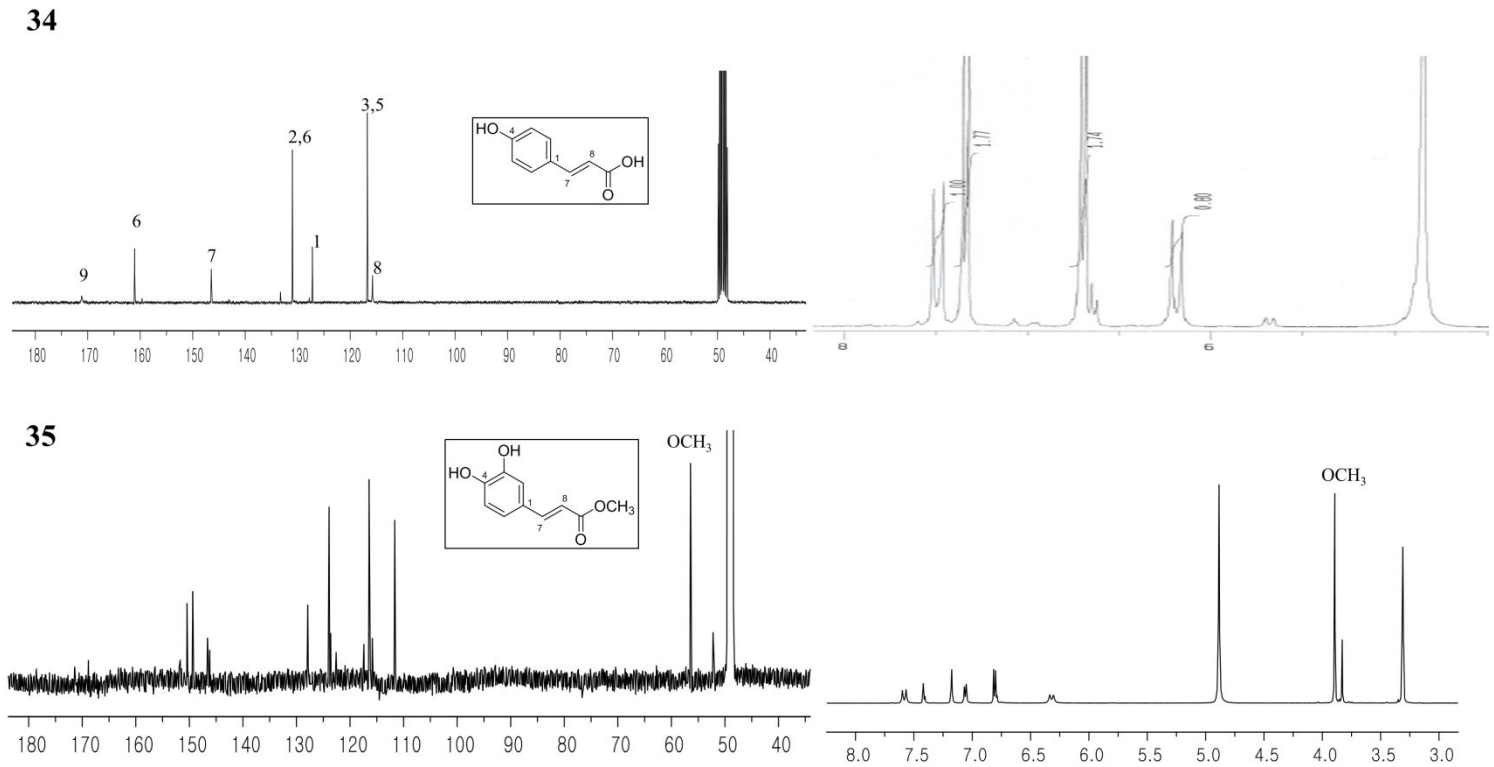

Figure 57. ^{1}H and ^{13}C NMR spectra of compounds **34** and **35** (CD_3OD, 300/75 MHz)

3.3.7. Compounds **36-39**

Compound **36** was obtained as a yellowish syrup. Its molecular formula was determined to be $C_{16}H_{18}O_9$ by ESI-MS at *m/z* 353.1 $[M-H]^-$ and ^{13}C NMR data. ^1H and HSQC spectra showed a (*E*)-caffeic acid moiety at δ_H 7.57 (1H, d, *J*=15.9 Hz, H-7′), 7.04 (1H, d, *J*=2.0 Hz, H-2′), 6.92 (1H, dd, *J*=8.2, 2.0 Hz, H-6′), 6.77 (1H, d, *J*=8.2 Hz, H-5′) and 6.30 (1H, d, *J*=15.9 Hz, H-8′), two methylene groups at δ_H 2.19 (1H, m, H-6a), 2.14 (2H, m, H-2a, 6b) and 1.95 (1H, dd, *J*=12.9, 9.7 Hz, H-2b) and three oxymethine groups at δ_H 5.35 (1H, m, H-5), 4.16 (1H, m, H-3) and 3.65 (1H, dd, *J*=8.5, 3.1 Hz, H-4) (Figure 58). The sequential correlations from H-2 to H-6 were shown in the COSY spectrum. From the HMBC spectrum, a carbonyl carbon at δ_C 178.5 (C-7) was coupled to H-2 and H-6, as well as a quaternary carbon at δ_C 75.4 (C-1) was coupled to H-2 and H-6, suggesting a quinic acid moiety. The HMBC correlation between C-9′ (δ_C 169.0) and H-5 assigned a linkage of caffeic acid with quinic acid. Based on these spectral data and comparison with literature, compound **36** was identified as neochlorogenic acid (3-*O*-caffeoylquinic acid) (Tatefuji et al. 1996).

Compound **37**, yellowish syrup, was determined to have a molecular formula of $C_{17}H_{20}O_9$ by the ^{13}C NMR and ESI-MS (*m/z* 369.1 $[M+H]^+$). ^1H NMR spectrum (Figure 59) was similar to compound **36** except for presence of a methoxy group. With these spectral data and literature (Zhu et al. 2005), compound **37** was identified and confirmed as neochlorogenic acid methyl ester.

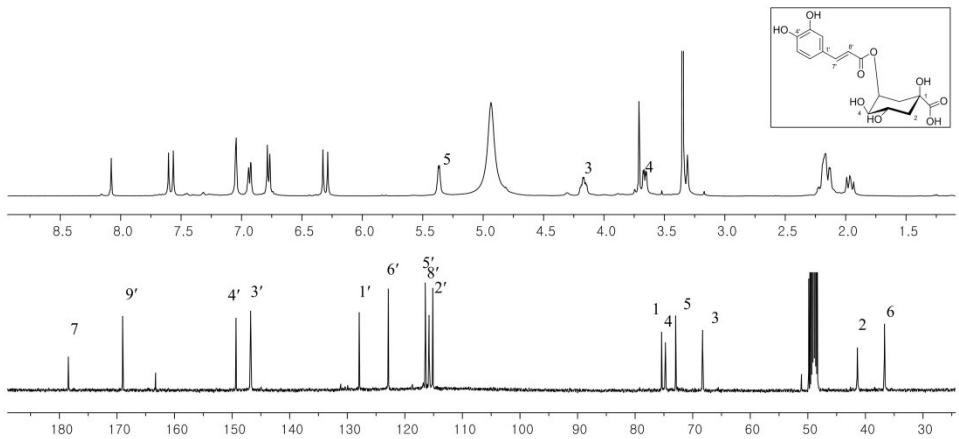

Figure 58. ^{1}H and ^{13}C NMR spectra of compound **36** (CD_3OD, 400/100 MHz)

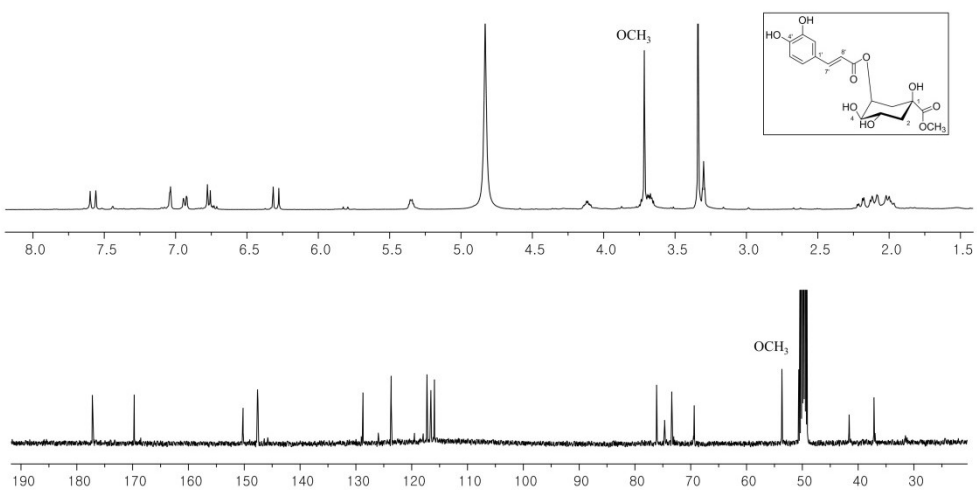

Figure 59. ^{1}H and ^{13}C NMR spectra of compound **37** (CD_3OD, 400/100 MHz)

Compound **38**, colorless syrup, was determined to have a molecular formula of $C_{16}H_{18}O_9$ by the ^{13}C NMR and ESI-MS (*m/z* 369.1 $[M+H]^+$). The spectral data (Figure 60) were similar to those of **36**. The position of the caffeoyl substitution at the quinic acid moiety was determined by the HMBC correlation between C-9′ (δ_C 169.0) and H-4 (δ_H 4.82, dd, *J*=9.3, 2.7 Hz, 1H). In addition, a downfield shift of H-4 and an upfield shift H-5 (δ_H 4.30, m, 1H) were observed. With these spectral data and literature (Dini et al. 2006), compound **38** was identified and confirmed as cryptochlorogenic acid (4-*O*-caffeoylquinic acid).

Compound **39**, yellowish syrup, was established as $C_{17}H_{20}O_9$ on the basis of ESI-MS data with an protonated ion at *m/z* 369.1 $[M+H]^+$ and ^{13}C NMR. 1D NMR spectrum was similar to compound **38**, but the signal corresponding a methoxy group (δ_C 52.9/ δ_H 3.72) was observed. With these spectral data and literature (Zhu et al. 2005), compound **39** was identified and confirmed as cryptochlorogenic acid methyl ester.

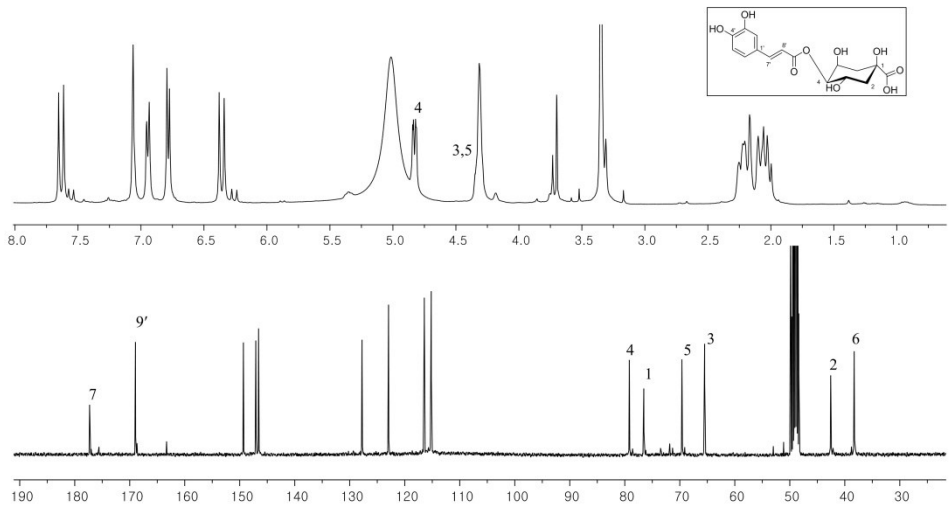

Figure 60. ^{1}H and ^{13}C NMR spectra of compound **38** (CD_3OD, 400/100 MHz)

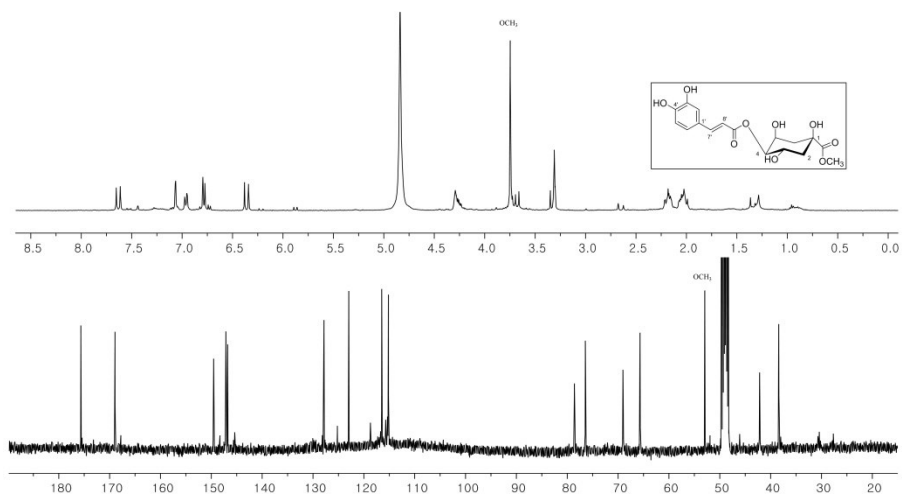

Figure 61. ^{1}H and ^{13}C NMR spectra of compound **39** (CD_3OD, 400/100 MHz)

3.3.8. Compounds **40**-**42**

Compound **40** was obtained as an amorphous brown powder. Its molecular formula was determined to be $C_8H_8O_4$ by ESI-MS at *m/z* 169.2 $[M+H]^+$ and ^{13}C NMR data. ^1H NMR spectrum (Figure 62) showed an 1,3,4-trisubstituted aromatic protons at δ_H 7.55 (1H, m, H-6), 7.53 (1H, m, H-2) and 6.82 (1H, d, *J*=8.8 Hz, H-5) and a methoxy group at δ_H 3.88 (3H, s, OCH_3). Based on these spectral data and comparison with literature, compound **40** was identified as vanillic acid (Yuan et al. 2017).

Compound **41**, colorless syrup, was established as $C_7H_6O_3$ on the basis of ESI-MS data with an protonated ion at *m/z* 139.1 $[M+H]^+$ and ^{13}C NMR. ^1H NMR spectrum (Figure 62) showed an 1,4-disubstituted benzene ring at δ_H 7.89 (2H, d, *J*=8.5 Hz, H-2,6) and 6.84 (2H, d, *J*=8.5 Hz, H-3,5). With these spectral data and literature (Yuan et al. 2017), compound **41** was identified and confirmed as 4-hydroxybenzoic acid.

Compound **42** was isolated as brown syrup. Its molecular formula was determined to be $C_7H_6O_3$ by ESI-MS at *m/z* 139.1 $[M+H]^+$ and ^{13}C NMR data. ^1H NMR spectrum (Figure 62) showed an 1,3-disubstituted aromatic protons at δ_H 7.30 (1H, dd, *J*=2.0, 7.7 Hz, H-6), 7.28 (1H, dd, *J*=2.0, 2.0 Hz, H-2), 7.26 (1H, dd, *J*=7.7, 7.7 Hz, H-5) and 6.95 (1H, dd, *J*=2.0, 7.7 Hz, H-4). Based on these spectral data and comparison with literature, compound **42** was identified as 3-hydroxybenzoic acid (Chimsook et al. 2013).

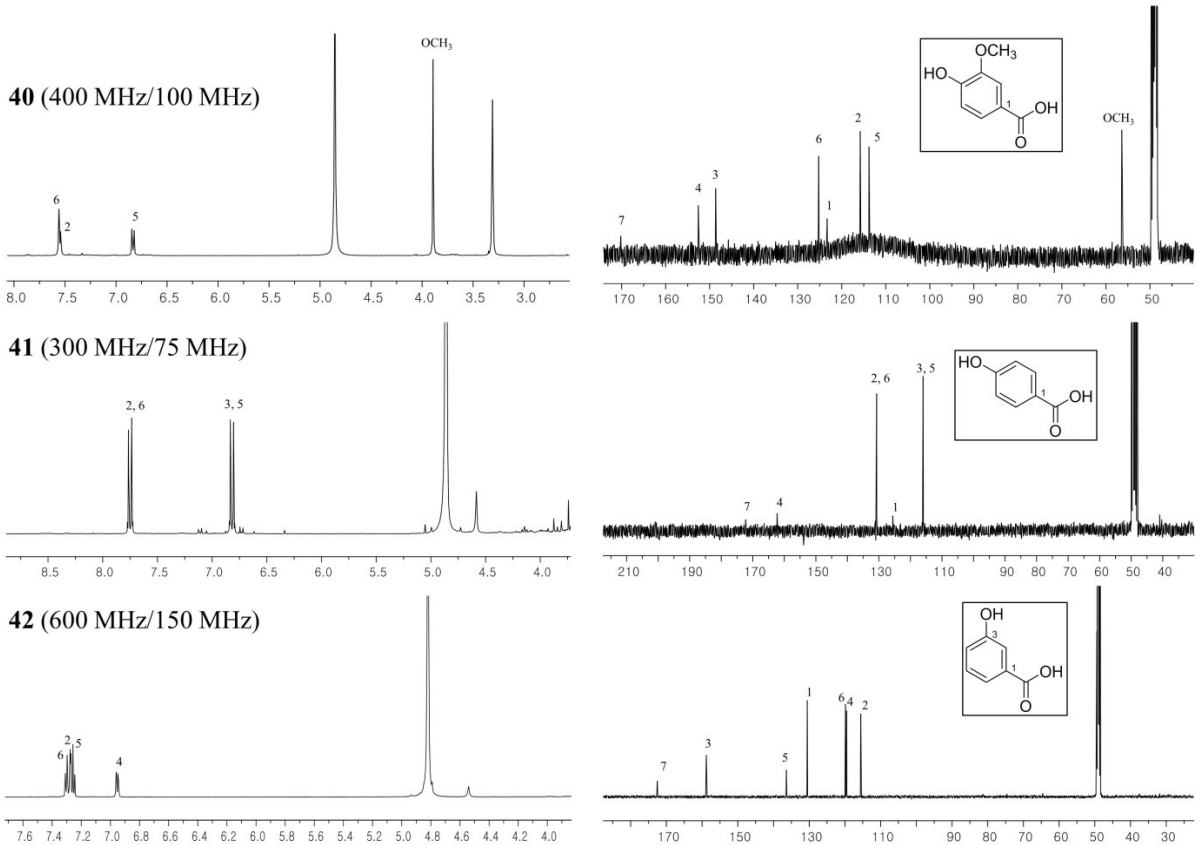

Figure 62. ^{1}H and ^{13}C NMR spectra of compounds **40**-**42** (CD_3OD)

3.3.9. Compounds **43-45**

Compound **43** was obtained as colorless syrup. Its molecular formula was determined to be $C_{13}H_{18}O_6$ by ESI-QTOF-MS at *m/z* 271.1178 $[M+H]^+$ (calcd. for $C_{13}H_{19}O_6$, 271.1176) and ^{13}C NMR data. ^1H and HSQC spectra showed a mono-substituted aromatic protons at δ_H 7.41 (2H, m, H-2, 6), 7.32 (2H, m, H-3, 5) and 7.26 (1H, m, H-4), an oxygenated methylene group at δ_H 4.92 (1H, d, *J*=12.2 Hz, H-7a) and 4.66 (1H, d, *J*=12.2 Hz, H-7b) and an anomeric proton at δ_H 4.36 (1H, d, *J*=7.7 Hz, H-1′) (Figure 63). The ^{13}C NMR spectrum showed a glucopyranosyl moiety (δ_C 103.3, 78.1, 78.0, 75.1, 71.7 and 62.8), and HPLC analysis of the thiocarbamoyl thiazolidine derivative of the acid hydrolysate reaffirmed a D-glucose group. Based on these spectral data and comparison with literature, compound **43** was identified as benzyl-*β*-D-glucopyranoside (Luyen et al. 2015).

Compound **44**, brown syrup, was established as $C_{14}H_{20}O_6$ on the basis of ESI-MS data with an protonated ion at *m/z* 285.1 $[M+H]^+$ and ^{13}C NMR. ^{13}C NMR spectrum was similar to compound **43**, but one more methylene group at δ_C 37.2 (C-7) was observed. ^1H and HSQC spectra showed a mono-substituted aromatic protons at δ_H 7.25 (4H, m, H-2, 3, 5, 6) and 7.17 (1H, m, H-4), two methylene groups at δ_H 4.09 (1H, m, H-8a), 3.75 (1H, m, H-8b) and 2.93 (2H, m, H-7) and an anomeric proton at δ_H 4.28 (1H, d, *J*=7.7 Hz, H-1′) (Figure 63). The ^{13}C NMR spectrum showed a glucopyranosyl moiety (δ_C 104.3, 78.1, 77.9, 75.1, 71.6 and 62.7). D-glucose group was confirmed again by HPLC analysis of the acid hydrolysate. With these spectral data and literature (Luyen et al. 2015), compound **44** was identified and confirmed as 2-phenylethyl-*β*-D-glucopyranoside.

Compound **45** was isolated as yellowish syrup. Its molecular formula was determined to be $C_{14}H_{20}O_8$ by ESI-MS at *m/z* 315.1 $[M-H]^-$ and ^{13}C NMR data. ^1H and HSQC spectra suggested an 1,3,4-trisubstituted aromatic ring at δ_H 6.68 (1H, d, *J*=1.8 Hz, H-2), 6.66 (1H, d, *J*=8.1 Hz, H-5) and 6.54 (1H, dd, *J*=1.8, 8.1 Hz, H-6), two methylene groups at δ_H 4.01 (1H, m, H-8a), 3.70 (1H, m, H-8b) and 2.76 (2H, m, H-7) and an anomeric proton at δ_H 4.27 (1H, d, *J*=7.8 Hz, H-1′) (Figure 63). The ^{13}C NMR spectrum showed a glucopyranosyl moiety (δ_C 104.3, 78.1, 77.9, 75.1, 71.6 and 62.7). D-glucose group was confirmed by HPLC analysis of thiocarbamoyl thiazolidine derivative of the acid hydrolysate. Based on these spectral data and comparison with literature, compound **45** was identified as dopaol-*β*-D-glucopyranoside (Franzyk et al. 2004).

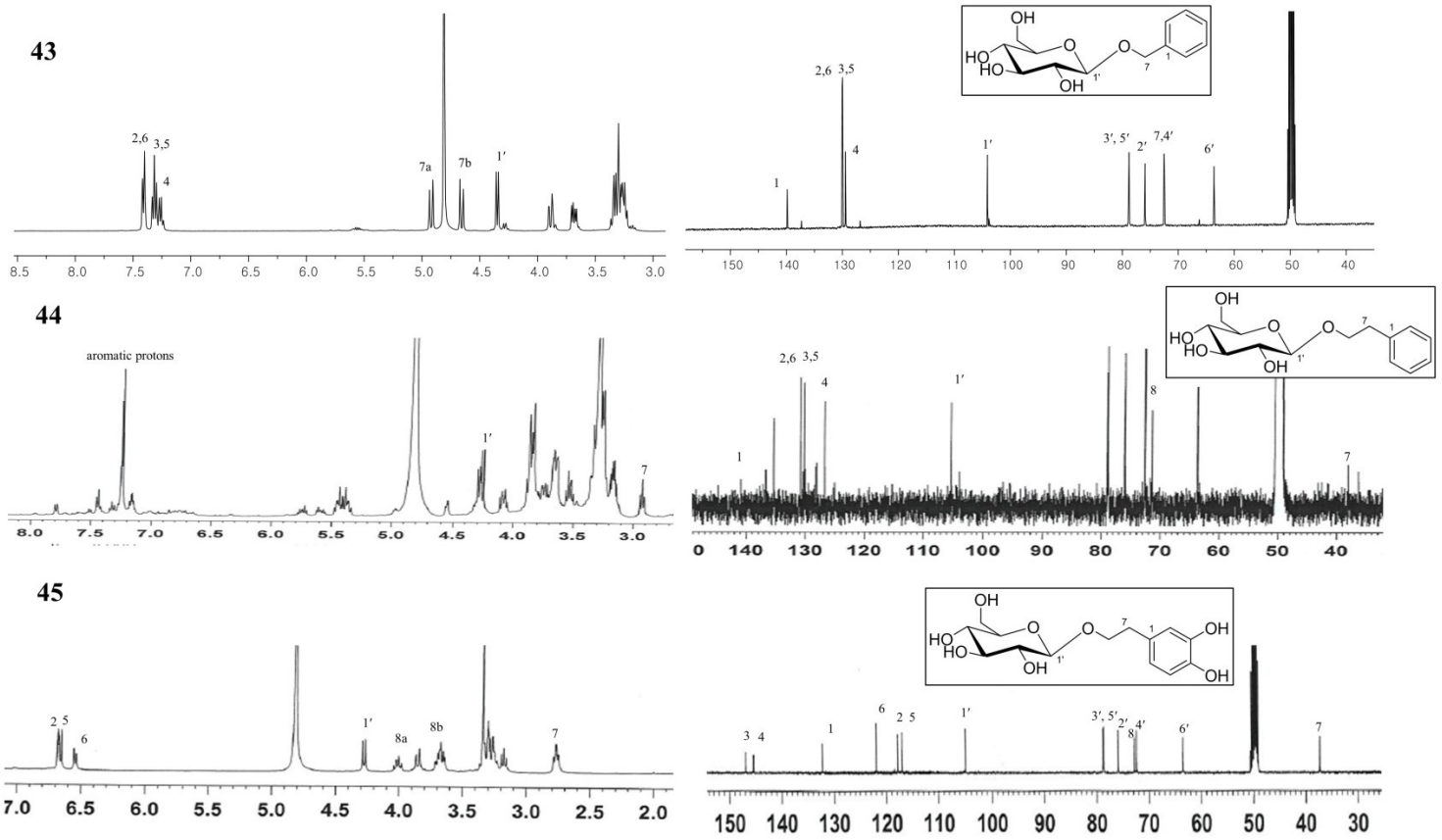

Figure 63. ^{1}H and ^{13}C NMR spectra of compounds **43-45** (CD_3OD, 400/100 MHz)

3.3.10. Compounds **46**, **47**

Compound **46** was obtained as colorless syrup. Its molecular formula was determined to be $C_{10}H_{14}O_5$ by ESI-MS at *m/z* 237.1 $[M+Na]^+$ and ^{13}C NMR data. ^1H and HSQC spectra showed an 1,3,4-trisubstituted aromatic ring at δ_H 6.98 (1H, d, *J*=1.8 Hz, H-2), 6.79 (1H, dd, *J*=1.8, 8.1 Hz, H-6) and 6.74 (1H, d, *J*=8.1 Hz, H-5), a methoxy group at δ_H 3.85 (3H, s, OCH_3), two oxygenated methine groups at δ_H 4.51 (1H, d, *J*=6.4 Hz, H-7) and 3.66 (1H, m, H-8) and an oxygenated methylene group at δ_H 3.48 (1H, m, H-9a) and 3.34 (1H, m, H-9b) (Figure 64). Based on these spectral data and comparison with literature, compound **46** was identified as *threo*-guaiacylglycerol (Gan et al. 2008).

Compound **47** was isolated as brown oil. Its molecular formula was determined to be $C_{16}H_{24}O_{10}$ by ESI-MS at *m/z* 421.1 $[M+HCOO]^-$ and ^{13}C NMR data. 1D NMR spectra (Figure 64) were similar to those of compound **46** except for presence of glucopyranosyl group. ^1H and HSQC spectra suggested an 1,3,4-trisubstituted aromatic ring at δ_H 6.94 (1H, brs, H-2), 6.68 (1H, m, H-5) and 6.73 (1H, m, H-6), a methoxy group at δ_H 3.74 (3H, s, OCH_3), two oxymethine groups at δ_H 4.52 (1H, d, *J*=6.4 Hz, H-7) and 3.64 (1H, m, H-8), an oxygenated methylene group at δ_H 3.35 (1H, m, H-9a) and 3.17 (1H, m, H-9b) and an anomeric proton at δ_H 4.24 (1H, d, J=7.5 Hz, H-1′). The ^{13}C NMR spectrum showed a glucopyranosyl moiety (δ_C 104.0, 76.8, 76.3, 73.8, 70.1 and 61.0). D-glucose group was confirmed by HPLC analysis of the acid hydrolysate. Based on these spectral data and comparison with literature, compound **47** was identified as *threo*-guaiacylglycerol 8-*O*-*β*-D-glucopyranoside (Gan et al. 2008).

46 (MeOD-d_4**)**

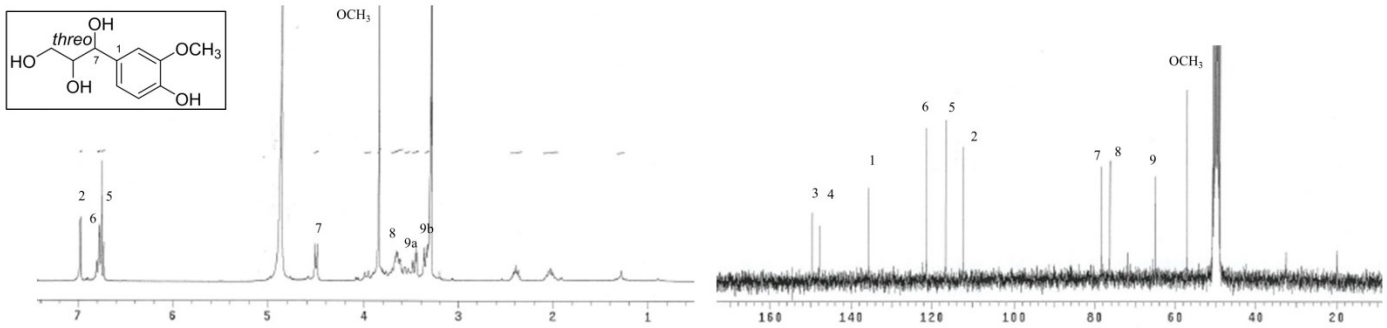

47 (DMSO-d_6)

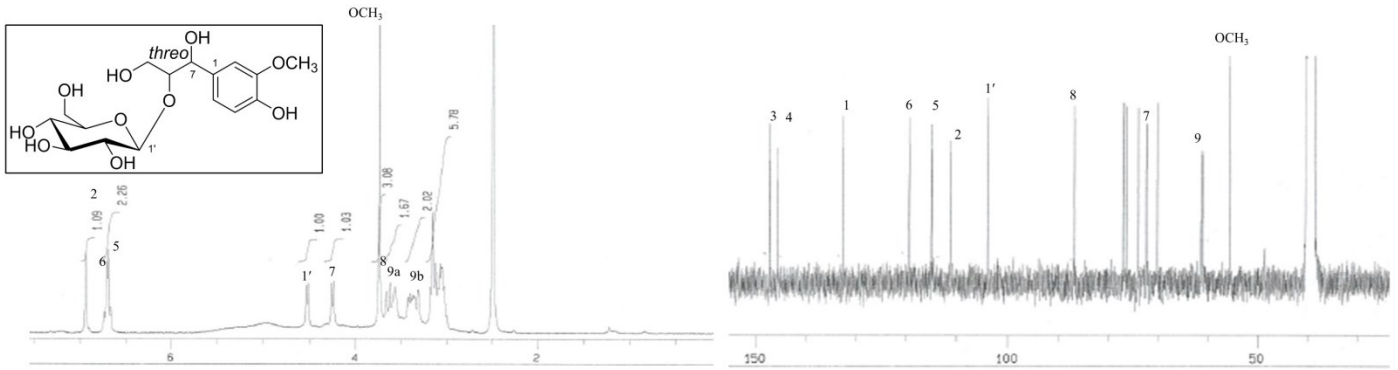

Figure 64. ^{1}H and ^{13}C NMR spectra of compounds **46**, **47** (300 MHz/75 MHz)

3.3.11. Compound **48**

Compound **48** was obtained as yellowish oil. Its molecular formula was determined to be $C_{19}H_{26}O_{10}$ by ESI-QTOF-MS at *m/z* 437.1407 $[M+H]^+$ (calcd. for $C_{19}H_{26}O_{10}Na$, 437.1418). The ^1H and HSQC spectra showed a mono-substituted benzene ring at δ_H 7.36 (2H, m, H-2, 6), 7.34 (2H, m, H-3, 5) and 7.28 (1H, m, H-4), four methylene groups at δ_H 4.76 (1H, d, *J*=12.3 Hz, H-7a), 4.54 (1H, d, *J*=12.3 Hz, H-7b), 4.35 (1H, d, *J*=11.4 Hz, H-6′a), 4.06 (1H, dd, *J*=11.4, 6.8 Hz, H-6′b), 2.64 (2H, m, H-2″) and 2.48 (2H, m, H-4″), five methine protons at δ_H 4.26 (1H, d, *J*=7.5 Hz, H-1′), 3.35 (1H, m, H-5′), 3.15 (1H, m, H-3′), 3.09 (1H, m, H-4′) and 3.05 (1H, m, H-2′) and a methyl group at δ_H 1.29 (3H, s, 3″-CH_3′) (Figure 65).

The sequential ^1H-^1H COSY correlations from H-1′ to H-6′ were observed, suggesting the presence of a sugar moiety. D-glucose was confirmed by the HPLC analysis of the acid hydrolysate. The *β*-configuration of D-glucose was determined based on the vicinal coupling constant of H-1′ (*J*=7.5 Hz). The downfield shift of H-6′ (δ_H 4.35, 4.06) and the ^{13}C NMR spectrum (δ_C 102.1, 76.3, 73.7, 73.3, 70.1 and 63.5) showed a 6-*O*-substituted glucopyranosyl moiety.

The HMBC correlations of H-7 with C-1′ (102.1) and C-1 (137.9) suggested the aglycone, phenylmethyl group. The HMBC correlations of methyl protons with C-2″, C-3″ and C-4″ were observed, and two carboxylic groups at δ_C 172.6 (C-5″) and 170.4 (C-1″) were coupled to H-4″ and H-2″, respectively. These HMBC correlations suggested HMG substructure (3-hydroxy-3-methylglutaryl group). From HMBC spectrum, the correlation between H-6′ and C-1″ suggested the location of HMG unit. *S*-configuration of the C-3″ was assumed because naturally

occurring HMG esters are formed via the acylation of the hydroxy group with (*S*)-HMG-CoA (Wu et al. 2011). Based on these spectral data and comparison with literature, compound **48** was identified as undatuside A (Wu et al. 2011).

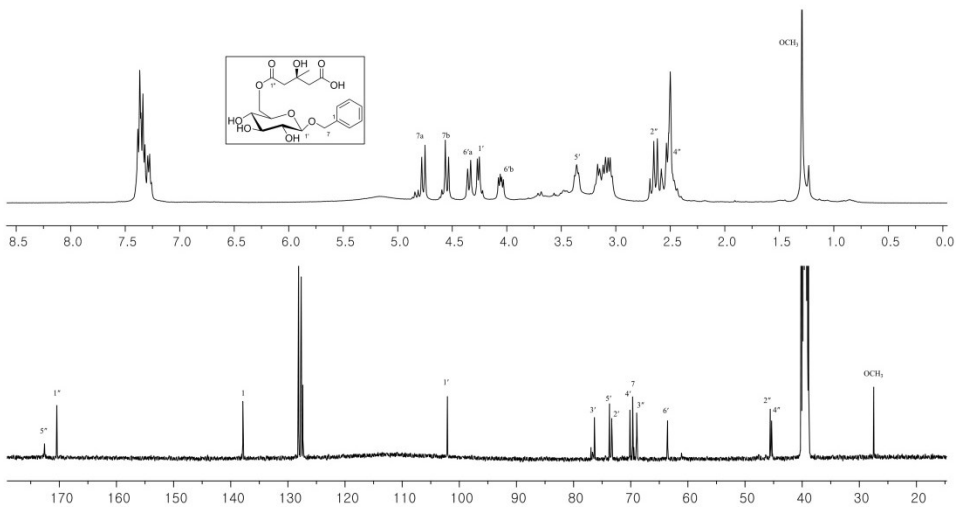

Figure 65. ^{1}H and ^{13}C NMR spectra of compound **48** (DMSO-d_6, 400/100 MHz)

3.3.12. Compound **49**

Compound **49** was obtained as yellowish oil. Its molecular formula was determined to be $C_{12}H_{22}O_6$ by ESI-MS at *m/z* 307.1 $[M+HCOO]^-$ and ^{13}C NMR data. ^{1}H and HSQC spectra showed an (*E*)-olefin at δ_H 5.75 (1H, m, H-4) and 5.58 (1H, m, H-3), an anomeric proton at δ_H 4.18 (1H, d, *J*=7.9 Hz, H-1′), four methylene groups at δ_H 4.31 (1H, m, H-1a), 4.08 (1H, m, H-1b), 3.85 (1H, m, H-6′a), 3.67 (1H, m, H-6′b), 2.04 (2H, m, H-2) and 1.42 (2H, m, H-5) and a methyl group at δ_H 0.93 (3H, t, *J* = 7.5 Hz, H-6). (Figure 66). The sequential COSY

correlations from H-1 to H-6 suggested presence of (*E*)-3-hexenyl group. D-glucose was confirmed by the HPLC analysis of the acid hydrolysate. The *β*-configuration of D-glucose was determined based on the vicinal coupling constant of H-1′ (*J*=7.9 Hz). Based on these spectral data and comparison with literature, compound **49** was identified as (*E*)-3-hexenyl-*β*-D-glucopyranoside (Lee et al. 2012).

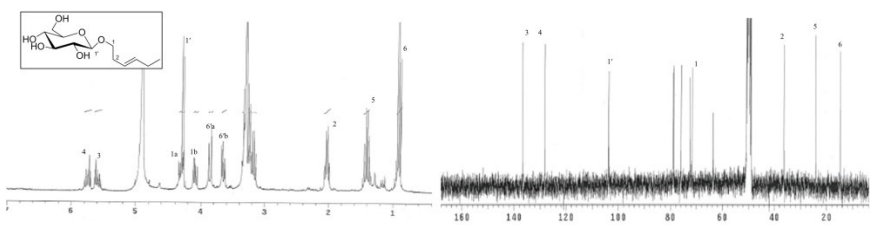

Figure 66. ^{1}H and ^{13}C NMR spectra of compound **49** (CD_3OD, 300 /75 MHz)

3.3.13. Compound **50**

Compound **50** was isolated as colorless oil. Its molecular formula was established as $C_{20}H_{24}O_7$ on the basis of positive mode ESI-QTOF-MS data with an adduct ion peak at *m/z* 399.1428 $[M+Na]^+$ (calcd. for $C_{20}H_{24}O_7Na$, 399.1414). The IR spectrum indicated that compound **50** possesses hydroxy (3400 cm^{-1}), phenyl (2936, 1514 cm^{-1}) and ether (1273 cm^{-1}) functional groups. The ^{1}H and HSQC spectra revealed the signals for two 1,2,4-trisubstituted benzene rings at [δ_H 6.82 (1H, d, *J*=1.8 Hz, H-2), 6.75 (1H, d, *J*=8.2 Hz, H-5) and 6.63 (1H, dd, *J*=1.8, 8.2 Hz, H-6)], [δ_H 7.61 (1H, d, *J*=2.0 Hz, H-2′), 6.86 (1H, d, *J*=8.4 Hz, H-5′) and 7.68

(1H, dd, *J*=2.0, 8.4 Hz, H-6′)], four methylenes at δ_H 4.01 (2H, m, H-9′), 3.52 (2H, t, *J*=6.5 Hz, H-9), 2.59 (2H, m, H-7) and 1.77 (2H, m, H-8), a methine at δ_H 5.50 (1H, dd, *J*=4.3, 5.5 Hz, H-8′) and two methoxy groups at δ_H 3.87 (3H, s, 3-OCH_3) and 3.77 (3H, s, 3′-OCH_3) (Figure 67).

Two 1,2,4-trisubsituted benzene ring was confirmed by the HMBC correlations of H-5 with C-1 (δ_C 138.1), C-3 (δ_C 151.0) and C-4 (δ_C 146.6) and H-5′ with C-1′ (δ_C 128.6), C-3′ (δ_C 149.1) and C-4′ (δ_C 153.9). The position of methoxy groups were suggested by the HMBC and NOESY spectra. From the HMBC spectrum, the correlations between δ_H 3.87 (3-OCH_3) and C-3 and between δ_H 3.77 (3′-OCH_3) and C-3′ were observed. The NOESY spectrum (Figure 70) showed the correlation of δ_H 3.87 (3-OCH_3) with H-2 and δ_H 3.77 (3′-OCH_3) with H-2′.

The COSY correlations of H-8 with H-7 and H-9 revealed the presence of 1-propanol. From the HMBC spectrum, H-7 was coupled to C-1, suggesting the presence of a 3-guaiacylpropanol substructure. A 2,3-dihydroxy-1-guaiacylpropan-1-one substructure was indicated by the COSY correlation between H-8′ and H-9′ and the HMBC correlations of a carbonyl carbon (δ_C 197.4) with H-2′, H-6′ and H-8′. In the HMBC spectrum, H-8′ was coupled to C-4, implying the connection of two substructures. The absolute configuration of C-8′ was determined as *R* by the negative exciton-split Cotton effect at 331 nm (Δε -0.10) and 272 nm (Δε +0.03) in compund **50** indicating that the transition dipole moments of two chromophores were oriented in an anticlockwise manner (Figure 71) (Yang et al. 2014). The π→π* transition (intramolecular charge-transfer transition) of benzoate chromophore show 280 nm in UV region, as calculated with empirical rules. By

the literature (Yang et al. 2016), the π→π* transition of benzene moiety is also 280 nm in UV region.

On the basis of these data, the structure of **50** was defined as (*R*)-4,9,9′-trihydroxy-3,3′-dimethoxy-7-oxo-8-*O*-4′-neolignan and named houttuylignan.

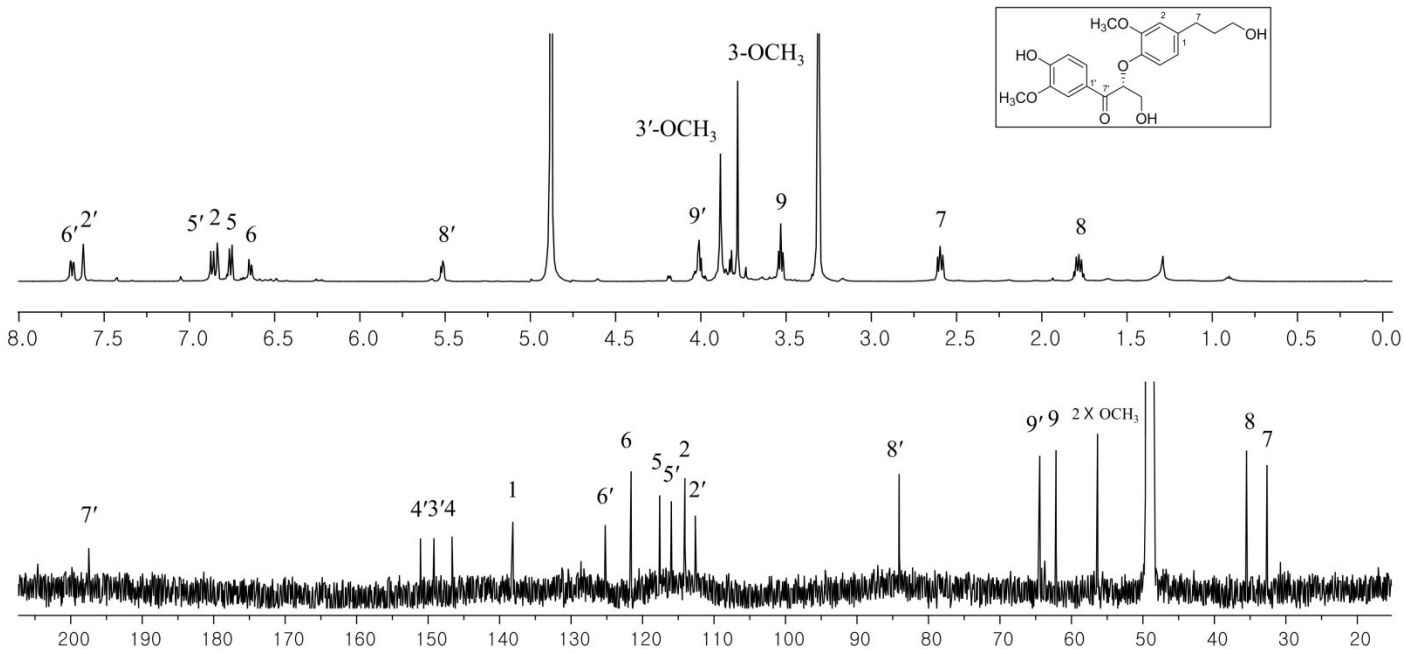

Figure 67. ^{1}H and ^{13}C NMR spectra of compound **50** (CD_3OD, 500/125 MHz)

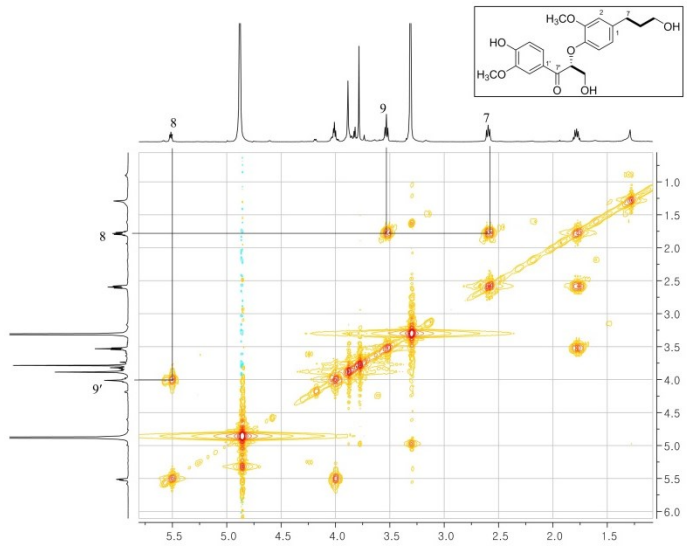

Figure 68. ^{1}H-^{1}H COSY spectrum of compound **50** (CD_3OD, 400 MHz)

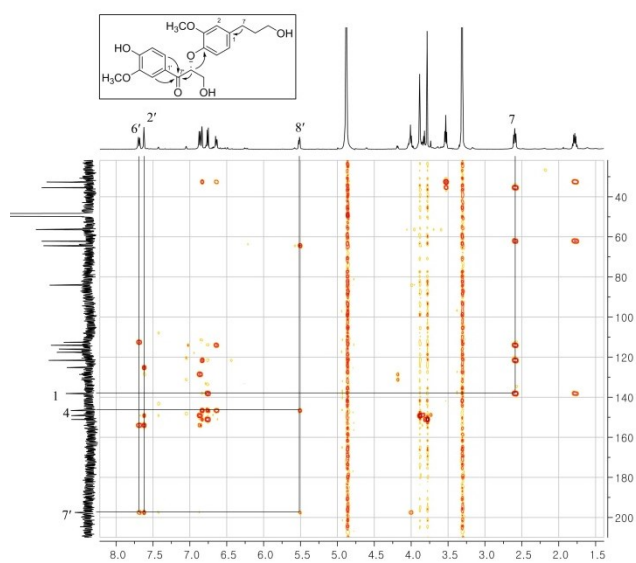

Figure 69. The HMBC spectrum of compound **50** (CD_3OD, 400 MHz)

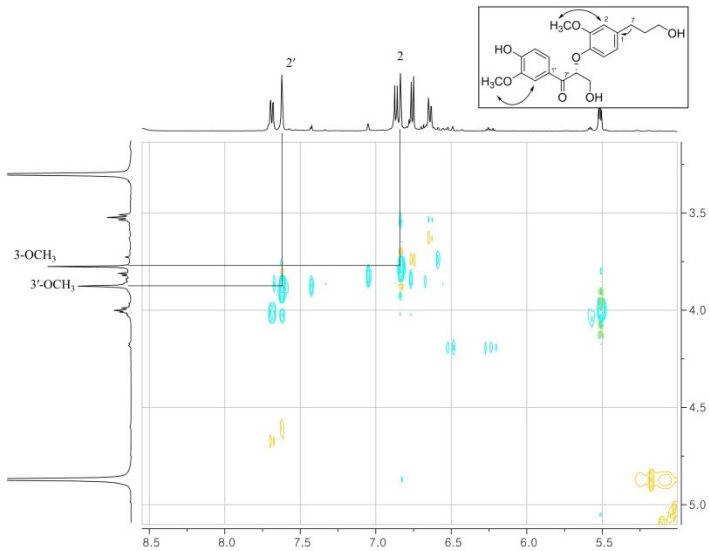

Figure 70. The NOESY spectrum of compound **50** (CD_3OD, 400 MHz)

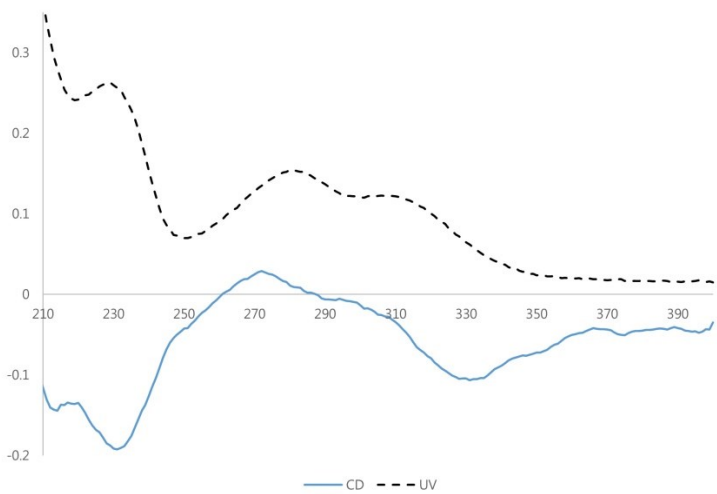

Figure 71. The CD and UV spectra of compound **50**

3.3.14. Compound **51**

Compound **51** was obtained as colorless oil. Its molecular formula was determined to be $C_{20}H_{24}O_6$ by ESI-QTOF-MS based on the adduct ion peak at *m/z* 383.1470 $[M+Na]^+$ (calcd. for $C_{20}H_{24}O_6Na$, 383.1465). The ^1H and HSQC spectra showed an 1,2,4-trisubstituted benzene ring at δ_H 6.94 (1H, d, *J*=1.8 Hz, H-2), 6.75 (1H, d, *J*=8.1Hz, H-5) and 6.81 (1H, dd, *J*=1.8, 8.1 Hz, H-6), two aromatic protons at δ_H 6.72 (2H, brs, H-2′,6′), four methylene at δ_H 3.81 (1H, m, H-9a), 3.74 (1H, dd, *J*=7.0, 11.0 Hz, H-9b), 3.56 (2H, t, *J*=6.4 Hz, H-9′), 2.62 (2H, t, *J*=7.6 Hz, H-7′) and 1.80 (2H, m, H-8′), two methine protons at δ_H 5.48 (1H, d, *J*=6.2 Hz, H-7) and 3.45 (1H, m, H-8) and two methoxy groups at δ_H 3.84 (3H, s, 3′-OCH_3) and 3.80 (3H, s, 3-OCH_3) (Figure 72).

The COSY correlations in combination with HMBC spectroscopic data suggested two C_6-C_3 units arising neolignan moiety. From the HMBC spectrum, the correlations between H-7 and C-4′ (δ_C 147.5) and between H-8 and C-5′ (δ_C 129.9) confirmed a neolignan skeleton of compound **51**. The relative configuration of H-7/H-8 was suggested to be *trans* form by the chemical shift of H-7 (δ_H 5.48, *J*=6.2 Hz). According to the literature (Li et al. 2014), the chemical shift of H-7 was a adequate tool to determine the relative configuration of H-7/H-8 of benzofuran-type neolignans. The absolute configuration of compound **51** was assigned to be the 7*S*, 8*R* configuration based on CD spectrum (Li et al. 2014). In which, the Cotton effect at 243 nm was negative. Compound **51** was identified as (7*S*, 8*R*)-dihydrodehydrodiconiferyl alcohol by comparison of the spectral data with those reported previously (Park et al. 2011).

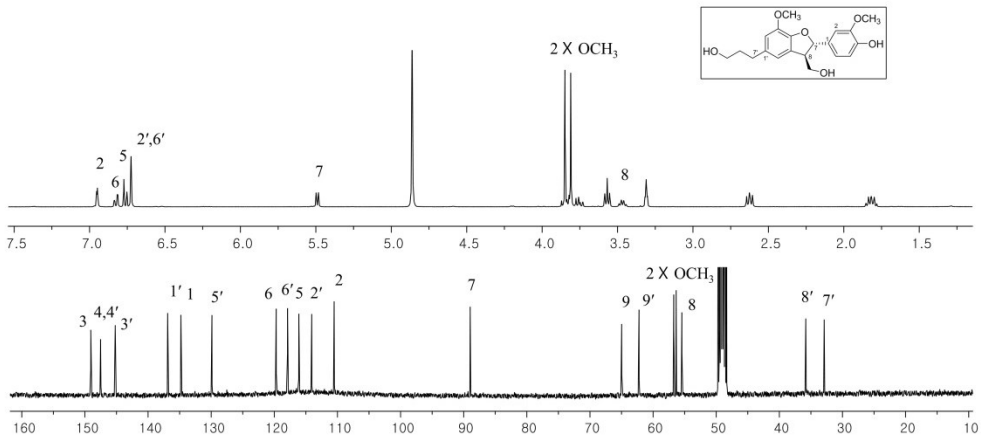

Figure 72. ^{1}H and ^{13}C NMR spectra of compound **51** (CD_3OD, 400 /100 MHz)

3.3.15. Compound **52**

Compound **52** was isolated as yellowish oil. Its molecular formula was determined to be $C_{20}H_{22}O_6$ by ESI-QTOF-MS at *m/z* 359.1493 $[M+H]^+$ (calcd. for $C_{20}H_{23}O_6$, 359.1489). 1D NMR spectra (Figure 73) were similar to those of compound **51** except for (*E*)-3-hydroxy-1-propenyl group at δ_H 6.54 (1H, d, *J*=15.8 Hz, H-7′) and 6.23 (1H, dt, *J*=15.8, 5.9 Hz, H-8′) instead of 1-propanol moiety in **51**. The relative configuration of H-7/H-8 was suggested to be *trans* form by the chemical shift of H-7 (δ_H 5.52, *J*=6.3 Hz). The absolute configuration of compound **52** was identified as 7*S*, 8*R* by comparison with the CD spectra of compound **51**. The CD spectrum of **52** showed a negative Cotton effect at 243 nm, similar to those of **51**. Thus, the structure of **52** was identified as (7*S*, 8*R*)-dehydrodiconiferyl alcohol by comparison of the spectral data with those reported previously (Feng et al. 2016)

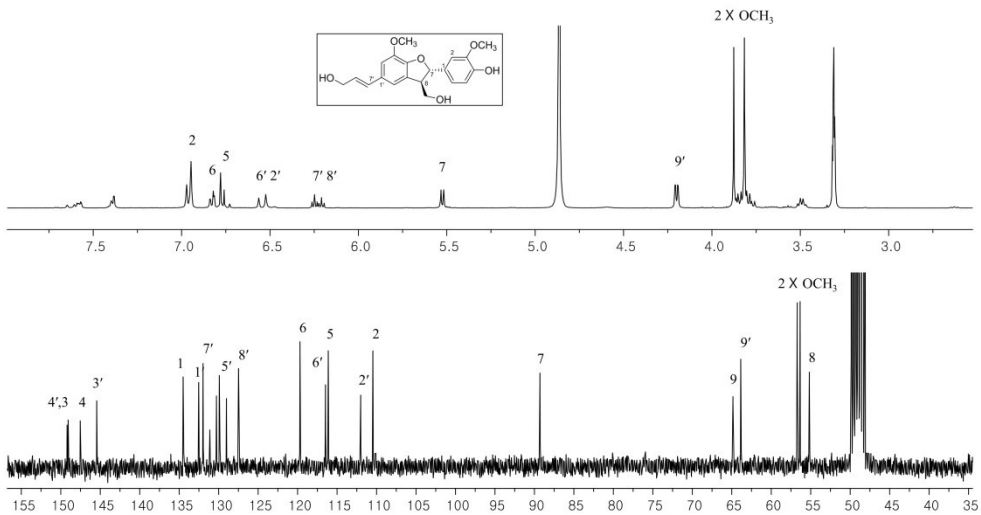

Figure 73. ^{1}H and ^{13}C NMR spectra of compound **52** (CD_3OD, 300 /75 MHz)

3.3.16. Compound **53**

Compound **53** was isolated as colorless oil. Its molecular formula was determined to be $C_{20}H_{24}O_6$ by ESI-QTOF-MS at *m/z* 383.1472 $[M+Na]^+$ (calcd. for $C_{20}H_{24}O_6Na$, 383.1465). The ^{1}H and HSQC spectra showed an 1,2,4-trisubstituted benzene ring at δ_H 6.72 (1H, d, *J*=8.0 Hz, H-5), 6.65 (1H, d, *J*=1.9 Hz, H-2) and 6.59 (1H, dd, *J*=1.9, 8.0 Hz, H-6), two aromatic protons at δ_H 6.63 (1H, s, H-2′) and 6.16 (1H, s, H-5′), three methylene at δ_H 3.71 (1H, dd, *J*=4.9, 11.0 Hz, H-9′a), 3.66 (1H, m, H-9a), 3.65 (1H, m, H-9′b), 3.37 (1H, dd, *J*=11.3, 4.1 Hz, H-9b) and 2.75 (2H, d, *J*=7.7 Hz, H-7′), three methine protons at δ_H 3.78 (1H, d, *J*=5.1 Hz, H-7), 1.98 (1H, m, H-8′) and 1.74 (1H, m, H-8) and two methoxy groups at δ_H 3.79 (3H, s, 3′-OCH_3) and 3.75 (3H, s, 3-OCH_3) (Figure 74).

The COSY correlations in combination with HMBC spectroscopic data

suggested the presence of two phenylpropanoid moieties in structure of **53**. The COSY spectrum revealed the linkage between H-8 and H-8′. The HMBC correlation of H-7 with C-6′ (δ_C 129.0) was observed. Based on these data and literature (Du et al. 2010), compound **53** was identified as isolariciresinol. The absolute configuration of **53** was identified as 7*R*, 8*S*, 8′*S* by comparison with the CD data reported previously (Lundgren et al. 1981). The CD spectrum of **53** showed a negative Cotton effect at 215 nm, negative at 239 nm, negative at 276 nm and positive at 293 nm. Thus, the structure of **53** was determined as (7*R*, 8*S*, 8′*S*)-isolariciresinol.

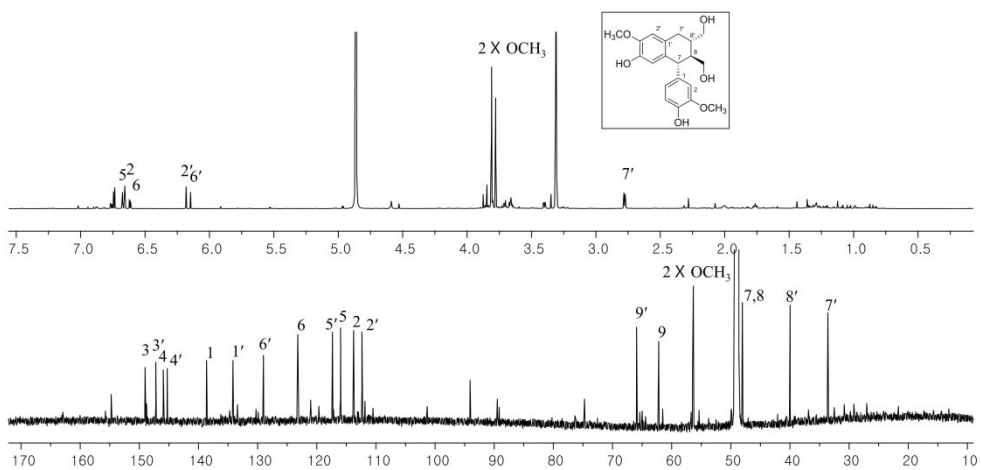

Figure 74. ^{1}H and ^{13}C NMR spectra of compound **53** (CD_3OD, 800 /200 MHz)

3.3.17. Compound **54**

Compound **54** was obtained as colorless oil. Its molecular formula was assigned as $C_{20}H_{26}O_6$ by ESI-QTOF-MS at *m/z* 385.1608 $[M+Na]^+$ (calcd. for $C_{20}H_{26}O_6Na$, 385.1622). The ^{13}C NMR and HSQC spectra showed ten carbon signals due to six

aromatic carbons, two methylene carbons at δ_C 36.0 and 62.1, a methoxy carbon at δ_C 56.1 and a methine carbon at δ_C 44.1. It could be deduced that compound **54** has a symmetrical structure. The ^{1}H spectrum revealed an 1,2,4-trisubstituted benzene ring at δ_H 6.65 (1H, d, *J*=7.9 Hz, H-5), 6.58 (1H, d, *J*=1.8 Hz, H-2) and 6.54 (1H, dd, *J*=1.8, 7.9 Hz, H-6) (Figure 75). Based on these data and literature, compound **54** was identified as secoisolariciresinol. The spectroscopic data was identical with those of (-)-secoisolariciresinol (Zeng et al. 2013), but the optical rotations were of opposite signs. The CD spectrum of **54** was opposite to (-)-secoisolariciresinol, with known absolute configuration (Xie et al. 2003). In which, the Cotton effect at 289 nm was positive. Compound **54** was identified as (+)-(8*S*,8′*S*)-secoisolariciresinol by comparison of the spectral data with literature.

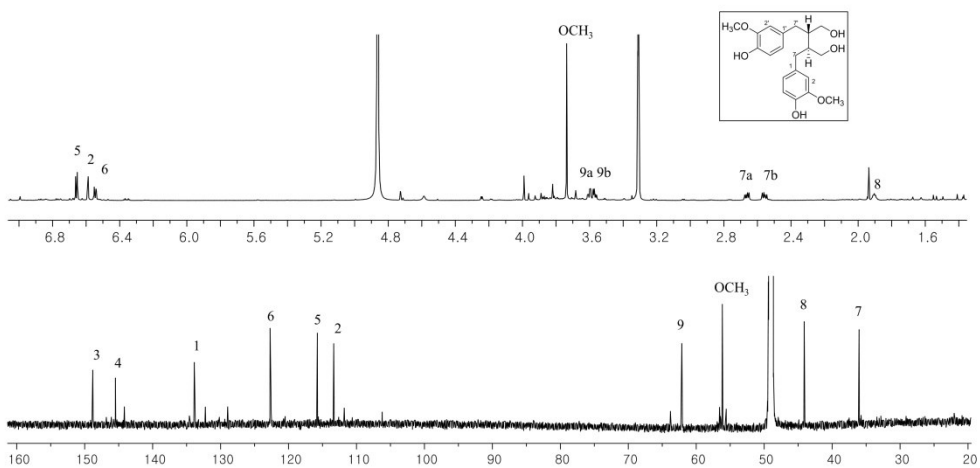

Figure 75. ^{1}H and ^{13}C NMR spectra of compound **54** (CD_3OD, 800 /200 MHz)

3.3.18. Compounds **55** and **56**

Compound **55** was obtained as colorless oil. Its molecular formula was determined to be $C_{21}H_{28}O_8$ by an adduct ion at *m/z* 431.1683 $[M+Na]^+$ (calcd. for $C_{21}H_{28}O_8Na$, 431.1676) in ESI-QTOF-MS. Peaks indicative of an 1,3,4-trisubstituted benzene ring at δ_H 6.98 (1H, d, *J*=1.7 Hz, H-2), 6.78 (1H, dd, *J*=1.7, 8.1 Hz, H-6) and 6.73 (1H, d, *J*=8.1 Hz, H-5), two aromatic protons at δ_H 6.53 (2H, s, H-2′,6′), four methylene groups at δ_H 3.87 (1H, dd, *J*=5.6, 12.0 Hz, H-9a), 3.56 (2H, t, *J*=6.5 Hz, H-9′), 3.52 (1H, dd, *J*=3.6, 12.0 Hz, H-9b), 2.63 (2H, dd, J=7.0, 8.5 Hz, H-7′) and 1.81 (2H, m, H-8′), two methine protons at δ_H 4.91 (1H, d, *J*=4.9 Hz, H-7) and 4.16 (1H, m, H-8) and three methoxy groups at δ_H 3.83 (3H, s, 3-OCH_3) and 3.80 (6H, s, 3′-OCH_3 and 5′-OCH_3) were observed in the ^1H and HSQC spectra (Figure 76). The COSY correlations in combination with HMBC spectroscopic data suggested the presence of a dihydrosinapyl alcohol and a guaiacylglycerol in structure of **55**. The HMBC correlation of H-8 with C-4′ suggested an 8-*O*-4′ neolignan structure. The coupling constant between H-7 and H-8 was measured to be 4.9 Hz, which resulted in an *erythro* configuration at C-7/C-8 (Jutiviboonsuk et al. 2005). Compound **55** was identified and confirmed as *erythro*-1-(4-hydroxy-3-methoxyphenyl)-2-[4-(3-hydroxypropyl)-2,6-dimethoxyphenoxy]-propane-1,3-diol by comparison with the literature (Jutiviboonsuk et al. 2005).

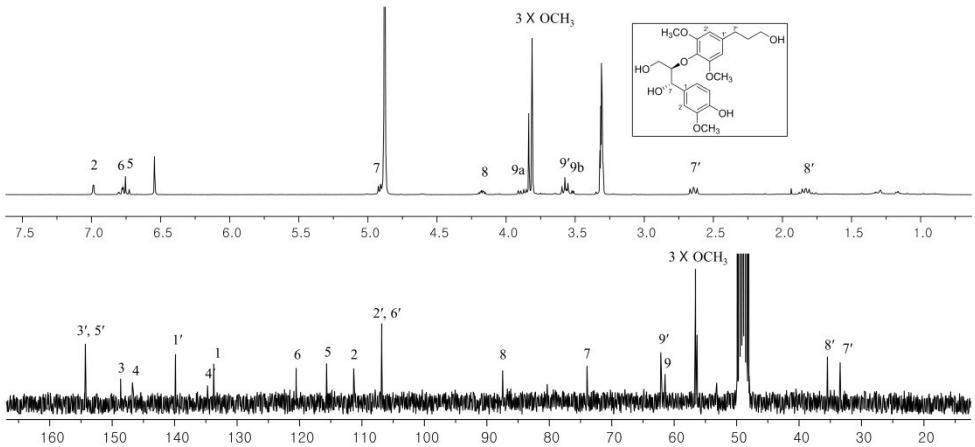

Figure 76. ^{1}H and ^{13}C NMR spectra of compound **55** (CD_3OD, 300 /75 MHz)

Compound **56** was isolated as brown oil. Its molecular formula was established as $C_{26}H_{36}O_{12}$ on the basis of ESI-QTOF-MS data with a pseudo-molecular ion peak at *m/z* 539.2136 $[M-H]^-$ (calcd. for $C_{26}H_{35}O_{12}$, 539.2134). 1D NMR spectra (Figure 77) were similar to those of compound **55** except for presence of a 3-guaiacylpropanol instead of a dihydrosinapyl alcohol. In addition, compound **56** has a sugar moiety. The sugar moiety was established to be *β*-D-glucose by the HPLC spectrum of the acid hydrolysate, with analysis of ^{13}C NMR spectrum. A glucopyranosyl moiety (δ_C 103.0, 76.8, 76.7, 73.5, 70.1 and 61.1) was observed in the ^{13}C NMR spectrum. The sugar moiety were defined as a *β*-glucose by coupling constants (*J*=7.6 Hz) of the anomeric protons. The HMBC correlations of H-8 (δ_H 4.21) with C-4′ (δ_C 146.0) and H-1″ (δ_H 4.10) with C-9′ (δ_C 67.9) were observed. The coupling constant ($J_{7,8}$) of H-7 (δ_H 4.70) was 5.3 Hz, which indicated an

erythro configuration at C-7/C-8 (Jutiviboonsuk et al. 2005). The absolute configuration of **56** was identified as 7*S*, 8*R* by comparison with the CD data of neolignans reported previously (Gan et al. 2008). The CD spectrum of **56** showed a negative Cotton effect at 236 nm. Compound **56** was identified and confirmed as *erythro*-(7*S*, 8*R*)-4,7,9-trihydroxy-3,3'-dimethoxy-8-*O*-4'-neolignan-9'-*O*-*β*-D-glucopy ranoside by comparison with the literature (Gan et al. 2008).

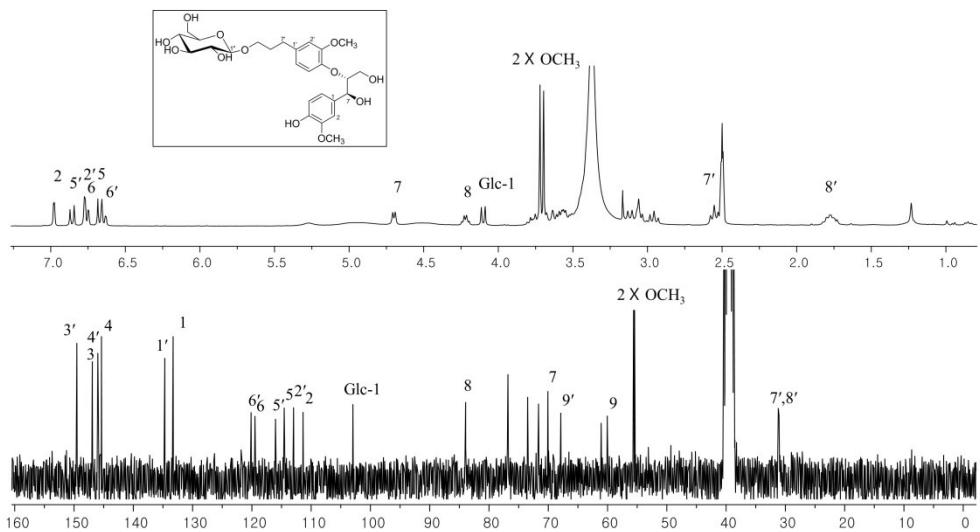

Figure 77. ^{1}H and ^{13}C NMR spectra of compound **56** (DMSO-d_6, 300 /75 MHz)

3.3.19. Compound **57**

Compound **57**, a colorless oil, was determined to have a molecular formula of $C_{17}H_{20}O_6$ by the ESI-QTOF-MS, which showed the pseudo-molecular ion at *m/z* 319.1190 $[M-H]^-$ (calcd. for $C_{17}H_{19}O_6$, 319.1187). ^{1}H NMR and HSQC spectra showed two 1,2,4-trisubstituted benzene rings at [δ_H 6.70 (1H, m, H-5′), 6.67 (1H, m, H-6′) and 6.63 (1H, m, H-2′)], [δ_H 6.66 (1H, m, H-2″), 6.62 (1H, m, H-6″) and

6.61 (1H, m, H-5″)], an oxygenated methylene at δ_H 3.84 (1H, dd, *J*=10.8, 6.5 Hz, H-3a) and 3.68 (1H, m, H-3b), two methine protons at δ_H 4.92 (1H, d, *J*=5.7 Hz, H-1) and 2.91 (1H, m, H-2) and two methoxy groups at δ_H 3.76 (3H, s, OCH_3) and 3.70 (3H, s, OCH_3) (Figure 78).

The COSY spectrum showed the correlations of H-2 with H-1 and H-3, suggesting an 1,2-disubstituted-propan-1,3-diol substructure. From the HMBC spectrum, the correlations of H-1 with C-2′ and C-6′ and H-2 with C-2″ and C-6″ were observed. Based on these data, compound **57** was identified as 1,2-bis-(4-hydroxy-3methoxyphenyl)propane-1,3-diol and confirmed by comparison with the literature (Zeng et al. 2013). The relative stereochemistry could be obtained from the ^{1}H NMR spectrum. The coupling constant of the signals for H-1 and H-2 is 5.7 Hz, suggesting *erythro* isomer (Berova et al. 1983). The CD spetrum showed negative Cotton effect at 236 nm.

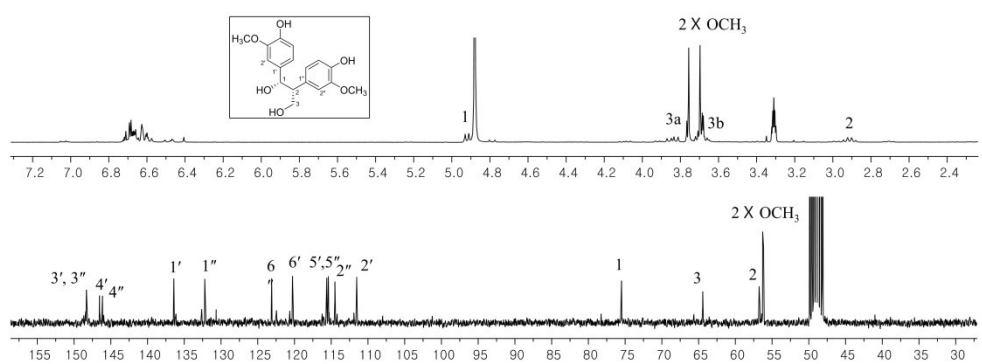

Figure 78. ^{1}H and ^{13}C NMR spectra of compound **57** (CD_3OD, 300 /75 MHz)

3.3.20. Compounds **58**, **59**

Compound **58** was obtained as colorless oil. Its molecular formula was established as $C_{18}H_{28}O_2$ by ESI-QTOF-MS at 277.2158 $[M+H]^+$ (calcd. for $C_{18}H_{29}O_2$, 277.2162) and ^{13}C NMR data. The ^{13}C NMR and HSQC spectra showed 18 carbons including a carboxyl carbon atom at δ_C 177.6 (C-1), six olefinic carbons at δ_C 136.6 (C-12), 134.5 (C-16), 133.0 (C-9), 129.3 (C-10), 126.6 (C-11) and 125.5 (C-15), nine methylene carbons at δ_C 36.3 (C-14), 35.0 (C-2), 30.7, 30.3, 30.2, 30.1 (C-4~7), 28.6 (C-8), 26.1 (C-3) and 21.7 (C-17), an oxymethine carbon at δ_C 73.2 (C-13) and a methyl group at δ_C 14.6 (C-18) (Figure 79). The sequential ^1H-^1H COSY correlations confirmed the linkage from C-2 to C-4 and from C-7 to C-18. In ^1H NMR spectrum, the splittings ($J_{9,10}$=11.2 Hz, $J_{11,12}$=15.2 Hz, $J_{15,16}$=10.9 Hz) of the signals for olefins suggested 9*Z*, 11*E*, 15*Z* configuration of compound **58**. From the HMBC spectrum, a carboxyl carbon was coupled to H-2. The optical rotation was positive. Based on these spectral data and comparison with literature, compound **58** was identified as (9*Z*, 11*E*, 13*S*, 15*Z*)-Octadeca-9,11,15-trien-13-olide (Schulz et al. 2007; Matsushita et al. 1997).

Compound **59** was isolated as colorless oil. Its molecular formula was determined to be $C_{18}H_{30}O_2$ by ESI-QTOF-MS at *m/z* 279.2326 $[M+H]^+$ (calcd. for $C_{18}H_{31}O_2$, 279.2319) and ^{13}C NMR data. 1D NMR spectra (Figure 80) were similar to those of compound **58** except for presence of two methylenes instead of a (*Z*)-olefin. The optical rotation was positive, suggesting that the configuration of **59** was *S* form. By analysis of these spectral data and comparison with literature, compound **59** was identified as (*S*)-coriolide (Schulz et al. 2007; Matsushita et al.

1997).

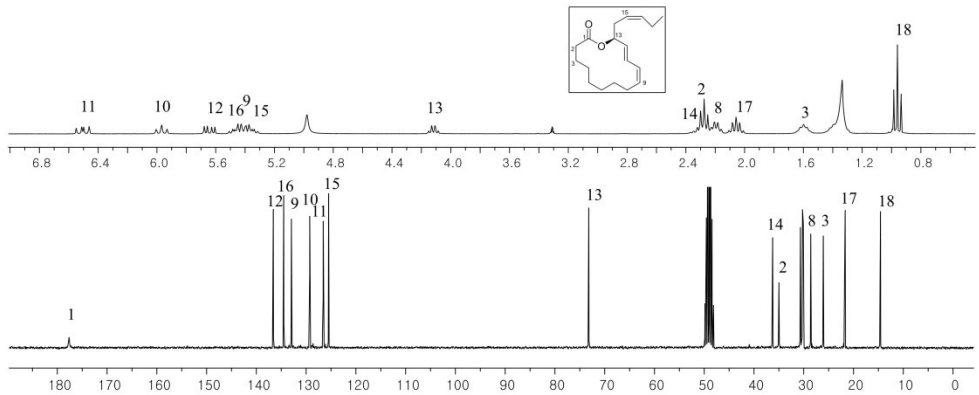

Figure 79. ^{1}H and ^{13}C NMR spectra of compound **58** (CD_3OD, 300 /75 MHz)

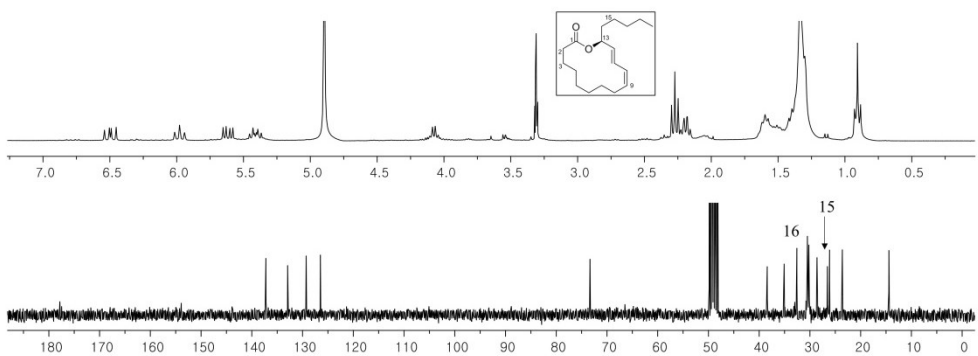

Figure 80. ^{1}H and ^{13}C NMR spectra of compound **59** (CD_3OD, 300 /75 MHz)

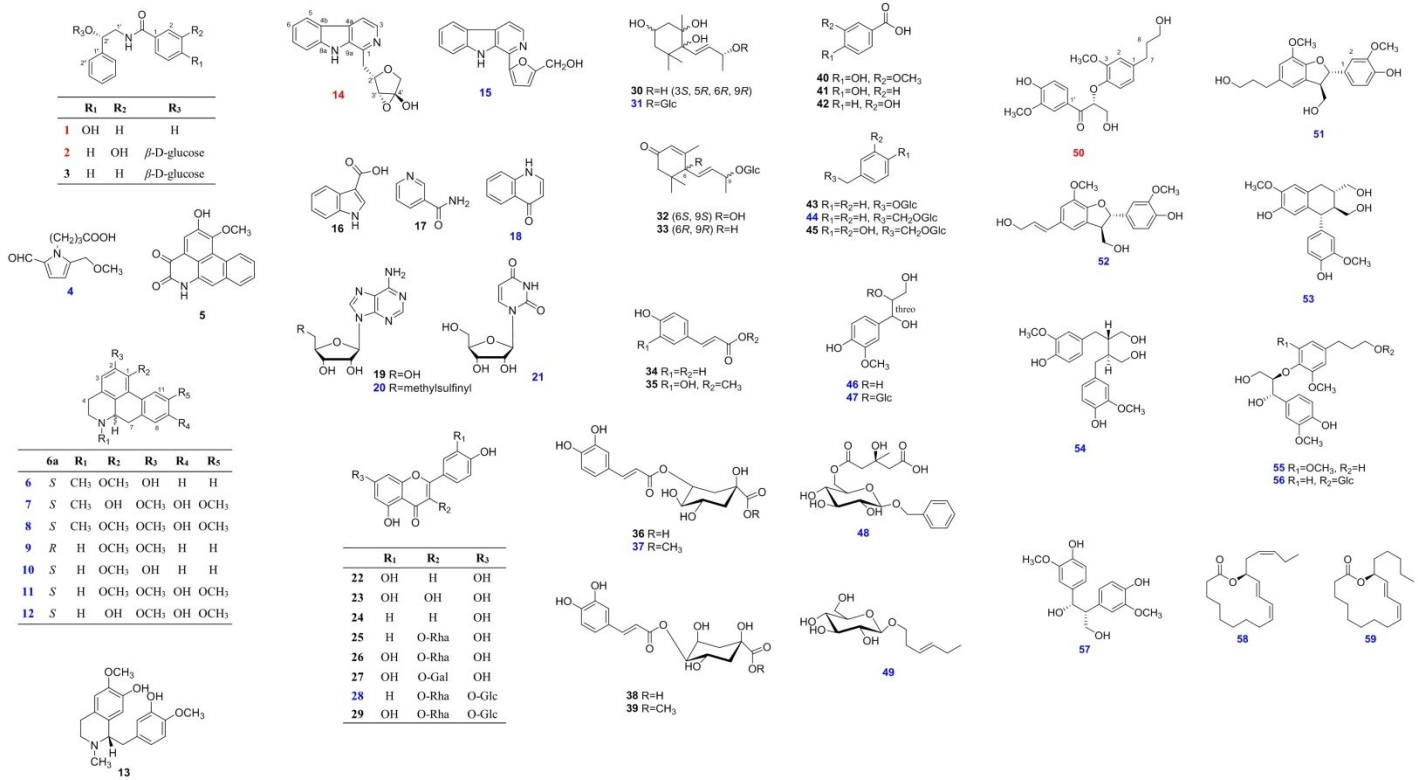

Figure 81. The isolated compounds from aerial parts of *H. cordata*

3.4. Inhibitory activity of isolates from H. cordata on NO production in LPS-stimulated RAW264.7 cells

Isolated compounds from aerial parts of *H. cordata* were tested for their inhibitory effects on LPS-induced NO production in RAW 264.7 cells. As shown Table 21, it was found that compounds **22-24**, **40**, **44**, **50-55**, **57-59** showed statistically significant effects on LPS-stimulated NO production in RAW264.7 cells. Cell viability was measured by MTT assay. All tested compounds had no toxicity at the concentration of 50 μM.

Table 21. The inhibitory activity of the compounds isolated from aerial parts of *H. cordata* on NO production in LPS-stimulated RAW264.7 cells

Compounds	IC_{50} (μM)	Compounds	IC_{50} (μM)	Compounds	IC_{50} (μM)
Dexamethasone	7.0	**34**	>100	**47**	>100
22	49.0 ± 6.7	**35**	-	**48**	>100
23	47.2 ± 0.2	**36**	>100	**49**	-
24	21.1 ± 3.7	**37**	>100	**50**	54.2 ± 1.5
25	>100	**38**	-	**51**	42.4 ± 1.7
26	>100	**39**	>100	**52**	4.4 ± 1.9
27	-	**40**	48.9 ± 1.5	**53**	46.1 ± 7.0
28	>100	**41**	>100	**54**	57.5 ± 13.4
29	-	**42**	>100	**55**	42.1 ± 11.6
30	>100	**43**	-	**56**	>100
31	>100	**44**	73.4 ± 10.2	**57**	55.5 ± 1.5
32	>100	**45**	>100	**58**	23.7 ± 3.0
33	>100	**46**	>100	**59**	18.0 ± 6.7

The values represent the mean ± S.D. of sample runs in triplicate.

4. Conclusion

This research was performed in order to investigate the alkaloids from the aerial parts of *Houttuynia cordata* and explore the biological activity of the isolated alkaloids to determine their anti-inflammatory properties.

The isolation of alkaloids from the MeOH extract of *H. cordata* was carried out. Twenty-one alkaloids were isolated and their structures were elucidated. Among them, two benzamids and one *β*-carboline alkaloids were isolated for the first time from nature. Their structures were defined as (*S*)-(-)-4-hydroxy-*N*-(2-hydroxy-2-phenylethyl) benzamide (**1**), (*S*)-(-)-3-hydroxy-*N*-(2-*β*-D-glucopyranosyl-2-phenylethyl)benzamide (**2**) and (2′*S*, 3′*R*, 4′*S*)-(3,4-epoxy-4-hydroxytetrahydro-furanyl)harmane (**14**). These compounds were named houttuynamide B (**1**), houttuynamide C (**2**) and houttuycorine (**14**), respectively. Also, the biosynthetic pathway of compound **14,** which have unusual partial structure (3,4-epoxy-4-hydroxytetrahydrofuran), were suggested to be generated from a tryptamine and a galactose.

The inhibitory effects of isolated alkaloids on LPS-induced NO production in a RAW 264.7 cell line were evaluated. Of the tested compounds, compound **15** showed moderate most potent inhibitory activity.

In addition, The constituents of *H. cordata* were further isolated. thirty-eight compounds including eight flavonoids (**22**-**29**), four megastigmane derivatives (**30**-**33**), eight phenylpropanoid derivatives (**34**-**39**, **46**, **47**), three benzoic acid

derivatives (**40**-**42**), five glycosides (**43**-**45**, **48**, **50**), two lignans (**53**, **54**), five neolignans (**50**-**52**, **55**, **56**), one bisphenylpropanol (**57**), two macrolides (**58**, **59**) were isolated and their structures were determined. Among them, a neolignan was newly reported from nature. Its structure was established to be (*R*)-4,9,9′-trihydroxy-3,3′-dimethoxy-7-oxo-8-*O*-4′-neolignan and named houttuylignan.

The inhibitory effects of isolates on LPS-induced NO production in a RAW 264.7 cells were evaluated. Of the tested compounds, compounds **22**-**24**, **40**, **44**, **50**-**55**, **57**-**59** showed moderate effects on LPS-stimulated NO production in RAW264.7 cells without cytotoxicity.

5. References

Ahmadinejad, N. & Tari, M.T., 2017. Nuclear Magnetic and Nuclear Quadrupole Resonance Parameters of *β*-Carboline Derivatives Calculated Using Density Functional Theory. *Russian Journal of Physical Chemistry A*, 91(4), pp.733–738. Available at: http://link.springer.com/10.1134/S0036024417040185.

Almeida, A.I.S., Silva, A.M.S. & Cavaleiro, J.A.S., 2010. Reactivity of 3-Iodo-4-quinolones in Heck Reactions: Synthesis of Novel (*E*)-3-Styryl-4-quinolones. *Synlett*, (3), pp.462–466.

Ang, K.K.H. et al., 2000. In Vivo Antimalarial Activity of the *Beta*-Carboline Alkaloid Manzamine A. *Antimicrobial Agents and Chemotherapy*, 44(6), pp.1645–1649.

Bauer, R. et al., 1996. Cyclooxygenase inhibitory constituents from *Houttuynia cordata*. *Phytomedicine*, 2(4), pp.305–308.

Berova, N., Kurtev, B. & Snatzke, G., 1983. Circular Dichroism of Optically Acitve 1,2-Disubstituted 1,2-Diphenylethanes-part I:The Cotton Effects within the *α*-band. *Tetrahedron*, 39(8), pp.1371–1378.

Boscá, L. et al., 2005. Nitric Oxide and Cell Viability in Inflammatory Cells: a Role for NO in Macrophage Function and Fate. *Toxicology*, 208(2), pp.249–258.

Braga, P.A.C. et al., 2007. In vitro Cytotoxicity Activity on Several Cancer cell lines of Acridone Alkaloids and *N*-Phenylethyl-Benzamide Derivatives from

Swinglea glutinosa (Bl.) Merr. *Natural product research*, 21(1), pp.47–55.

Briejer, M.R., Akkermans, L.M.A. & Schuurkes, J.A.J., 1995. Gastrointestinal Prokinetic Benzamides:The Pharmacology Underlying Stimulation of Motility. *Pharmacological Reviews*, 47(4), pp.631–651.

Calis, I. et al., 2002. (6*S*)-Hydroxy-3-oxo-*α*-ionol glucosides from *Capparis spinosa* fruits. *Phytochemistry*, 59(4), pp.451–457.

Carvalho, A. et al., 2017. A Harmine-derived *beta*-Carboline Displays Anti-cancer Effects in vitro by Targeting Protein Synthesis. *European Journal of Pharmacology*, 805, pp.25–35.

Cebrián-Torrejón, G. et al., 2015. Harvesting Canthinones:Identification of the Optimal Seasonal Point of Harvest of *Zanthoxylum chiloperone* leaves as a Source of 5-Methoxycanthin-6-one. *Natural Product Research*, 29(21), pp.2054–2058.

Chapla, V.M. et al., 2014. Antifungal Compounds Produced by *Colletotrichum gloeosporioides*, an Endophytic Fungus from *Michelia champaca*. *Molecules*, 19(11), pp.19243–19252.

Chen, J. et al., 2013. Aporphine Alkaloids : A Kind of Alkaloids' Extract Source, Chemical Constitution and Pharmacological Actions in Different Botany. *Asian Journal of Chemistry*, 25(18), pp.10015–10027.

Chen, S.D. et al., 2012. Houttuynoids A-E, Anti-Herpes Simplex Virus Active Flavonoids with Novel Skeletons from *Houttuynia cordata*. *Organic Letters*, 14(7), pp.1772–1775.

Chen, Y.F. et al., 2013. *Houttuynia cordata* Thunb extract modulates G_0/G_1 arrest and Fas/CD95-mediated death receptor apoptotic cell death in human lung cancer A549 cells. *Journal of Biomedical Science*, 20(1), pp.1–8.

Chen, Y.F. et al., 2010. *β*-Carboline Alkaloids from Stellaria dichotoma var. lanceolata and Their Anti-inflammatory Activity. *Journal of Natural Products*, 73(12), pp.1993–1998.

Chiang, L.-C. et al., 2003. Anti-Herpes Simplex Virus Activity of *Bidens pilosa* and *Houttuynia cordata*. *The American Journal of Chinese Medicine*, 31(3), pp.355–362.

Chimsook, T. et al., 2013. Structure-spectroscopic relationship of co-crystals between a rare chromone structure type of barakol and some organic acids. *Journal of Molecular Structure*, 1054–1055, pp.188–198.

Chin, Y.-W. et al., 2003. Hepatoprotective Pyrrole Derivatives of *Lycium chinense* fruits. *Bioorganic and Medicinal Chemistry Letters*, 13, pp.79–81.

Chou, S.-C. et al., 2009. The Constituents and Their Bioactivities of *Houttuynia cordata*. *Chemical & Pharmaceutical Bulletin*, 57(11), pp.1227–1230.

Craig, J.C. & Roy, S.K., 1965. Optical Rotatory Dispersion and Absolute Configuration-II. *Tetrahedron*, 21, pp.395–399.

Dewick, P.M., 2009. *Medicinal Natural Products : A Biosynthetic Approach-3rd edition*.

Dibinlal, Seethadevi & Sukumaran, S., 2015. Antioxidant activity of acetone extract of *Naravelia zeylanica*. *Journal of Pharmacognosy and*

Phytochemistry, 3(5), pp.131–133.

Dinesh, P. & Rasool, M., 2017. Berberine, an isoquinoline alkaloid suppresses TXNIP mediated NLRP3 inflammasome activation in MSU crystal stimulated RAW 264.7 macrophages through the upregulation of Nrf2 transcription factor and alleviates MSU crystal induced inflammation in rats. *International Immunopharmacology*, 44, pp.26–37.

Dini, I., Tenore, G.C. & Dini, A., 2006. New Polyphenol Derivative in *Ipomoea batatas* Tubers and Its Antioxidant Activity. *Journal of Agricultural and Food Chemistry*, 54(23), pp.8733–8737.

Dong, Z.B. et al., 2015. Screening for Anti-inflammatory Components from *Corydalis bungeana* Turcz. based on Macrophage Binding Combined with HPLC. *BMC Complementary and Alternative Medicine*, 15(363). Available at: http://www.biomedcentral.com/1472-6882/15/363.

Du, J.L. et al., 2010. Chemical Investigation of *Ervatamia yunnanensis*. *Chemistry of Natural Compounds*, 46(3), pp.459–461.

Fan, H. et al., 2013. In vitro and in vivo Anti-inflammatory Effects of 4-Methoxy-5- hydroxycanthin-6-one, a Natural Alkaloid from *Picrasma quassioides*. *Phytomedicine*, 20, pp.319–323.

Feng, J. et al., 2016. Radical Scavenging Constituents from Leaf of *Humulus scandens*. *Asian Journal of Chemistry*, 28(8), pp.1820–1822.

Franzyk, H., Olsen, C.E. & Jensen, S.R., 2004. Dopaol 2-Keto- and 2,3-Diketoglycosides from *Chelone obliqua*. *Journal of Natural Products*, 67(6), pp.1052–1054.

Fu, J. et al., 2013. Houttuynia cordata Thunb: A Review of Phytochemistry and Pharmacology and Quality Control. *Chinese medicine*, 4, pp.101–123.

Gan, M. et al., 2008. Glycosides from the Root of *Iodes cirrhosa*. *Journal of Natural Products*, 71(4), pp.647–654.

Gao, Y. et al., 2012. Anti-inflammatory effects of sophocarpine in LPS-induced RAW 264.7 cells via NF-κB and MAPKs signaling pathways. *Toxicology in Vitro*, 26, pp.1–6.

Guinaudeau, H., Leboeuf, M. & Cave, A., 1979. Aporphine Alkaloids II. *Journal of natural products*, 42(4), pp.325–360.

Guo, S. & DiPietro, L.A., 2010. Factors Affecting Wound Healing. *Journal of dental research*, 89(3), pp.219–229.

Han, E.H. et al., 2009. *Houttuynia cordata* water extract suppresses anaphylactic reaction and IgE-mediated allergic response by inhibiting multiple steps of FcεRI signaling in mast cells. *Food and Chemical Toxicology*, 47, pp.1659–1666.

Herraiz, T. et al., 2010. *β*-Carboline alkaloids in *Peganum harmala* and inhibition of human monoamine oxidase (MAO). *Food and Chemical Toxicology*, 48, pp.839–845.

Hopkinson-Woolley, J. et al., 1994. Macrophage recruitment during limb development and wound healing in the embryonic and foetal mouse. *Journal of Cell Science*, 107, pp.1159–1167.

Horsman, M.R., 1995. Nicotinamide and Other Benzamide Analogs as Agents for Overcoming Hypoxic Cell Radiation Resistance in Tumours. *Acta oncologica*, 34(5), pp.571–587.

Hotamisligil, G.S., 2006. Inflammation and Metabolic Disorders. *Nature*, 444, pp.860–867.

Hu, Y. et al., 2016. (±)-Homocrepidine A, a Pair of Anti-inflammatory Enantiomeric Octahydroindolizine Alkaloid Dimers from *Dendrobium crepidatum*. *Journal of Natural Products*, 79, pp.252–256.

Iman, V. et al., 2017. Anticancer and Anti-inflammatory Activities of Girinimbine Isolated from *Murraya koenigii*. *Drug Design, Development and Therapy*, 11, pp.103–121.

Jiang, Y. et al., 2014. Anti-complementary constituents of *Houttuynia cordata* and their targets in complement activation cascade. *Natural Product Research*, 28(6), pp.407–410.

Jiao, W.-H. et al., 2015. (±)-Quassidines I and J, Two Pairs of Cytotoxic Bis-*β*-carboline Alkaloid Enantiomers from *Picrasma quassioides*. *Journal of Natural Products*, 78, pp.125–130.

Jung, M. & Park, M., 2007. Acetylcholinesterase Inhibition by Flavonoids from *Agrimonia pilosa*. *Molecules*, 12, pp.2130–2139.

Jutiviboonsuk, A. et al., 2005. Bioactive constituents from roots of *Bursera tonkinensis*. *Phytochemistry*, 66, pp.2745–2751.

Kang, C.K. et al., 2012. Evaluation of the Genotoxicity of Extracts of *Houttuynia cordata* Thunb. *The American Journal of Chinese Medicine*, 40(5), pp.1019–1032.

Kawagishi, H. et al., 1993. 5′-Deoxy-5′-methylsulphinyladenosine, A Platelet Aggregation Inhibitor from *Ganoderma lucidum*. *Phytochemistry*, 32(2), pp.239–241.

Keinath, A.P. & Kousik, C.S., 2011. Sensitivity of Isolates of *Phytophthora capsici* from the Eastern United States to Fluopicolide. *Plant Disease*, 95(11), pp.1414–1419.

Kim, G.S. et al., 2008. Biological and Antibacterial Activities of the Natural Herb *Houttuynia cordata* Water Extract against the Intracellular Bacterial Pathogen *Salmonella* within the RAW 264.7 Macrophage. *Biological and Pharmaceutical bulletin*, 31(11), pp.2012–2017.

Kim, H.M. et al., 2016. A New Canthinone-Type Alkaloid Isolated from *Ailanthus altissima* Swingle. *molecules*, 21, pp.1–10.

Kim, I.S. et al., 2007. The inhibitory effect of *Houttuynia cordata* extract on stem cell factor-induced HMC-1 cell migration. *Journal of Ethnopharmacology*, 112(1), pp.90–95.

Kim, R.P.T. et al., 2013. Cytotoxic and Antioxidant Compounds from the Stem Bark of *Goniothalamus tapisoides* Mat salleh. *Molecules*, 18, pp.128–139.

Kumar, S. & Das, P., 2013. Solid-Supported Ruthenium(0): an Efficient Heterogeneous Catalyst for Hydration of Nitriles to Amides under Microwave Irradiation. *New Journal of Chemistry*, 37, pp.2987–2990.

Kumar, V., Yadav, N. & Kartha, K.P.R., 2014. In(III) triflate-catalyzed detritylation and glycosylation by solvent-free ball milling. *Carbohydrate Research*, 397, pp.18–26.

Lau, K.-M. et al., 2008. Immunomodulatory and anti-SARS activities of *Houttuynia cordata*. *Journal of Ethnopharmacology*, 118, pp.79–85.

Leardkamolkarn, V. et al., 2012. The inhibitory actions of *Houttuynia cordata* aqueous extract on dengue virus and dengue-infected cells. *Journal of Food Biochemistry*, 36, pp.86–92.

Lee, B.G. et al., 2000. Suppression of inducible nitric oxide synthase expression in RAW 264.7 macrophages by two *β*-carboline alkaloids extracted from *Melia azedarach*. *European Journal of Pharmacology*, 406, pp.301–309.

Lee, J.-S. et al., 2008. Suppressive effects of *Houttuynia cordata* Thunb (Saururaceae) extract on Th2 immune response. *Journal of Ethnopharmacology*, 117, pp.34–40.

Lee, S.-S. & Doskotch, R.W., 1999. Four Dimeric Aporphine-Containing Alkaloids from *Thalictrum fauriei*. *Journal of Natural Products*, 62(6), pp.803–810.

Lee, S.Y. et al., 2012. A New Flavonol Glycoside from *Hylomecon vernalis*. *Archives of Pharmacal Research*, 35(3), pp.415–421.

Lee, S.Y. et al., 2014. Antibacterial Effects of Afzelin Isolated from *Cornus macrophylla* on *Pseudomonas aeruginosa*, a Leading Cause of Illness in Immunocompromised Individuals. *Molecules*, 19, pp.3173–3180.

Li, C. et al., 2014. Quinoid glycosides from *Forsythia suspensa*. *Phytochemistry*, 104, pp.105–113.

Liu, J. et al., 2015. Anti-inflammatory alkaloid glycoside and quinoline alkaloid derivates from the stems of *Clausena lansium*. *RSC Advances*, 5, pp.80553–80560.

Liu, Q.-L. et al., 2017. A new indole alkaloid with anti-inflammatory activity from *Nauclea officinalis*. *Natural Product Research*, pp.1–6. Available at: https://www.tandfonline.com/doi/full/10.1080/14786419.2016.1277351.

Lundgren, L.N., Popoff, T. & Theander, O., 1981. Dilignol glycosides from needles of *Picea abies*. *Phytochemistry*, 20(8), pp.1967–1969.

Luyen, B.T.T. et al., 2015. Anti-inflammatory components of *Chrysanthemum indicum* flowers. *Bioorganic and Medicinal Chemistry Letters*, 25, pp.266–269.

Ma, C. et al., 2014. Purification and Characterization of Aporphine Alkaloids from Leaves of *Nelumbo nucifera* Gaertn and Their Effects on Glucose Consumption in 3T3-L1 Adipocytes. *International Journal of Molecular Sciences*, 15, pp.3481–3494.

Ma, Q. et al., 2017. Bioactive alkaloids from the aerial parts of *Houttuynia cordata*. *Journal of Ethnopharmacology*, 195, pp.166–172.

Matsunami, K. et al., 2009. Absolute configuration of (+)-pinoresinol 4-O-[6″-O-galloyl]-*β*-D-glucopyranoside, macarangiosides E, and F isolated from the leaves of *Macaranga tanarius*. *Phytochemistry*, 70, pp.1277–1285.

Matsushita, Y. et al., 1997. Enantioselective Synthases of 10-Oxo-11(*E*)-octadecen-13-olide and Related Fatty Acid. *Tetrahedron Letters*, 38(34), pp.6055–6058.

Meng, Y. et al., 2016. The anti-inflammation and pharmacokinetics of a novel alkaloid from *Portulaca oleracea* L. *Journal of Pharmacy and Pharmacology*, 68, pp.397–405.

Min, H.-Y. et al., 2010. Inhibition of Lipopolysaccharide-Induced Nitric Oxide Production by Antofine and Its Analogues in RAW 264.7 Macrophage Cells. *Chemistry and Biodiversity*, 7, pp.409–414.

Miyata, M., Koyama, T. & Yazawa, K., 2010. Water Extract of *Houttuynia cordata* Thunb. Leaves Exerts Anti-Obesity Effects by Inhibiting Fatty Acid and Glycerol Absorption. *Journal of nutritional science and vitaminology*, 56, pp.150–156.

Moustafa, A.M.Y. et al., 2007. Phytochemical Investigation and Biological Evaluation of *Schinus terebinthifolius*. *Research Journal of Phytochemistry*, 1(1), pp.1–11.

Ndi, C.P. et al., 2016. Antiproliferative Aporphine Alkaloids from *Litsea glutinosa* and Ethnopharmacological Relevance to Kuuku I'yu Traditional Medicine. *Australian Journal of Chemistry*, 69, pp.145–151.

Nemoto, K. et al., 2016. Me2AlCl-mediated carboxylation, ethoxycarbonylation, and carbamoylation of indoles. *Tetrahedron*, 72, pp.734–745.

De Oliveira, A.L.L. et al., 2012. Chemical constituents from red algae *Bostrychia radicans* (Rhodomelaceae): New amides and phenolic compounds. *Quimica Nova*, 35(11), pp.2186–2188.

Oltmanns, D. et al., 2009. Benzamides as Melanotropic Carriers for Radioisotopes, Metals, Cytotoxic Agents and as Enzyme Inhibitors. *Current Medicinal Chemistry*, 16, pp.2086–2094.

Otsuka, H. et al., 2003. Stereochemistry of megastigmane glucosides from *Glochidion zeylanicum* and *Alangium premnifolium*. *Phytochemistry*, 62, pp.763–768.

Pandurangan, A.K. et al., 2016. Boldine suppresses dextran sulfate sodium-induced mouse experimental colitis: NF-κB and IL-6/STAT3 as potential targets. *BioFactors*, 42(3), pp.247–258.

Park, C.H. et al., 2011. Phenolic constituents of *Acorus gramineus*. *Archives of Pharmacal Research*, 34(8), pp.1289–1296.

Prommaban, A. et al., 2012. *Houttuynia cordata* Thunb Fraction Induces Human Leukemic Molt-4 Cell Apoptosis through the Endoplasmic Reticulum Stress Pathway. *Asian Pacific Journal of Cancer Prevention*, 13, pp.1977–1981.

Rajemiarimoelisoa, C.F. et al., 2016. Chemical composition of the pods of *Albizia polyphylla*. *Natural Product Research*, 30(13), pp.1557–1560.

Rossini, A.F.C. et al., 2015. Total Syntheses of Aporphine Alkaloids via Benzyne

Chemistry: An Approach to the Formation of Aporphine Cores. *Journal of Organic Chemistry*, 80, pp.10033–10040.

Schulz, S. et al., 2007. Macrolides from the scent glands of the tropical butterflies *Heliconius cydno* and *Heliconius pachinus*. *Organic & biomolecular chemistry*, 5, pp.3434–3441.

Seco, J.M., Qui'noá, E. & Riguera, R., 2004. The Assignment of Absolute Configuration by NMR. *Chemical Reviews*, 104, pp.17–117.

Sharaf, M., El-Ansari, M.A. & Saleh, N.A.M., 1997. Flavonoids of four *Cleome* and three *Capparis* species. *Biochemical Systematics and Ecology*, 25(2), pp.161–166.

Shim, S.-Y., Seo, Y.-K. & Park, J.-R., 2009. Down-Regulation of FcεRI Expression by *Houttuynia cordata* Thunb Extract in Human Basophilic KU812F Cells. *Journal of medicinal food*, 12(2), pp.383–388.

Shin, S. et al., 2010. Anti-inflammatory effects of a *Houttuynia cordata* supercritical extract. *Journal of Veterinary Science*, 11(3), pp.273–275.

Shou, Q. et al., 2013. Parvifloranines A and B, Two 11-Carbon Alkaloids from *Geijera parviflora*. *Journal of Natural Products*, 76, pp.1384–1387.

Tanaka, T. et al., 2007. Facile Discrimination of Aldose Enantiomers by Reversed-Phase HPLC. *Chemical and Pharmaceutical Bulletin*, 55(6), pp.899–901.

Tatefuji, T. et al., 1996. Isolation and Identification of Compounds from Brazilian Propolis which Enhance Macrophage Spreading and Mobility. *Biological and Pharmaceutical bulletin*, 19(7), pp.966–970.

Vijayalakshmi, U. & Shourie, A., 2013. Gas chromatography-mass spectrometric analysis of ethanolic extracts of *Glycyrrhiza glabra* Linn. roots. *International Journal of Pharma and Bio Sciences*, 4(4), pp.741–755.

Vilegas, J.H.Y. et al., 1989. Aporphine Alkaloids from *Ocotea caesia*. *Phytochemistry*, 28(12), pp.3577–3578.

Vodovotz, Y. et al., 1993. Mechanisms of Suppression of Macrophage Nitric Oxide Release by Transforming Growth Factor *β*. *The Journal of experimental medicine*, 178, pp.605–613.

Wagner, D.J. et al., 2017. Potent inhibition of human organic cation transporter 2 (hOCT2) by *β*-carboline alkaloids. *Xenobiotica*, pp.1–9.

Wei, Z. et al., 2015. Norisoboldine, an Anti-Arthritis Alkaloid Isolated from Radix Linderae, Attenuates Osteoclast Differentiation and Inflammatory Bone Erosion in an Aryl Hydrocarbon Receptor-Dependent Manner. *International Journal of Biological Sciences*, 11(9), pp.1113–1126.

Williams, C.S., Mann, M. & DuBois, R.N., 1999. The role of cyclooxygenases in inflammation, cancer, and development. *Oncogene*, 18, pp.7908–7916.

Won, T.H. et al., 2012. Brominated Aromatic Furanones and Related Esters from the *Ascidian synoicum* sp. *Journal of Natural Products*, 75, pp.2055–2061.

Wu-Bao, W. et al., 2005. Flavonoids in *Sabina vulgaris* Antoine. *Chemistry of Natural Compounds*, 41(4), pp.473–474.

Wu, X. et al., 2011. Three new glycosides from *Hylocereus undatus*. *Journal of Asian Natural Products Research*, 13(8), pp.728–733.

Xia, R. et al., 2014. Efficient Synthesis of Nebularine and Vidarabine via Dehydrazination of (Hetero)aromatics Catalyzed by $CuSO_4$ in Water. *Green Chemistry*, 16(3), pp.1077–1081.

Xie, L.-H. et al., 2003. Biotransformation of Pinoresinol Diglucoside to Mammalian Lignans by Human Intestinal Microflora , and Isolation of *Enterococcus faecalis* Strain PDG-1 Responsible for the Transformation of (+)-Pinoresinol to (+)-Lariciresinol. *Chemical and Pharmaceutical Bulletin*, 51(5), pp.508–515.

Xu, M., Shen, L. & Wang, K., 2009. A new biflavonoid from *Daphniphyllum angustifolium* Hutch. *Fitoterapia*, 80, pp.461–464.

Yan, Q. et al., 2017. A Unified Approach to the Isomeric *α*-, *β*-, *γ*-, and *δ*-Carbolines via their 6,7,8,9-Tetrahydro Counterparts. *The Journal of Organic Chemistry*, 82, pp.4328–4335.

Yang, L. et al., 2016. Monitoring quality consistency of *Ixeris sonchifolia* (Bunge) Hance injection by integrating UV spectroscopic fingerprints, a multi-wavelength fusion fingerprint method, antioxidant activities and UHPLC/Q-TOF-MS. *RSC Advances*, 6, pp.87616–87627. Available at: http://dx.doi.org/10.1039/C6RA16436F.

Yang, L. & Jiang, J.-G., 2009. Bioactive components and functional properties of *Hottuynia cordata* and its applications. *Pharmaceutical Biology*, 47(12), pp.1154–1161.

Yang, Y.-N. et al., 2014. Hepatoprotective Activity of Twelve Novel 7′-Hydroxy Lignan Glucosides from *Arctii Fructus*. *Journal of Agricultural and Food Chemistry*, 62, pp.9095–9102.

Ying, Y.-M. et al., 2013. Alkaloids and Nucleoside Derivatives from a Fungal Endophyte of *Huperzia serrata*. *Chemistry of Natural Compounds*, 49(1), pp.184–186.

Yoon, J.W. et al., 2005. *β*-Carboline Alkaloid Suppresses NF-κB Transcriptional Activity Through Inhibition of IKK Signaling Pathway. *Journal of Toxicology and Environmental Health, Part A*, 68(23–24), pp.2005–2017.

Yuan, X. et al., 2017. Phenolics from *Lagotis brevituba* Maxim. *Natural Product Research*, 31(3), pp.362–366.

Zeng, Q. et al., 2013. Chemical constituents from *Aphanamixis grandifolia*. *Chemistry of Natural Compounds*, 49(3), pp.486–492.

Zhang, S. et al., 2015. Characterization and simultaneous quantification of biological aporphine alkaloids in *Litsea cubeba* by HPLC with hybrid ion trap time-of-flight mass spectrometry and HPLC with diode array detection. *Journal of Separation Science*, 38(15), pp.2614–2624.

Zhang, X. et al., 2010. Chemical constituents from the leaves of *Cerbera manghas*. *Asian Pacific Journal of Tropical Medicine*, 3(2), pp.109–111.

Zhu, X. et al., 2005. Phenolic compounds from *Viburnum cylindricum*. *Helvetica Chimica Acta*, 88(2), pp.339–342.

국문초록

약모밀(*Houttuynia cordata* Thunb.)은 삼백초과(Saururaceae)의 식물로, 어성초는 약모밀의 꽃필 때의 지상부이다. 한국, 중국, 일본 등 동북아시아에 분포하고 있으며, 전통적으로 해열, 해독, 소염약으로 사용되어 왔다. 어성초에서 분리 보고된 성분으로는 flavonoids, flavonoid glycosides, ionones와 alkaloid 등이 있으며, 어성초 추출물은 항균, 항진균, 항염, 항암 등의 다양한 생리 활성이 보고되어 있다.

Alkaloid는 질소 원자를 함유하고 있는 유기화합물의 통칭으로 식물계에 널리 분포하며 생리 작용이 뚜렷한 것이 많다고 알려져 있다. quinoline, isoquinoline, indole alkaloid와 benzamide 등의 다양한 모핵을 지니며, 모핵에 따라 항염, 항암 등을 포함한 다양한 생리 활성을 지닌다.

어성초에서 분리된 alkaloid로는 주로 benzamide와 isoquinoline 모핵을 지닌 물질 등이 보고되어 있으나 그 종류는 많지 않았다. 또한 어성초에서 분리, 보고된 alkaloid들에 대한 항염활성도 보고된 바 없었다.

본 연구에서는 어성초의 alkaloid성분 연구를 위해 어성초 메탄올 추출물에서 alkaloid를 선택적으로 분리하였고, 그에 대한 항염활성을 확인하고자 대식세포 내 산화질소 생성 저해능을 평가하였다. 총 21종의 alkaloid를 분리하였고, 이 중 1, 2, 14번 화합물이 천연에서 처음으로 분리, 보고되는 물질이다.

이화학적 및 분광학적 분석을 통해 그 구조를 각각 (*S*)-(-)-4-hydroxy-*N*-(2-hydroxy-2-phenylethyl) benzamide (**1**), (*S*)-(-)-3-hydroxy-*N*-(2-*β*-D-glucopyranosyl-2-phenylethyl)benzamide (**2**), (2′*S*, 3′*R*, 4′*S*)-(3,4-epoxy-4-hydroxytetrahydrofuranyl)-harmane (**14**)로 확인하였으며 각각 houttuynamide B (**1**), houttuynamide C (**2**), houttuycorine (**14**)로 명명하였다. 1, 2번 화합물은 그 구조가 어성초의 구성성분으로 보고되어 있는 houttuyamide A와 유사함을 확인하여 그 이름을 houttuynamide B, C로 명명하였다. 어성초에서 분리한 21종의 alkaloid에 대하여 RAW 264.7 세포주에서의 산화질소 생성 억제능을 평가한 결과, *β*-carboline 모핵을 지닌 15번 화합물만이 뚜렷한 활성을 나타냈다. (IC_{50} 8.7 μM)

또한 어성초의 성분연구를 추가적으로 진행하여 flavonoid 8종, megastigmane 유도체 4종, phenylpropanoid 유도체 8종, benzoic acid 유도체 3종, lignan 2종, neolignan 5종, bisphenylpropanol 1종, 배당체 5종, macrolide 2종을 포함하여 총 38종의 화합물을 추가로 분리하였다. 이 중 50번 화합물은 천연에서 처음으로 분리, 보고되는 물질로, (*R*)-4,9,9′-trihydroxy-3,3′-dimethoxy-7-oxo-8-*O*-4′-neolignan으로 확인하였으며 houttuylignan으로 명명하였다.

주요어 : 어성초, 삼백초과, alkaloids, 산화질소 생성 저해활성

학번 : 2011-21735